NATIONAL TECHNICAL UNIVERSITY OF ATHENS

SCHOOL OF APPLIED MATHEMATICAL AND PHYSICAL SCIENCES

Differential Gene Expression in Human Fibroblasts Simultaneously Exposed to Ionizing Radiation and Simulated Microgravity

Dissertation of:

Polina Malatesta

Dissertation Advisor:

Alexandros G. Georgakilas

February 2024

ΕΘΝΙΚΟ ΜΕΤΣΟΒΙΟ ΠΟΛΥΤΕΧΝΕΙΟ

ΣΧΟΛΗ ΕΦΑΡΜΟΣΜΕΝΩΝ ΜΑΘΗΜΑΤΙΚΩΝ ΚΑΙ ΦΥΣΙΚΩΝ ΕΠΙΣΤΗΜΩΝ

Διαφορική Γονιδιακή Έκφραση σε Ανθρώπινους Ινοβλάστες Εκτεθειμένους Ταυτοχρόνων σε Ιοντίζουσα Ακτινοβολία και Προσομοιωμένη Μικροβαρύτητα

Διπλωματική της:

Πολίνα Μαλατέστα

Υπεύθυνος Καθηγητής:

Αλέξανδρος Γεωργακίλας

Φεβρουάριος 2024

NATIONAL TECHNICAL UNIVERSITY OF ATHENS

SCHOOL OF APPLIED MATHEMATICAL AND PHYSICAL SCIENCES

Differential Gene Expression in Human Fibroblasts Simultaneously Exposed to Ionizing Radiation and Simulated Microgravity

Dissertation of:

Polina Malatesta

Dissertation Advisor:

Alexandros G. Georgakilas

Dissertation Committee:

Dr. Alexandros G. Georgakilas	Dr. Maria Diakaki	Dr. Ioannis Michalopoulos

Athens, February 2024

ACKNOWLEDGEMENTS

This dissertation would not have been possible without the help, guidance and support of several individuals who contributed their valuable assistance in preparation and completion of this study.
Starting off, I would like to express my deepest appreciation to my dissertation supervisor, Dr. Alexandros G. Georgakilas. He is the professor during my studies at the National Technical University of Athens, who inspired me to choose a path that interconnects applications of physics in the medical field. Without him, I would have never been exposed to the opportunity of pursuing an internship at the Biomedical Research Foundation Academy of Athens. Furthermore, his help and advice carried me through all stages of writing my dissertation. He offered me the chance of publishing the work of this project and having my first paper publication. Thank you for everything.
Likewise, I would like to express my greatest gratitude to Dr. Ioannis Michalopoulos, the head of the bioinformatics lab of the Biomedical Research Foundation, Academy of Athens, where I pursued my internship. He was the one who saw something in me and selected me to be the student that takes on this project. This project was a collaboration between NASA and JAXA and through this project I had the opportunity to meet incredible researchers, remarkable people, present at a NASA Workshop in Texas, write this dissertation, and have my first paper publication. Without Dr. Michalopoulos believing in me, none of this would have happened. I am truly grateful for the chance you offered me, and all the time you devoted to helping me during this long, difficult but wonderful journey. Thank you.
I want to thank Dr. Maria Diakaki for being part of my dissertation committee. She is an inspirational professor at the National Technical University of Athens and her courses in Nuclear Physics were very helpful for the understanding and writing of this study.
I am also thankful for Mr. Kostantinos Kyriakidis's contribution to this study. His assistance during the bioinformatics analysis was essential for the progression of this project.
Next, I would like to thank Dr. Megumi Hada. She is the PI of this project and without her, this project would not have been possible. She was eager to collaborate with me and allowed me to contribute to her project. When I went to Texas to present at the NASA Workshop, she generously let me stay at her house and was extremely friendly and welcoming. She really made my whole experience unforgettable. I truly admire her dedication to her work, her innovative ideas, and most of all, her genuine kindness and generosity. Thank you from the bottom of my heart.
Moving on, I would like to thank Dr. Premkumar B. Saganti. I would like to express my appreciation for his help and contribution to this study. Furthermore, during my stay in Texas, he kindly gave me the amazing opportunity of presenting our study at Prairie View A&M University. He is extremely passionate, friendly, and encouraging. Thank you for everything.
Additionally, I would like to thank Dr. Akihisa Takahashi and Dr. Hiroko Ikeda. I find Dr. Takahashi's dedication to his work and his innovative ideas admirable. He developed the clinostat and open-handedly shared preliminary data that was crucial to this study. Dr. Ikeda, who analyzed the preliminary data before this study, was eager to help me and her findings were the inspiration of our current study. Dr. Takahashi and Dr. Ikeda trusted and allowed me to contribute to their study and I am truly grateful for that. Thank you.
I would also like to give a special thanks to my friends Alexandra, Marisevi, Demosthene and Kosma, who even though I met in university, I know we will keep our friendship lifelong. They made my university years truly memorable and during the writing of my dissertation, they were very supportive. I would also like to thank my childhood friend Stella who is always there for me, encourages me, and believes that I can do anything I put my mind to.
Last, but definitely not least, I would like to thank my family. I would like to thank my two wonderful sisters, Maria and Katerina. You are my best friends and your love, encouragement, and understanding have been my pillars of strength. Finally, I would like to thank my parents, Patty and Anthony. Thank you for standing by me through the ups and downs, for believing in me, and for providing a foundation of love and security. I dedicate this dissertation to my mother who has been my role model since day one and is the driving force behind my accomplishments. I feel very lucky and grateful to have such a loving and supportive family. Thank you.

.....
Polina Malatesta

ABSTRACT

During future space missions, astronauts will be exposed to cosmic radiation and microgravity (μG), known to be health risk factors. To examine the differentially expressed genes (DEGs) and their prevalent biological processes and pathways as a response to these two risk factors simultaneously, 1BR-hTERT human fibroblast cells were cultured under 1 gravity (1G) or simulated μG for 48 hrs in total and collected 0 (sham-irradiated), 3 or 24 hrs after 1 Gy of X-ray or Carbon-ion (C-ion) irradiation. A three-dimensional clinostat was used for the simulation of μG and the simultaneous radiation exposure of the samples. RNA-seq method was used to produce lists of differentially expressed genes between different environmental conditions. Over-representation analyses were performed and the enriched biological pathways and targeting transcription factors were identified. Comparing sham-irradiated cells under simulated μG and 1G conditions, terms related to response to oxygen levels and muscle contraction were identified. After irradiation with X-rays or C-ions under 1G, identified DEGs were found to be involved in DNA damage repair, signal transduction by p53 class mediator, cell cycle arrest and apoptosis pathways. The same enriched pathways emerged when cells were irradiated under simulated μG condition. Nevertheless, the combined effect attenuated the transcriptional response to irradiation which may pose a subtle risk in space flights.

Keywords: Space flight; Cosmic radiation; Microgravity; Differentially Expressed Genes; Gene networks

ΠΕΡΙΛΗΨΗ

Κατά τη διάρκεια μελλοντικών διαστημικών αποστολών, οι αστροναύτες θα εκτίθενται σε κοσμική ακτινοβολία και μικροβαρύτητα (μG) και είναι γνωστό ότι αποτελούν παράγοντες κινδύνου για την υγεία. Για να εξεταστούν τα διαφορετικά εκφραζόμενα γονίδια (DEGs) και οι επικρατούσες βιολογικές διεργασίες και μονοπάτια τους ως απόκριση σε αυτούς τους δύο παράγοντες κινδύνου ταυτόχρονα, κύτταρα ανθρώπινων ινοβλαστών 1BR-hTERT καλλιεργήθηκαν υπό 1 βαρύτητα (1G) ή προσομοίωση μG για 48 ώρες συνολικά και συλλέχθηκαν 0 (εικονική ακτινοβολία), 3 ή 24 ώρες μετά από 1 Gy ακτινοβολίας ακτίνων X ή ιόντων άνθρακα (ιόντων C). Ένας τρισδιάστατος κλινοστάτης χρησιμοποιήθηκε για την προσομοίωση της μG και την ταυτόχρονη έκθεση των δειγμάτων σε ακτινοβολία. Χρησιμοποιήθηκε η μέθοδος RNA-seq για την παραγωγή καταλόγων γονιδίων που εκφράζονται διαφορετικά μεταξύ διαφορετικών περιβαλλοντικών συνθηκών. Πραγματοποιήθηκαν αναλύσεις υπερεκπροσώπησης και εντοπίστηκαν τα εμπλουτισμένα βιολογικά μονοπάτια και οι μεταγραφικοί παράγοντες-στόχοι. Συγκρίνοντας τα κύτταρα που ακτινοβολήθηκαν με εικονική ακτινοβολία υπό προσομοιωμένες συνθήκες μG και 1G, εντοπίστηκαν όροι που σχετίζονται με την απόκριση στα επίπεδα οξυγόνου και τη μυϊκή συστολή. Μετά από ακτινοβόληση με ακτίνες X ή ιόντα C υπό 1G, διαπιστώθηκε ότι οι εντοπισμένοι DEGs εμπλέκονται στην επιδιόρθωση βλαβών του DNA, στη μεταγωγή σήματος από τον μεσολαβητή της τάξης p53, στη διακοπή του κυτταρικού κύκλου και στα μονοπάτια της απόπτωσης. Τα ίδια εμπλουτισμένα μονοπάτια προέκυψαν όταν τα κύτταρα ακτινοβολήθηκαν υπό συνθήκες προσομοίωσης μG. Παρ' όλα αυτά, η συνδυασμένη επίδραση εξασθένισε τη μεταγραφική απόκριση στην ακτινοβολία, η οποία μπορεί να αποτελέσει έναν ανεπαίσθητο κίνδυνο στις διαστημικές πτήσεις.

Λέξεις-κλειδιά: Διαστημική πτήση, Κοσμική ακτινοβολία, Μικροβαρύτητα, Διαφορικά Εκφρασμένα Γονίδια, Δίκτυα γονιδίων

Table of Figures

Table of Contents

1. INTRODUCTION

Space flight conditions differ to those on Earth due to cosmic ionizing radiation (IR) and the absence of gravity, known as microgravity (μG), both of which pose health risk factors to humans, causing complex DNA damage and genome instability (Hada et al., 2018; H. Ikeda et al., 2019; Maxwell et al., 2008; Michalettou et al., 2021; Yamanouchi et al., 2021). It is crucial to gain more insights on these factors, as astronauts will be continuously exposed to them in long-duration exploration missions, such as those to the Moon or Mars, which require humans to remain in space for days, months and even years.

The space environment, comprising galactic cosmic rays (GCRs) and reduced gravity, necessitates testing for possible additive or synergistic effects. Altered DNA repair mechanisms due to gravity changes can impede cellular responses to space radiation, increasing the risk of DNA damage accumulation and tumorigenesis (Moreno-Villanueva & Wu, 2019). Recent studies highlight that spaceflight stressors like ionizing radiation (IR) and/or microgravity, disrupt the wound healing process, affecting pathways like inflammation and proliferation (Radstake et al., 2023). Microgravity significantly impacts cell death, migration, and gene expression in tumor cells, including cancer stem cells, and alters the effects of chemotherapeutic drugs (Topal & Zamur, 2021). While extensive research has focused on the impact of either radiation or microgravity alone, limited studies address their combined effects. Previous attempts were found to be challenging, as older clinostats had to pause rotation which simulates microgravity to irradiate the cells (Indo et al., 2015; T. Wang et al., 2015), potentially introducing additional gravitational stimuli, and thus activating specific signaling cascades.

In deep space beyond the Van Allen belts, galactic cosmic rays consist of both high-energy and low-energy radiation. To investigate the combined effects of space radiation and microgravity, considering lunar and Mars explorations and long-term stays in space in the near future, it was decided to use carbon ions as high-energy radiation and X-rays as low-energy radiation. To maintain the consistent simulated μG condition before, during, and after exposure to radiation, a 3D clinostat that allows samples to be rotated and irradiated simultaneously was developed (H. Ikeda et al., 2017) and used in this study. The raw transcriptomic data that was produced (H. Ikeda et al., 2019), was analyzed and applying a systems biology approach, all differentially expressed genes between various conditions and their predominant processes they participate were identified.

1.1. Radiation

Radiation refers to the emission and transmission of energy in the form of particles or electromagnetic waves through space or a medium. It encompasses a wide spectrum of phenomena, from natural processes like sunlight and heat, to human-made sources such as X-rays and radio waves. Radiation can be categorized into two main types: ionizing and non-ionizing radiation. Ionizing radiation possesses enough energy to remove tightly bound electrons from atoms, leading to the formation of charged particles known as ions. This type of radiation includes X-rays, gamma rays, and some forms of ultraviolet radiation. On the other hand, non-ionizing radiation has lower energy levels and does not have sufficient energy to ionize atoms. Examples of non-ionizing radiation are visible light, infrared waves, radio waves, and microwaves. Understanding and managing radiation is crucial as it has diverse applications in medicine, communication, energy production, and scientific research, while also posing potential risks to human health and the environment when not properly controlled.

1.1.1. Ionizing Radiation

Ionizing Radiation (IR) is a type of energy emitted by atoms in the form of electromagnetic waves or particles and its interaction with matter is capable of ionizing its atoms, breaking chemical bonds and causing damage to living organisms (Ahnstrom, Ehrenberg, & Graslund, 1978). Ionization is the phenomenon where a neutral atom or molecule acquires a negative or positive charge upon the addition or removal of an electron due to exogenous factors. The genetic material of cells of living organisms may be damaged due to the properties of ionizing radiation. The probability of genetic alterations and cancer being caused by ionizing radiation depends on the Absorbed Dose (D), which is measured in Gray (Gy = $J*kg^{-1}$) and is the amount of the energy deposited in matter by ionizing radiation per unit mass. Equivalent dose (H) quantifies the probabilistic health impacts of low levels of ionizing radiation exposure on the human body. It reflects the probability of radiation-induced cancer and genetic damage. While it stems from the absorbed dose, it also considers the biological effectiveness of the radiation, influenced by factors such as radiation type and energy. The Equivalent dose is measured in Sievert (Sv) in the International System of Units (SI). The effective dose is calculated by multiplying the equivalent dose by a tissue weighting factor and it is also measured in Sv. The relative biological effectiveness (RBE) is the ratio of the absorbed dose of one type of ionizing radiation relative to another, to produce the same biologic effect (Castro, Blakely, Tsujii, & Schulz-Ertner, 2010). The mission of the International Commission on Radiological Protection (ICRP) is to protect individuals, animals, and the environment against the negative impacts of ionizing radiation. The ICRP provides recommendations that serve as the foundation for global radiological protection policies, regulations, guidelines, and practices (https://www.icrp.org/). It has been estimated that the probability of fatal cancer induction is 5% per Sv (Mazrani, McHugh, & Marsden, 2007). Finally, the sources of ionizing radiation can be natural or man-made. Natural sources include cosmic radiation, ground radiation and the food chain. Artificial sources include radiotherapy, radiodiagnostics and the use of radioisotopes in medical applications and in the broader context, radioactive dust from nuclear tests, nuclear waste and nuclear reactors. The unit of measurement of radioactivity is Becquerel (Bq = $1s^{-1}$) and corresponds to one nuclear decay per second of a radioactive atom.

1.1.1.1. X-rays

X-rays, also known as Röntgen rays, are a part of the electromagnetic spectrum that ranges in the 10pm to 10nm wavelength region. X-rays correspond to frequency that ranges from 30 PHz to 30 EHz and energy that ranges from 100 eV to 200 keV. They are divided into two categories (Sort and Hard) according to their wavelength, frequency and energy. Soft X-rays are 100nm to 100pm, 30 PHz to 3 EHz and 120 eV to 12 keV while hard X-rays are 100pm to 10pm, 3 EHz to 30 EHz and 12 keV to 120 keV. When X-rays penetrate any material, some of the radiation is absorbed by that material and the absorption of the radiation depends on the nature of the material, as well as the wavelength of the radiation. The higher the atomic number (Z) of the atoms of the material that absorbs the radiation, the higher the absorption of the radiation. Furthermore, the absorption of radiation increases as the wavelength of the radiation increases.

1.1.1.2. Gamma Rays

Gamma radiation is high-energy photon radiation and corresponds to the wavelength range of 1 nm to 10 pm, with a frequency range of 50 EHz to 30 ZHz and an energy range of 100 keV to 8 MeV. Even though gamma rays are quite similar the x-rays (Dendy & Heaton, 2011),gamma rays originate from the nucleus of the atom while X-rays originate from the electron cloud (L'Annunziata, 2003). Gamma rays have higher energy than X-rays and have a higher penetrating power. Gamma rays often accompany nuclear reactions of all types.

1.1.1.3. Alpha Rays

Alpha particles, also called alpha rays, consist of two protons and two neutrons bound together in a particle identical to a ^{4}He (helium-4) nucleus and are produced in the process of alpha decay, i.e. by nuclear fission of heavy and unstable nuclei. A-decay is essentially a nuclear decay process in which alpha particles are emitted.

1.1.1.4. Beta Ray

Beta ray is defined as the emission of beta particles, either electrons or positrons, from unstable radioactive nuclei. The emission of beta particles is achieved through beta decay, i.e., when a neutron decays to produce a proton, an electron and an electron antineutrino.

1.1.1.5. Neutron Radiation

Neutron radiation is commonly referred to as indirectly ionizing radiation. Unlike charged particles such as protons and electrons, neutrons lack charge and do not ionize atoms in the same manner. However, neutron interactions largely result in ionization. Due to their lack of charge, neutrons exhibit greater penetration compared to alpha or beta radiation. In some instances, neutrons can surpass gamma radiation in penetration, especially in materials with high atomic numbers that impede gamma radiation. Nevertheless, in materials with low atomic numbers, like hydrogen, a low-energy gamma ray may exhibit greater penetration than a high-energy neutron. In the field of health physics, neutron radiation presents a form of radiation hazard. A more serious aspect of neutron radiation is its potential for neutron activation, in which the radiation can induce radioactivity in most encountered substances, including bodily tissues (Preston et al., 2004). This phenomenon arises from the capture of neutrons by atomic nuclei, leading to a transformation into another nuclide, often a radionuclide. The process of neutron activation contributes significantly to the release of radioactive materials following the detonation of a nuclear weapon.

1.1.1.6. Ionizing Radiation in Space

The particles associated with ionizing radiation in space are categorized into three main groups relating to the source of the radiation: radiation belt particles (Van Allen Belts) trapped in space around the Earth, solar energetic particles (SEPs) and galactic cosmic rays (GCRs).

1.1.1.6.1. Van Allen Radiation

The Van Allen radiation belts refer to regions of intense radiation surrounding the Earth, named after scientist James Van Allen who discovered them in 1958 (Van Allen, McIlwain, & Ludwig, 1959). These belts are composed of charged particles, trapped by the Earth's magnetic field. There are two main regions of the Van Allen belts: the inner belt and the outer belt.

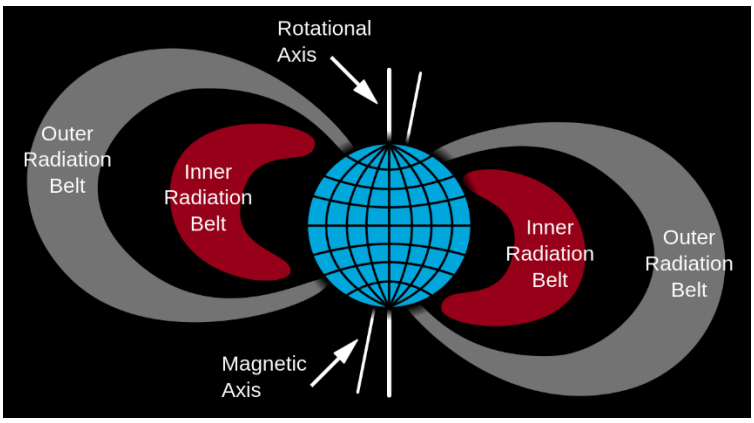

Figure 1. A cross section of Van Allen radiation belts.
(https://en.wikipedia.org/wiki/Van_Allen_radiation_belt#/media/File:Van_Allen_radiation_belt.svg)

1.1.1.6.2. Solar Energetic Particles

Solar wind is a stream of changed particles, with its plasma consisting of electrons, protons, alpha particles, charge state and elemental composition of nearly 40 ion species of He, C, N, O, Ne, Mg, Si, S, and Fe that are emitted by the Sun (von Steiger et al., 2000). The solar wind is created by the outermost layer of the Sun's atmosphere, known as the corona. Coronal Mass Ejections (CMEs) and solar flares are closely related phenomena that occur on the Sun. A coronal mass ejection (CME) is a significant ejection of plasma and magnetic field from the Sun's corona into space (Schwenn et al., 2006). A solar flare is an intense localized eruption of electromagnetic radiation in the Sun's atmosphere. During the solar cycle, the solar wind influences the presence of lower-energy GCR particles, preventing most of them from reaching Earth during periods of high solar activity. However, during solar minimum, when there is less solar activity, GCR particles have an easier time reaching Earth. The GCR cycle follows a similar 11-year pattern to the solar cycle, but its peak occurs during solar minimum. Unlike the solar cycle, which can experience sudden changes, the energy and composition of GCR particles remain relatively stable over time, changing slowly.

1.1.1.6.3. Galactic Cosmic Rays

Cosmic rays, also known as astroparticles, are high energy particles traveling through space at nearly the speed of light. The arriving flux consists of approximately 2% electrons and 98% nuclei. The nuclear component consists of ~87% hydrogen, ~12% helium and ~1% of high atomic number and energy (HZE) particles (Simpson, 1983). Even though the flux levels of GCR particles are very low, these high-linear energy transfer (LET) particles produce intense ionization as they pass through matter (Maalouf, Durante, & Foray, 2011; Nelson, 2016). In deep space, the exposure is equivalent to approximately 1-2 mSv per day and half this value on planetary surfaces (Cucinotta & Durante, 2006). When cosmic rays encounter Earth's atmosphere, they generate showers of secondary particles, with some reaching the Earth's surface. However, the majority are redirected into space by the magnetosphere or heliosphere.

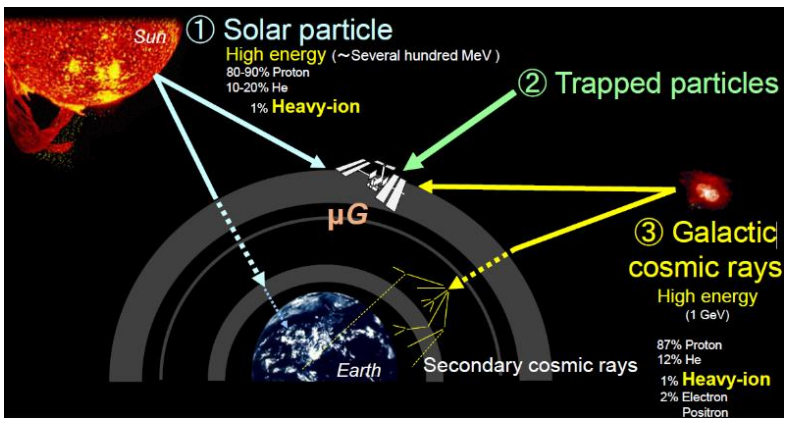

Figure 2. Space Environment Discription (http://www.radconsult.eu/)

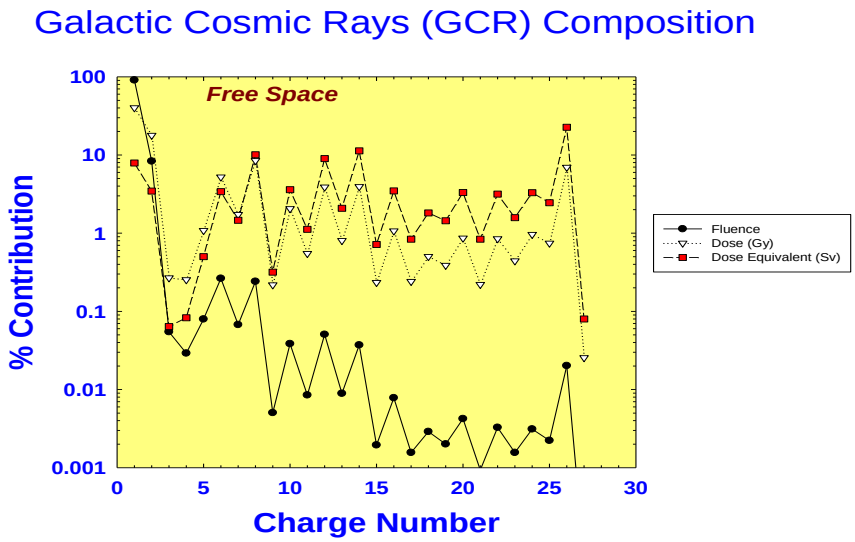

Figure 3. Galactic Cosmic Rays Composition (https://www.icrp.org/docs/Gunther%20Dietze%20Assessment%20of%20Radiation%20Exposure%20of%20Astronauts%20in%20Space.pdf)

1.1.2. Properties of Radiation

1.1.2.1. The Bethe formula

The Bethe formula or Bethe–Bloch formula defines the mean energy loss per distance travelled of charged particles, such as protons, alpha particles, atomic ions, traversing matter, also known as the stopping power. The stopping power depends mainly on the Z/A ratio, which is the ratio of atomic number to mass. (Ziegler, Ziegler, & Biersack, 2010). The general form of the Bethe-Bloch equation is:

$$-\frac{dE}{dx} = \left(\frac{1}{4\pi\varepsilon_{\circ}}\right)^2 \frac{4\pi z^2 e^4}{mu^2} \frac{Z}{A} \ln\left(\frac{mu^2}{I}\right)$$

, where $(1/4\pi\varepsilon_o)$ is a constant from Coulomb's Law, m, z and u are determined by the radiation (mass, atomic number, e.g. z=1 for protons, velocity), e is the electron charge, and I is the ionization potential.

For electrons relativistic corrections at the Bethe-Bloch formula are made and due to their small mass, the energy loss differs to some extent, as they undergo more substantial losses through Bremsstrahlung (Porter, 1985). The swift movement of charged particles through a substance, results in interactions with the electrons of atoms within the material. These interactions either excite or ionize the atoms, leading to the dissipation of energy by the traveling particle.

1.1.2.2. Bremsstrahlung radiation

Bremsstrahlung radiation is type of electromagnetic radiation, which is produced when a charged particle, like an electron, slows down or changes direction due to interacting with another charged particle, usually an atomic nucleus. As the particle loses speed, it releases energy in the form of radiation, specifically photons (Low, 1958). When a free electron approaches the nucleus of an atom or another charged particle, the potent electric field of the nucleus attracts the electron, causing it to change both direction and speed, effectively accelerating it. As the electron loses energy during this acceleration, it emits X-ray photons. The energy of these emitted photons varies, with more energetic electrons producing higher-energy X-rays and less energetic electrons emitting lower-energy photons. The X-rays generated through this process are referred to as bremsstrahlung. The

kinetic energy lost by the first (moving) particle is converted into a photon to satisfy the law of conservation of energy. For large momenta, hence large energies, the produced photons (bremsstrahlung radiation) exhibit large frequencies.

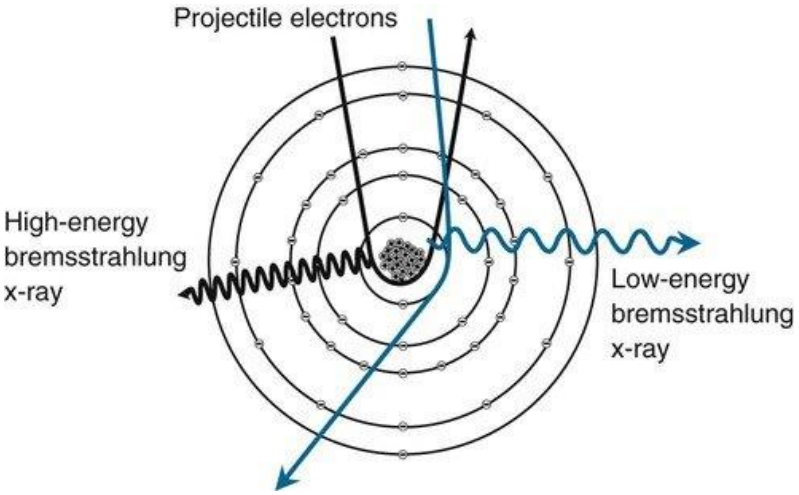

Figure 4. Bremsstrahlung (https://physicsopenlab.org/2017/08/02/bremsstrahlung-radiation/)

1.1.2.3. Bragg peak

The Bragg peak is an evident peak on the Bragg curve that plots the energy loss of ionizing radiation during its travel through matter. It was discovered in 1903 by William Henry Bragg, and it was named after him. The peak occurs instantly before particles (protons, α-rays, and other ion rays) come to rest (C. M. C. Ma & Lomax, 2012). The Bragg peak plays a pivotal role in determining the dose distribution of ionizing radiation within a material, especially in applications like radiation therapy. As charged particles, such as protons or alpha particles, traverse through a medium, their energy loss is graphically represented by the Bragg curve. The Bragg peak represents a concentrated release of energy, occurring just before the particles come to rest. In the context of dose, the Bragg peak is strategically utilized in radiation therapy to target tumors. By adjusting the energy of the particles, medical professionals can precisely position the Bragg peak at the depth of the tumor. This targeted delivery allows for maximum energy deposition at the tumor site, ensuring effective destruction of cancer cells while minimizing damage to surrounding healthy tissues.

1.1.2.4. Linear Energy Transfer (LET)

Linear Energy Transfer (LET) is the amount of energy that an ionizing particle transfers to the material traversed per unit distance. It is measured in MeV/cm.

$$\text{LET}=\frac{dE}{dx}$$

,where dE is the energy loss of the charged particle due to electronic collisions while transferring a distance dx

It describes the action of radiation into matter. High-LET radiation deposits a higher concentration of energy in a shorter distance when traversing tissue compared with low-LET radiation (Russ et al., 2022). High LET usually refers to heavily charged particles, such as Carbon ion (C-ion) radiation and causes more tissue damage than low LET radiation, such as electrons and photons. High LET particles deposit more energy in the targeted areas of a tumor (this effect is called Bragg Peak) and also have a higher Relative Biological Effectiveness (RBE).

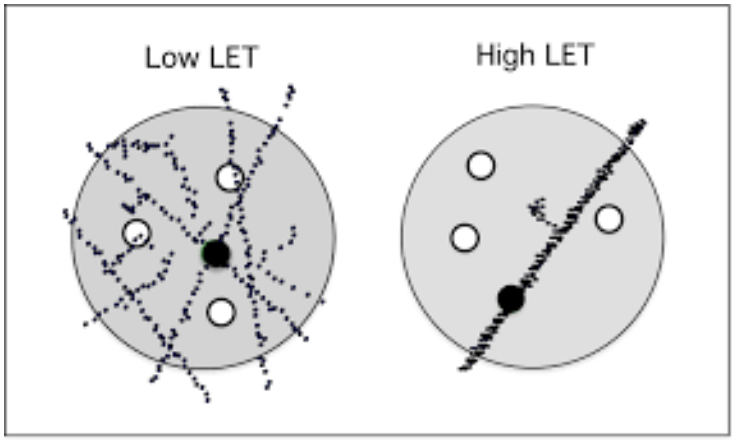

Figure 5. Schematic representation of particle tracks for low-LET (left) and high-LET (right) radiation. (https://arxiv.org/ftp/arxiv/papers/1804/1804.08500.pdf)

1.2. Space

1.2.1. International Space Station

The International Space Station (ISS) is a research space station that is a multinational collaboration between the space agencies NASA (USA), Roscosmos (Russia), JAXA (Japan), ESA (Europe), and CSA (Canada). The assembly of the 108 m long station began in November 1998 and the first crew was installed in November 2000. The ISS is located about 420 km above the Earth's surface and moves at a speed of 28,000 km/h. Because of this, the ISS makes a full orbit around the Earth approximately every 90 minutes and therefore its crew sees the sunrise and sunset 16 times in one day. The gravity at the ISS altitude is about 89% of that of the Earth (Earth's gravity ≈ 9.807 m/s^2).

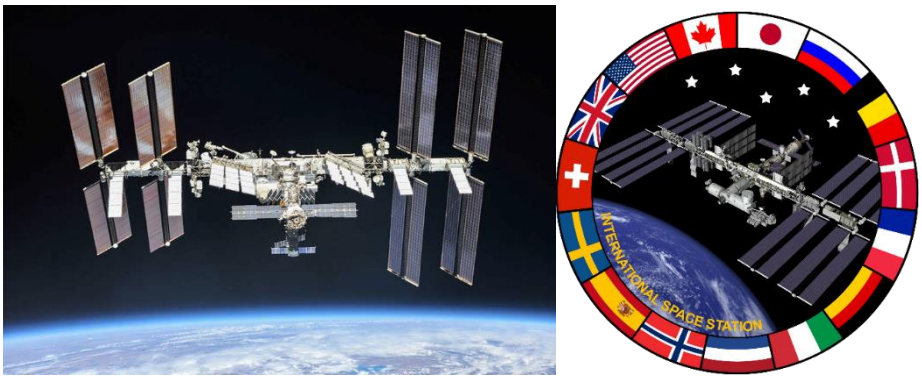

Figure 6. International Space Station (left) (https://www.nasa.gov/news-release/nasa-administrator-statement-on-russian-asat-test/) and Emblem of the ISS (right) (https://en.wikipedia.org/wiki/International_Space_Station_programme#/media/File:ISS_emblem.png)

1.2.2. Moon

The Moon is Earth's only natural satellite and the fifth largest natural satellite in the solar system. The average distance of the Moon is 384,400 km from Earth. The gravity on the Moon is 1.6 m/s^2, which is a weaker gravitational field than Earth, about 1/6 that of Earth (0.17 G).

1.2.3. Mars

Mars is the fourth planet in our solar system, next to Earth. It is a rocky planet and is about 228 million kilometers from the Sun, 52% more than Earth. It takes 687 days to make a full orbit. Its mass is 11% of Earth's mass and its diameter is 53% of Earth's diameter. Therefore, it has a weaker

gravitational field than the Earth, about 0.38G (3/8) of it (Kiss, 2014). Mars' red color is due to the fact that it is covered by huge amounts of iron oxides. The composition of the Martian atmosphere is very different from Earth's atmosphere. It consists of 95% carbon dioxide, 2.8% nitrogen, 2% argon and 0.2% other substances. The atmospheric pressure is 0.6% of Earth's (Franz et al., 2017). On Mars, there are pronounced temperature differences. The average surface temperature is about -60°C. At the equator, temperatures of about 20°C are observed, while at the poles the temperature can drop below -150°C. On the surface of Mars, water goes directly from solid to gaseous form. However, there is water in frozen form at the poles, which is covered by a surface layer of frozen carbon dioxide. However, the possibility of liquid water in the subsurface of the planet cannot be ruled out. Per square meter of surface area, Mars receives 44% of the solar power that reaches Earth.

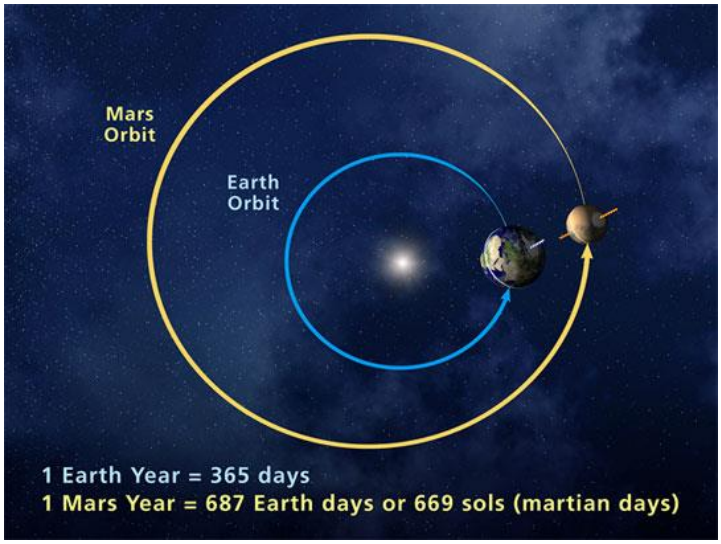

Figure 7. Mars and Earth Orbit (https://twitter.com/NEUDOSE/status/1119354023860166662)

1.2.4. Hohmann Transfer

The transfer between two circular orbits is done most efficiently using the Hohmann (Hohmann, 1925). A Hohmann transfer, named after German engineer Walter Hohmann, is an orbital maneuver commonly used in space travel to transfer a spacecraft between two circular orbits. This transfer is executed by raising the spacecraft's orbit in a more elliptical trajectory until it intersects with the target orbit. Subsequently, the spacecraft performs a burn at the apoapsis (the highest point of the elliptical orbit), increasing its velocity and transitioning to the new circular orbit. This maneuver is particularly efficient in terms of fuel consumption and is widely employed for missions to celestial bodies within our solar system. The Hohmann transfer provides a balanced compromise between energy efficiency and travel time, making it a preferred method for interplanetary missions, such as those to Mars or other distant destinations. In the case of the planetary transfer from Earth to Mars and back, the total duration of a manned mission (with an 11-month stay on Mars), is estimated to be two to three years (Owen et al., 2019).

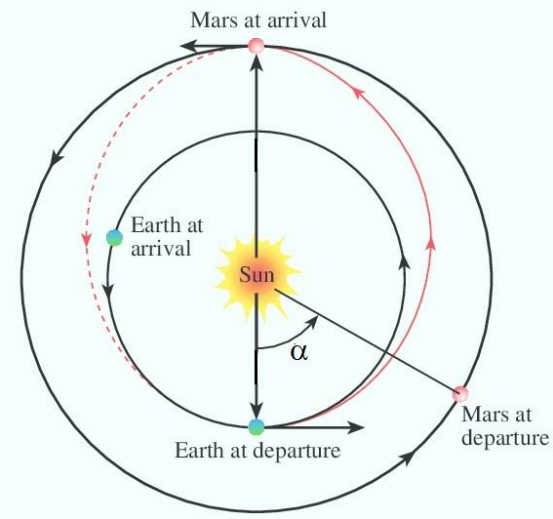

Figure 8. Hohmann transfer orbit between Earth and Mars (https://medium.com/@robertlufkinmd/mars-mission-launch-guide-july-2020-b3941facb3c0)

1.3. DNA

1.3.1. DNA Structure

The structure of DNA, discovered by James Watson and Francis Crick in 1953, is a marvel of molecular architecture that underpins the inheritance of genetic information. DNA is a double helix, resembling a spiraled staircase, composed of two long strands running in opposite directions. Each strand is a chain of nucleotides, with a deoxyribose sugar and a phosphate group forming the backbone. The distinctive rungs of the helical ladder are crafted by pairs of nitrogenous bases – adenine (A) bonds with thymine (T), and guanine (G) pairs with cytosine (C) through hydrogen bonds. This complementary base pairing ensures the stability and specificity of the DNA structure. The antiparallel arrangement of the two strands is a critical feature. One strand runs from 5' to 3', while the other runs from 3' to 5'. This arrangement is vital for processes like DNA replication, where the enzyme DNA polymerase synthesizes a new strand by adding nucleotides in the 5' to 3' direction (Sinden, 1994).

1.3.2. Central Dogma of Molecular Biology

The central dogma of molecular biology is a fundamental framework that outlines the flow of genetic information within a biological system. Proposed by Francis Crick (F. H. Crick, 1958) and later elaborated (F. Crick, 1970), the central dogma describes the sequential processes by which genetic information stored in DNA is used to build proteins and, in some cases, RNA molecules. The central dogma consists of three main stages: Replication, Transcription and Translation. Replication involves the copying of genetic information from DNA to form an identical DNA molecule. It occurs before cell division, ensuring that each daughter cell receives a complete set of genetic instructions. In the transcription stage, genetic information from DNA is transcribed into RNA. RNA, a single-stranded molecule, serves as an intermediary carrier of genetic information. The enzyme RNA polymerase synthesizes an RNA molecule complementary to one strand of the DNA. The final step is the translation of the RNA code into proteins. This occurs at cellular structures called ribosomes, where transfer RNA (tRNA) molecules interpret the RNA code and assemble amino acids in the correct sequence to form a functional protein.

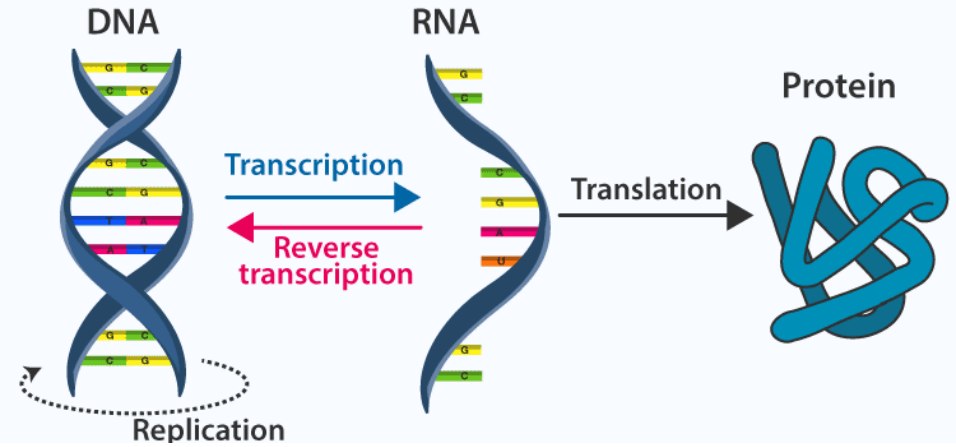

Figure 9. Central Dogma: DNA to RNA to Protein (https://byjus.com/biology/central-dogma-inheritance-mechanism/)

1.3.3. Cell Cycle

A cell cycle is a sequence of events that occurs within a cell as it undergoes growth and division. The majority of a cell's time is spent in a phase known as interphase, during which it grows, duplicates its chromosomes, and prepares itself for cell division. Subsequently, the cell exits interphase, proceeds through mitosis, and concludes its division process. The resulting cells, referred to as daughter cells, each initiate their own interphase, indicating the start of a new cycle of cell division. The term "cell cycle" describes the mechanism by which cells replicate and generate two new cells. This process consists of distinct phases called G1, S, G2, and M. In the G1 phase, the cell prepares for division, followed by entry into the S phase, during which all the DNA is copied, hence the "S" stands for DNA synthesis. After the DNA has been completely duplicated, the cell advances into the G2 phase, where it arranges and condenses the genetic material in preparation for division. The subsequent stage is known as M, that stands for mitosis, where the cell separates the two copies of genetic material into the two daughter cells. Once the M phase is completed, cell division occurs, resulting in the formation of two cells, and the cell cycle can begin again.

1.3.3.1. Cell Cycle Regulation

The regulation of the cell cycle (activation and inhibition) depends on specific checkpoints during the cell cycle, which prevent abnormal activation and continuation of the cell cycle. For example, the G2/M checkpoint ensures that cells containing damaged DNA do not enter the mitotic phase. The regulatory process of the cell cycle is ensured by checkpoints through the coordinated action of Cyclin-Dependent Kinases (CDK -1, -2, -4, -6, -8, -12) that induce the action of a cyclin (heterodimeric protein complexes divided into families (A, B, $D_{1,2,3}$, E) and each family having the responsibility of controlling a different phase) (Funk, 1999).

When the cell is exposed to ionizing radiation, a complex response is activated that includes: the arrest of cell cycle progression in phases G1, S, G2, the process of apoptosis and DNA repair. The delay and/or arrest of the G1 phase seems to be regulated by the activation or not of the tumor suppressor gene TP53 (p53), that acts as a barrier to cell cycle continuation, with two distinct mechanisms (Teyssier, Bay, Dionet, & Verrelle, 1999):

- DNA damage → Activation of p53 → Activation of Cyclin-Dependent Kinase Inhibitor $p21^{WAF1/CIP1}$ (Cyclin-Dependent Kinase Inhibitor - CKI) → Arrest of G1 progression to S phase
- DNA damage → Activation of p53 → Activation of Programmed Cell Death (Apoptosis)

The delay in phase S is observed after relatively high doses of radiation. This delay corresponds to inhibition of DNA replication (Bernhard, Maity, Muschel, & McKenna, 1995).

1.3.4. DNA Damage

DNA damage refers to any alteration in the structure of DNA molecules that deviate from the normal, undamaged state. DNA is susceptible to various forms of damage due to both endogenous factors (internal cellular processes) and exogenous factors (external sources).

1.3.4.1. Single Strand Break

A single-strand break (SSB) is a type of DNA damage that involves the disruption of one of the two complementary strands of the DNA double helix. In simpler terms, it is a break in just one of the DNA strands, leaving the complementary strand intact. Single-strand breaks can occur due to various factors, including exposure to ionizing radiation, certain chemicals, or as a result of normal cellular processes (Shiraishi, Shikazono, Suzuki, Fujii, & Yokoya, 2017). While single-strand breaks are generally less severe than double-strand breaks, they can still impact the normal functioning of the cell. If not repaired promptly and accurately, single-strand breaks can lead to mutations or errors during DNA replication. Cells have mechanisms to repair single-strand breaks, and several repair pathways are involved in fixing this type of DNA damage.

1.3.4.2. Double Strand Break

A double-strand break (DSB) is a more severe form of DNA damage that involves the simultaneous breakage of both complementary strands of the DNA double helix. This type of DNA break is considered more challenging to repair than single strand breaks because it requires the reconnection of broken ends from both strands. Double-strand breaks can occur due to various factors, including exposure to ionizing radiation, certain chemicals, or as a result of errors during DNA replication. Unrepaired or improperly repaired double-strand breaks can lead to chromosomal abnormalities, genomic instability, and may contribute to the development of various genetic disorders, including cancer. Cells have evolved complex mechanisms to repair double-strand breaks. Two main pathways involved in the repair of double-strand breaks are non-homologous end joining (NHEJ) and homologous recombination (HR). NHEJ rejoins the broken ends directly, often introducing small insertions or deletions, while HR uses an undamaged homologous DNA sequence as a template for repair, resulting in more accurate restoration of the DNA sequence (Nikitaki, Michalopoulos, & Georgakilas, 2015).

1.3.4.3. Alteration of a Base

An alteration of a base in the context of genetics and molecular biology refers to a change or modification in one of the nitrogenous bases that make up DNA. DNA is composed of four types of nitrogenous bases: adenine (A), thymine (T), cytosine (C), and guanine (G). These bases form the genetic code that carries instructions for the synthesis of proteins and other cellular functions. An alteration of a base occurs when there is a change in the sequence of DNA due to a substitution, insertion, or deletion of one or more bases (Mavragani et al., 2017). This alteration can be caused by various factors, including exposure to mutagenic agents, errors during DNA replication, or spontaneous chemical changes. There are different types of base alterations, including:

- Point Mutations: A single base is changed, substituted with another base.
- Insertions: One or more bases are added to the DNA sequence.
- Deletions: One or more bases are removed from the DNA sequence.

1.3.4.4. Loss of a Base

The loss of a base, often referred to as an abasic site or an apurinic/apyrimidinic (AP) site, occurs when one of the nitrogenous bases (adenine, thymine, cytosine, or guanine) is spontaneously removed from the DNA sequence. This can happen due to various factors, including exposure to environmental agents, radiation, or chemical reactions. The term "apurinic/apyrimidinic" reflects the

loss of either a purine (adenine or guanine) or a pyrimidine (thymine or cytosine) base from the DNA sequence (Rodriguez-Rocha, Garcia-Garcia, Panayiotidis, & Franco, 2011).

1.3.4.5. Hydrogen Bond Breakage

The hydrogen bond breakage between two chains refers to the disruption of hydrogen bonds that normally hold together the complementary nitrogenous bases on opposite strands of the DNA double helix. DNA consists of two strands that are held together by hydrogen bonds between specific pairs of nitrogenous bases: adenine (A) pairs with thymine (T) through two hydrogen bonds, and guanine (G) pairs with cytosine (C) through three hydrogen bonds. The hydrogen bonds play a crucial role in maintaining the stability and integrity of the DNA double helix (Y. Zhang et al., 2022).

1.3.4.6. Crosslinks

Transverse connections between helices, often referred to as crosslinks, describe the bonds or linkages that occur between the two strands of the double helical structure of DNA. These crosslinks can form covalent or non-covalent connections between the helices, contributing to the stability and structural integrity of the overall molecular complex. In the context of DNA, transverse connections or crosslinks can be induced by various factors, including chemical agents, radiation, or certain cellular processes. These connections can have both natural and artificial origins. Crosslinks can have significant biological implications. In the case of DNA, if the crosslinks are not properly repaired, they can lead to structural distortions, hinder essential cellular functions, and even contribute to genetic mutations or genomic instability (Kojima & Machida, 2020).

1.3.4.7. Chromosome Aberrations

Chromosome aberrations, also known as chromosomal abnormalities or anomalies, refer to structural or numerical abnormalities in the chromosomes. Chromosomes carry genetic information in the form of genes, and any deviation from the normal structure or number can have significant consequences on an individual's health and development. The main types of chromosome aberrations are:

- Structural Chromosome Aberrations:
  - Deletions: A portion of a chromosome is missing or deleted.
  - Duplications: Extra copies of a portion of a chromosome are present.
  - Inversions: A segment of a chromosome is flipped or reversed.
  - Translocations: Parts of two different chromosomes are exchanged.
- Numerical Chromosome Aberrations:
  - Aneuploidy: An abnormal number of chromosomes. It can be trisomy (one extra chromosome) or monosomy (one missing chromosome).
  - Polyploidy: More than two complete sets of chromosomes are present. Triploidy (three sets) or tetraploidy (four sets) are examples.

Chromosome aberrations can be spontaneous or induced by various factors, including:

- Genetic Factors: Inherited genetic mutations.
- Environmental Factors: Exposure to certain chemicals, radiation, or infections during pregnancy (Hada et al., 2018).
- Errors in Cell Division: Mistakes during meiosis (gamete formation) or mitosis (cell division) can lead to chromosome aberrations.

1.3.4.8. Reactive Oxygen Species

Reactive Oxygen Species (ROS) are chemically reactive molecules containing oxygen. They are produced as natural byproducts of normal cellular metabolism, particularly in the mitochondria,

which are the energy-producing organelles within cells. ROS includes free radicals such as superoxide anion, hydroxyl radical, and non-radical species like hydrogen peroxide. Free radicals are atoms, molecules, or ions that have unpaired electrons in their outermost electron shell. The presence of unpaired electrons makes these molecules highly reactive and unstable. Free radicals can be generated through various processes, including exposure to ultraviolet (UV) radiation, environmental pollutants, certain chemicals, and normal cellular metabolism (Nishikawa, 2008).

1.3.5. 1BR-hTERT human fibroblast

Human primary fibroblasts are crucial for maintaining the structural integrity of connective tissue and for the synthesis of extracellular matrix proteins like collagens, glycosaminoglycans, and glycoproteins. The appearance of fibroblasts varies in terms of morphology and is dependent on their in vivo location and activity. In response to tissue damage, fibroblasts are stimulated to generate proteins essential for wound healing. Fibroblasts are mediators in cancer, inflammation, angiogenesis, and pathological tissue fibrosis. They are commonly used in research related to wound healing, tissue engineering, as well as in assisting the growth and establishment of pluripotent stem (iPS) cells. The development of human telomerase reverse transcriptase (hTERT)-immortalized primary cells marks a significant advancement in cell biology research. These cells blend the in vivo characteristics of primary cells with the enduring in vitro survival capacity typically found in traditional cell lines.

1.4. Bioinformatics

1.4.1. RNA-Seq Method

RNA-Seq, short for RNA sequencing, is a next-generation sequencing (NGS) method employed to show the presence and quantity of RNA in a biological sample, indicating an aggregated snapshot of (Chu & Corey, 2012; Z. Wang, Gerstein, & Snyder, 2009).

RNA-Seq analysis involves two primary steps: the in vitro biological experiment and the construction of libraries, followed by in silico computational transcript analysis. The transcript analysis, preparing for the intended library construction, the appropriate RNA fraction encompasses the isolation and preservation of, followed by its conversion into complementary DNA (cDNA). This cDNA synthesis occurs through the enzymatic action of reverse transcriptase (RT) and mRNA priming with deoxynucleotides. The initial cDNA is then synthesized on an RNA template via the reverse transcriptase's activity. Prior to the RNA-Seq technique, the de facto study of gene expression relied on microarrays, based on hybridization. However, due to the limited dynamic range and the necessity for a priori knowledge of transcript sequences, sequencing-based technologies that depend on sequence alignment became necessary. Furthermore, the need for high-throughput data generation led to the obsolescence of Sanger sequencing methods. The most common technique used for validating RNA-Seq data is qPCR.

1.4.2. FASTQ

FASTQ files are a standard format used in bioinformatics to represent nucleotide sequences and their corresponding quality scores. These files are commonly generated by high-throughput sequencing technologies, such as those used in next-generation sequencing (NGS) platforms. A FASTQ file typically contains a series of records, each representing a sequence read along with quality scores for each base in the sequence.
FASTQ files contain 4 distinct lines. Here is a breakdown of the components:

1. Sequence Identifier Line (Header):
    - Begins with '@' character.
    - Contains information about the sequence read, such as an identifier or a label.

2. Sequence Line:

- Contains the nucleotide sequence.

3. Quality Score Header Line:
    - Begins with the '+' character.
    - Optional and often included for human readability but does not carry additional information.

4. Quality Scores Line:
    - Contains ASCII-encoded quality scores for each base in the sequence.
    - Dbdb

ASCII_BASE=33 Illumina, Ion Torrent, PacBio and Sanger

Q	P_error	ASCII	Q	P_error	ASCII	Q	P_error	ASCII	Q	P_error	ASCII
0	1.00000	33 !	11	0.07943	44 ,	22	0.00631	55 7	33	0.00050	66 B
1	0.79433	34 "	12	0.06310	45 -	23	0.00501	56 8	34	0.00040	67 C
2	0.63096	35 #	13	0.05012	46 .	24	0.00398	57 9	35	0.00032	68 D
3	0.50119	36 $	14	0.03981	47 /	25	0.00316	58 :	36	0.00025	69 E
4	0.39811	37 %	15	0.03162	48 0	26	0.00251	59 ;	37	0.00020	70 F
5	0.31623	38 &	16	0.02512	49 1	27	0.00200	60 <	38	0.00016	71 G
6	0.25119	39 '	17	0.01995	50 2	28	0.00158	61 =	39	0.00013	72 H
7	0.19953	40 (	18	0.01585	51 3	29	0.00126	62 >	40	0.00010	73 I
8	0.15849	41)	19	0.01259	52 4	30	0.00100	63 ?	41	0.00008	74 J
9	0.12589	42 *	20	0.01000	53 5	31	0.00079	64 @	42	0.00006	75 K
10	0.10000	43 +	21	0.00794	54 6	32	0.00063	65 A			

Figure 10. Quality (Phred) Scores (https://www.drive5.com/usearch/manual/quality_score.html)

Here is an example of a FASTQ file:

```
@MM123:002:FC123AB:3:2208:3330:9840 2:Y:18:ATCACG
AGGATACTAGCATAGATACCCTAGATAGTCATAGATCATGATAGGGAGATCTA
+
IJJJJJJIIIIIJIIIIIFFFEEEEEDDDDDDCABBBBB@@00))))*(*&%!
```

Figure 11. Example of the sequencing data found in a FASTQ file representing a given read. (https://zymoresearch.eu/blogs/blog/fastq-file-format)

Paired end DNA sequencing provides additional information about the sequence data that is used in sequence assembly, mapping, and other downstream bioinformatics analysis. Paired end reads are usually provided as two FASTQ-format files, with each file representing one end of the read.

1.4.3. qPCR

Quantitative Polymerase Chain Reaction (qPCR) is a molecular biology technique used to amplify and quantify DNA (Deoxyribonucleic Acid) in a sample. PCR itself is a method that allows for the exponential amplification of specific DNA sequences, making it possible to produce a large amount of DNA from a very small initial amount (Mullis, 1990; Saiki et al., 1985). The DNA sample is initially heated to a high temperature (94–98°C), causing the double-stranded DNA to denature into two single strands. In the next step, the temperature is lowered (50–65°C), allowing short DNA sequences called primers to bind to the single-stranded DNA at the target regions. The temperature is raised again (72°C), and a DNA polymerase enzyme synthesizes a new complementary strand for each single-stranded template, effectively duplicating the DNA. A fluorescent dye or probe, such as SYBR Green or TaqMan, is introduced. This dye binds specifically to the newly synthesized DNA during each cycle. Unlike traditional PCR, qPCR allows real-time monitoring of the amplification process. This is done by measuring the fluorescence at each cycle during the PCR reaction. This data is used to generate a quantification curve, correlating the fluorescence intensity with the amount of DNA present and a predetermined fluorescence threshold is set. The cycle at which the fluorescence signal crosses this threshold is used for quantification. The number of cycles needed to reach the threshold is inversely proportional to the initial amount of DNA in the sample. The fewer cycles required, the higher the initial DNA concentration of the target DNA (Mullis, 1990).

2. MATERIALS AND METHODS

2.1. Sample Curation

1BR-hTERT human fibroblast cells were cultured in CO2-independent medium (Thermo Fisher Scientific, Waltham, MA, USA) supplemented with 10% (v/v) fetal bovine serum (MP Biomedicals, Santa Ana, CA, USA), 200 mM L-glutamine (Thermo Fisher Scientific), and penicillin-streptomycin mixed solution (Nacalai Tesque, Kyoto, Kyoto, Japan) at 37°C under 1G or simulated µG for 48 hrs in total. The samples were collected 0 (sham-irradiated), 3 or 24 hrs after X-ray or C-ion irradiation at 1 Gy. X-ray irradiation was performed using an X-ray generator (200 kV, 14.6 mA, aluminum filter (0.3 mm thick), MultiRad225, Faxitron Bioptics, LLC, Tucson, AZ, USA) equipped with a high-speed shutter. C-ion irradiation was performed using a synchrotron (Gunma University Heavy Ion Medical Center (GHMC), Maebashi, Gunma, Japan) and respiratory gating signals with a dose-averaged LET of 50 keV/µm at the center of the 6-cm spread-out Bragg peak of the beam with energy of 290 MeV/. The dose rate was approximately 0.03 Gy/min for both X-ray and C-ion irradiation under the simulated µG or 1G conditions. Simulated µG was accomplished using a three-dimensional clinostat (Hiroko Ikeda et al., 2016; H. Ikeda et al., 2017). This device can manipulate the effect of gravity through the 3D rotation of two orthogonal axes and by continuously changing the direction of gravity. The X:Y ratios of clino-rotation were set at 11:13 rpm and 66°/s:78°/s using a special controller to maintain suitable conditions, which means that it does not use random speed and random direction. The rotation angle between the Z-axis of the 3D clinostat (i.e., the axis of radiation exposure) and the normal line of the sample holder on the 3D clinostat, θ, was kept at less than 12°, assuming the X:Y ratio of the clino-rotation was 11:13 rpm. Because different research groups are performing simulated microgravity experiments under various conditions with different types of simulators and cell line, we think that it is important to carefully consider the experimental conditions and provide details such as simulator limitations in order to avoid misinterpretation of the results (Hauslage, Cevik, & Hemmersbach, 2017). Among such limitations, we use adherent human fibroblasts in a thin culture vessel completely filled with medium (without bubbles) to minimize stress on the cells as much as possible. It is not necessary to change the medium under our simulated microgravity conditions until the sampling. From our previous data of cell growth, which did not differ significantly between rotating and standing conditions after 48 h of culture, we believe that it is unlikely that cells are subjected to shear stress under our experimental conditions using our system The samples were irradiated when in horizontal position, without pausing the rotation, for 0.2 seconds every minute. In total, 12 conditions were studied (Table 1) in triplicate (H. Ikeda et al., 2019).

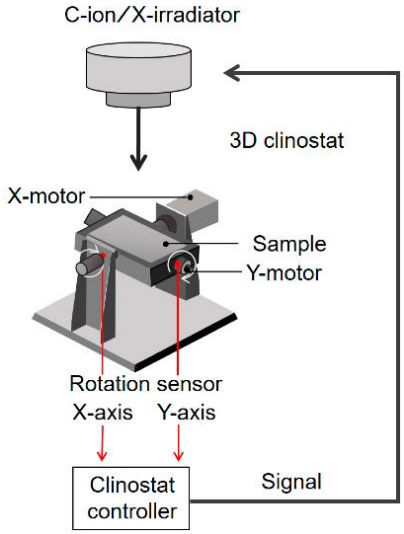

Figure 12. Diagram of 3D clinostat synchronized irradiation systems for examining the combined effects of radiation and simulated µG. (https://www.mdpi.com/1422-0067/20/19/4791)

Table 1. Names and combinations of the type of radiation (C-ion or X-ray), collection time points (0 (sham-irradiated), 3 or 24 hrs) and gravity (1G or simulated μG) for the 12 conditions studied.

Name	Irradiation		Maintenance Time			Gravity	
	C-ion	X-ray	0 hrs	3 hrs	24 hrs	1G	Simulated μG
C0G	-	-	+	-	-	+	-
C0μG	-	-	+	-	-	-	+
C3G	+	-	-	+	-	+	-
C3μG	+	-	-	+	-	-	+
C24G	+	-	-	-	+	+	-
C24μG	+	-	-	-	+	-	+
X0G	-	-	+	-	-	+	-
X0μG	-	-	+	-	-	-	+
X3G	-	+	-	+	-	+	-
X3μG	-	+	-	+	-	-	+
X24G	-	+	-	-	+	+	-
X24μG	-	+	-	-	+	-	+

2.2. RNA-Sequencing

RNA from each of the 36 samples, was extracted using TRIzol™ Reagent (Thermo Fisher Scientific) and its quality was assessed using RNA 6000 Pico Kit (Agilent). rRNA was depleted using NEBNext® rRNA Depletion Kit (New England Biolabs). Then, RNA-Seq library was prepared using NEBNext® Ultra™ Directional RNA Library Prep Kit for Illumina® (New England Biolabs). Paired-end sequencing (2x36bp) was performed with NextSeq500 (Illumina) at Tsukuba i-Laboratory LLP (Ibaraki, Japan) (H. Ikeda et al., 2019). 4 FASTQ files were produced from each sample.

2.3. Data Extraction and Concatenation

A zip file containing the FASTQ files from the RNA-Sequencing was shared through Google Drive and were downloaded and saved using a SanDisk USB and the given passwords needed to access this data. The data was then transferred to the lab's supercomputer (Genome), using FilleZilla. The zip file was then unzipped.

Table 2. The environmental conditions corresponding to each directory.

<table>
<tr><th>Name</th><th colspan="3">Treatment</th></tr>
<tr><td>LAB-014-1</td><td rowspan="9">Standing</td><td rowspan="3">Non-IR</td><td rowspan="3">-</td></tr>
<tr><td>LAB-014-2</td></tr>
<tr><td>LAB-014-3</td></tr>
<tr><td>LAB-014-4</td><td rowspan="6">C-ion</td><td rowspan="3">3h</td></tr>
<tr><td>LAB-014-5</td></tr>
<tr><td>LAB-014-6</td></tr>
<tr><td>LAB-014-7</td><td rowspan="3">24h</td></tr>
<tr><td>LAB-014-8</td></tr>
<tr><td>LAB-014-9</td></tr>
<tr><td>LAB-014-10</td><td>Rotation</td><td>Non-IR</td><td>-</td></tr>
</table>

LAB-014-11			
LAB-014-12			
LAB-014-13		C-ion	3h
LAB-014-14			
LAB-014-15			
LAB-014-16			24h
LAB-014-18			
LAB-014-19			
LAB_109_07	Standing	Non-IR	-
LAB_109_08			
LAB_109_09			
LAB_109_10		X-ray	3h
LAB_109_11			
LAB_109_12			
LAB_109_13			24h
LAB_109_14			
LAB_109_15			
LAB_109_16	Rotation	Non-IR	-
LAB_109_18			
LAB_109_19			
LAB_109_20		X-ray	3h
LAB_109_21			
LAB_109_22			
LAB_109_23			24h
LAB_109_25			
LAB_109_27			

The integrity of each directory was checked, using Ubuntu Linux 22.04 LTS, by opening the Terminal and using the command: “gunzip -t *.gz”.
For example:

```
cd Lab_014/
cd 'LAB_014 fastq'/
cd LAB-014-01-41041/

gunzip -t *.gz
```

This was done another 35 times, until the integrity of all 36 directories were checked.
Each directory contained 8 FASTQ files:

```
LAB-a-i_Si_L001_R1_001.fastq.gz
LAB-a-i_Si_L001_R2_001.fastq.gz
LAB-a-i_Si_L002_R1_001.fastq.gz
LAB-a-i_Si_L002_R2_001.fastq.gz
LAB-a-i_Si_L003_R1_001.fastq.gz
LAB-a-i_Si_L003_R2_001.fastq.gz
LAB-a-i_Si_L004_R1_001.fastq.gz
LAB-a-i_Si_L004_R2_001.fastq.gz
```

, where is an index number ranging from 014 to 109 and i the number that corresponds to each directory.
The FASTQ files come from paired end DNA sequencing since there are two FASTQ files (R1 and R2) for each DNA fragment.
The FASTQ files of each direction were concatenated by creating 2 FASTQ files instead of 8, for each directory. This was done by concatenating all reads from one strand together (R1) and all reads from the other strand together (R2).
For example:

```
zcat LAB-014-1_S1_L001_R1_001.fastq.gz LAB-014-1_S1_L002_R1_001.fastq.gz LAB-014-1_S1_L003_R1_001.fastq.gz LAB-014-1_S1_L004_R1_001.fastq.gz | concatenate.php | gzip > LAB-014-1_S1_R1_001.fastq.gz &

zcat LAB-014-1_S1_L001_R2_001.fastq.gz LAB-014-1_S1_L002_R2_001.fastq.gz LAB-014-1_S1_L003_R2_001.fastq.gz LAB-014-1_S1_L004_R2_001.fastq.gz | concatenate.php | gzip > LAB-014-1_S1_R2_001.fastq.gz &
```

This was done for all directories by using the in-house script “concatenate” written. This program imports the content of all 4 FASTQ files and exports it as one conjoined FASTQ file. Using the command gzip >, conjoined FASTQ file is then saved. The “concatenate” script is presented below:

```
<?php
while(!feof(STDIN)){
   $line = fgets(STDIN);
   $line = rtrim($line);
   if($line) {
         echo "$line\n";
   }
}
?>
```

2.4. Differentially Expressed Gene Analysis

After FASTQ files of each sample were concatenated, and the integrity of the resulting files was checked, quality control and alignment of their reads were carried out via the RNA-seq workflow from the bcbio-nextgen bioinformatics framework (version 1.2.9) (Chapman et al., 2021) (Figure 13). To ensure that the library generation and sequencing quality were suitable for further analysis, FastQC (Andrews, 2010) was used to examine the raw reads for quality issues. Then, raw reads were aligned to the GRCh38 (hg38) version of the human reference genome (FASTA and GTF files) with the splice-aware aligner STAR (version 2.6.1d) in two-pass mode (the first pass discovers new splice junctions and inserts them into the junction database, and the second pass calls junctions and calculates their counts) (Dobin et al., 2013). Moreover, Salmon (version 1.7.0) was run in alignment-based mode, using the genome alignments from STAR (BAM files) and the reference transcriptome FASTA file, to generate abundance estimates for known splice isoforms (Patro, Duggal, Love, Irizarry, & Kingsford, 2017). Bcbio assessed the complexity and quality of the RNA-seq data by quantifying ribosomal RNA (rRNA) content and the genomic context of alignments in known transcripts and introns using a combination of custom tools and Qualimap (García-Alcalde et al., 2012). MultiQC (Ewels, Magnusson, Lundin, & Käller, 2016) was then used for quality control and assurance analysis of the resulting BAM files by comparing to metrics gathered from bcbio-nextgen, samtools (H. Li et al., 2009), Salmon, STAR, Qualimap and FastQC. Next, we quantitated reads by assigning them to genes (features) annotated in Ensembl (release 105) and counting them with the featureCounts tool (Yang Liao, Smyth, & Shi, 2013) or preferably tximport (Soneson, Love, & Robinson, 2016). Gene counts were processed for DGEA, using DESeq2 (version 1.38.2) (Love, Huber, & Anders, 2014) default settings through the bcbioRNASeq R package (version 0.5.1) (Steinbaugh et al., 2018) (Figure 13). Moreover, log fold change shrinkage for visualization and ranking was performed calling the lfcShrink function of the DESeq2 package, replacing p-values with s-values produced by the apeglm estimation method (A. Zhu, Ibrahim, & Love, 2018). S-value was proposed as a statistic giving the aggregate false sign rate for tests with equal or lower s-value than the one considered (Stephens, 2016). Exported lists containing statistically significant differentially expressed genes (DEGs) include metrics such as Log2 Fold Change (Log2FC) and s-values for each gene. The lists were further annotated by bcbioRNASeq to include HGNC (Seal et al., 2023) gene symbols and names. The threshold for statistical significance was set at s-value < 0.001, as suggested (A. Zhu, Ibrahim, & Love, 2022). Using this method, the statistically significant differentially expressed genes between various pairs of biological conditions (Table 3) were identified (Malatesta et al., 2024).

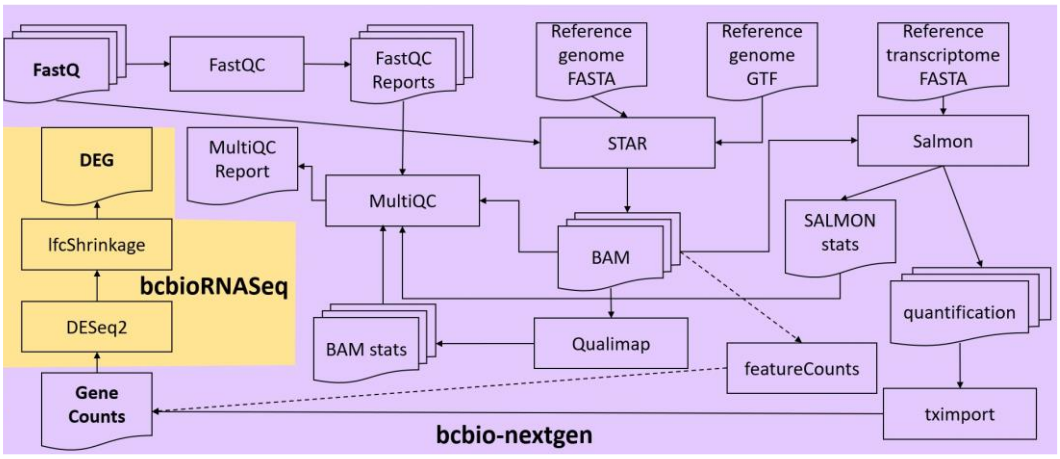

Figure 13. RNA-seq Analysis Pipeline. Gene counts were produced from FASTQ files, through the bcbio-nextgen pipeline (in lavender background). Lists of differentially expressed genes were produced through the bcbioRNASeq pipeline (in peach background).

Table 3. Comparisons between biological conditions that were analyzed to identify the statistically significant differentially expressed genes.

Comparisons	Description
X3G-X0G	Early response to X-ray under 1G
X3µG-X0µG	Early response to X-ray under µG
X0µG-X0G	Response to µG in sham-X-ray-irradiated cells
X3µG-X3G	Response to µG in cells collected 3 hrs after X-ray-irradiation
(X3µG-X0µG)-(X3G-X0G)	Interaction between early response to X-ray and response to µG
X24G-X0G	Late response to X-ray under 1G
X24µG-X0µG	Late response to X-ray under µG
X24µG-X24G	Response to µG in cells collected 24 hrs after X-ray-irradiation
(X24µG-X0µG)-(X24G-X0G)	Interaction between late response to X-ray and response to µG
X24G-X3G	Late vs early response to X-ray under 1G
X24µG-X3µG	Late vs early response to X-ray under µG
(X24µG-X3µG)-(X24G-X3G)	Interaction between late vs early response to X-ray and response to µG
X3µG-X0G	Early response to X-ray irradiation and µG combined effect
X24µG-X0G	Late response to X-ray irradiation and µG combined effect
C3G-C0G	Early response to C-ion under 1G
C3µG-C0µG	Early response to C-ion under µG
C0µG-C0G	Response to µG in sham-C-ion-irradiated cells
C3µG-C3G	Response to µG in cells collected 3 hrs after C-ion-irradiation
(C3µG-C0µG)-(C3G-C0G)	Interaction between early response to C-ion and response to µG
C24G-C0G	Late response to C-ion under 1G
C24µG-C0µG	Late response to C-ion under µG
C24µG-C24G	Response to µG in cells collected 24 hrs after C-ion-irradiation
(C24µG-C0µG)-(C24G-C0G)	Interaction between late response to C-ion and response to µG
C24G-C3G	Late vs early response to C-ion under 1G
C24µG-C3µG	Late vs early response to C-ion under µG
(C24µG-C3µG)-(C24G-C3G)	Interaction between late vs early response to C-ion and response to µG
C3µG-C0G	Early response to C-ion irradiation and µG combined effect
C24µG-C0G	Late response to C-ion irradiation and µG combined effect

2.5. Biological Term Enrichment Analysis

Gene term enrichment analyses were performed to identify the prevalent biological processes and pathways over- and under-expressed genes of each DEG analysis, participate in, using WebGestalt (Y. Liao, Wang, Jaehnig, Shi, & Zhang, 2019). Over-Representation Analysis (ORA) method (Khatri, Sirota, & Butte, 2012) was employed, applying BH (Benjamini & Hochberg, 1995) multiple test adjustment. The threshold for statistical significance was set at false discovery rate (FDR) < 0.05. The functional databases that were used for biological term enrichment, were Biological Process, Cellular Component and Molecular Function from Gene Ontology (Gene Ontology Consortium, 2023), KEGG (Kanehisa, Furumichi, Sato, Kawashima, & Ishiguro-Watanabe, 2023) and Transcription Factor Targeting and miRNA Targeting networks from MSigDB (Liberzon et al., 2015). In order to identify and depict overlapping genes or biological terms between comparisons of conditions, Venn diagrams were produced using a webtool developed by the Bioinformatics & Evolutionary Genomics group of Ghent University (https://bioinformatics.psb.ugent.be/webtools/Venn/).

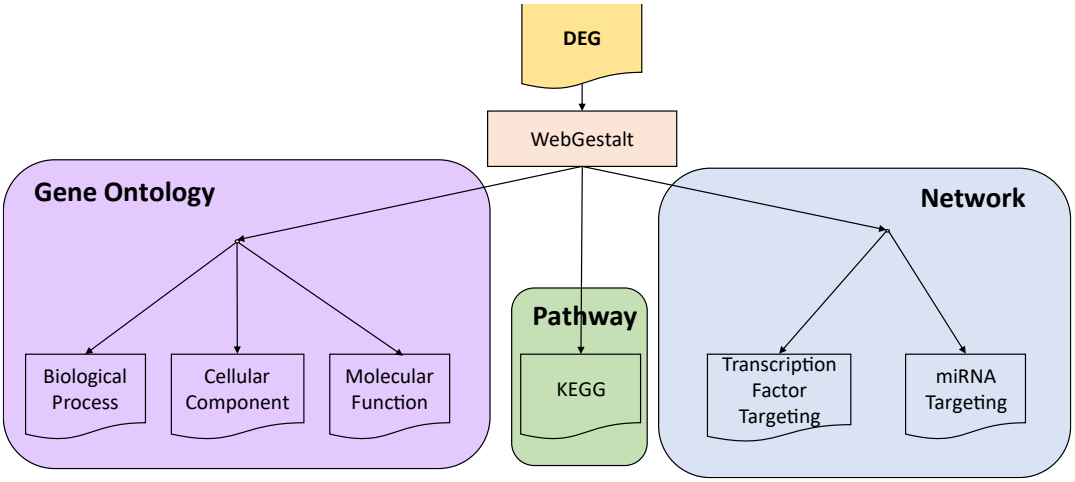

Figure 14. Gene term enrichment analyses using WebGestalt.

2.6. Protein-Protein Interaction Network Analysis

STRING (Szklarczyk et al., 2022) based protein-protein interaction (PPI) network analyses were performed for the DEGs and PPI networks were constructed for each DEG analysis from all comparisons in order to discover their functional associations. The average local clustering coefficient (Watts & Strogatz, 1998) served as a measure of how connected the produced PPI networks were and PPI enrichment p-values provide the probability to get the observed number of edges by chance. To identify the hub genes of the PPI networks, i.e. the genes with the highest degree of connectivity, the interactions of each gene were counted and genes with the highest number of edges were pinpointed.

3. RESULTS

Lists of up- and down regulated genes were produced through the DEG analysis from all comparisons between two different biological conditions and subsequently, biological term over-representation analyses were performed.

3.1. Early response genes to X-ray irradiation under 1G

From the comparison between X-ray (low LET) irradiated cells collected 3 hrs post-irradiation and sham-irradiated ones under 1G (X3G-X0G), 112 over-expressed genes were found in total, and among them, *CDKN1A*, *MDM2*, *PURPL*, *PTCHD4*, *TP53INP1*, *PAPPA* and *BTG2* stood out. In particular, the expression of *CDKN1A* and *MDM2* had approximately quadrupled. Likewise, 108 genes were found to be statistically significant under-expressed ones. Down-regulated genes *FAM111B*, *ZNF367* and *MCM10* stood out. Concerning the over-expressed genes, enrichment analyses for Gene Ontology biological processes and KEGG pathways highlighted the p53 signaling pathway. Biological processes related to response to stimulus and apoptosis were also identified. Focusing on under-expressed genes, biological term over-representation analyses in all Gene Ontology aspects, as well as in KEGG pathways, highlighted cell cycle and carcinogenesis related terms. E2F was identified as a transcription factor targeting down-regulated genes.

Table 4. Top up-regulated genes from the comparison between X-ray irradiated cells collected 3 hrs post-irradiation and sham-irradiated ones under 1G.

Gene Id	Gene Name	Description	svalue
ENSG00000124762	*CDKN1A*	cyclin dependent kinase inhibitor 1A [Source:HGNC Symbol;Acc:HGNC:1784]	1.21E-75
ENSG00000135679	*MDM2*	MDM2 proto-oncogene [Source:HGNC Symbol;Acc:HGNC:6973]	7.16E-68
ENSG00000256664	*NA*	ribosomal L24 domain containing 1 (RSL24D1) pseudogene	4.01E-36
ENSG00000250337	*PURPL*	p53 upregulated regulator of p53 levels [Source:HGNC Symbol;Acc:HGNC:48995]	2.38E-31
ENSG00000244694	*PTCHD4*	patched domain containing 4 [Source:HGNC Symbol;Acc:HGNC:21345]	9.41E-25
ENSG00000164938	*TP53INP1*	tumor protein p53 inducible nuclear protein 1 [Source:HGNC Symbol;Acc:HGNC:18022]	6.40E-21
ENSG00000182752	*PAPPA*	pappalysin 1 [Source:HGNC Symbol;Acc:HGNC:8602]	1.80E-20
ENSG00000048392	*RRM2B*	ribonucleotide reductase regulatory TP53 inducible subunit M2B [Source:HGNC Symbol;Acc:HGNC:17296]	9.02E-19
ENSG00000159388	*BTG2*	BTG anti-proliferation factor 2 [Source:HGNC Symbol;Acc:HGNC:1131]	2.57E-18
ENSG00000028277	*POU2F2*	POU class 2 homeobox 2 [Source:HGNC Symbol;Acc:HGNC:9213]	2.86E-17
ENSG00000172667	*ZMAT3*	zinc finger matrin-type 3 [Source:HGNC Symbol;Acc:HGNC:29983]	2.79E-15
ENSG00000161513	*FDXR*	ferredoxin reductase [Source:HGNC Symbol;Acc:HGNC:3642]	5.44E-15
ENSG00000080546	*SESN1*	sestrin 1 [Source:HGNC Symbol;Acc:HGNC:21595]	1.24E-14
ENSG00000174307	*PHLDA3*	pleckstrin homology like domain family A member 3 [Source:HGNC Symbol;Acc:HGNC:8934]	1.67E-14
ENSG00000120889	*TNFRSF10B*	TNF receptor superfamily member 10b [Source:HGNC Symbol;Acc:HGNC:11905]	1.07E-13
ENSG00000154767	*XPC*	XPC complex subunit, DNA damage recognition and repair factor [Source:HGNC Symbol;Acc:HGNC:12816]	5.48E-13
ENSG00000026103	*FAS*	Fas cell surface death receptor [Source:HGNC Symbol;Acc:HGNC:11920]	1.65E-12
ENSG00000164125	*GASK1B*	golgi associated kinase 1B [Source:HGNC Symbol;Acc:HGNC:25312]	1.62E-11
ENSG00000130513	*GDF15*	growth differentiation factor 15 [Source:HGNC Symbol;Acc:HGNC:30142]	3.48E-11
ENSG00000168497	*CAVIN2*	caveolae associated protein 2 [Source:HGNC Symbol;Acc:HGNC:10690]	1.30E-10

Table 5. Top down-regulated genes from the comparison between X-ray irradiated cells collected 3 hrs post-irradiation and sham-irradiated ones under 1G.

Gene Id	Gene Name	Description	svalue
ENSG00000285920	*NA*	novel protein	8.97E-15
ENSG00000189057	*FAM111B*	FAM111 trypsin like peptidase B [Source:HGNC Symbol;Acc:HGNC:24200]	6.57E-11
ENSG00000165244	*ZNF367*	zinc finger protein 367 [Source:HGNC Symbol;Acc:HGNC:18320]	9.55E-11
ENSG00000270882	*H4C14*	H4 clustered histone 14 [Source:HGNC Symbol;Acc:HGNC:4794]	1.85E-08
ENSG00000130816	*DNMT1*	DNA methyltransferase 1 [Source:HGNC Symbol;Acc:HGNC:2976]	2.61E-08
ENSG00000065328	*MCM10*	minichromosome maintenance 10 replication initiation factor [Source:HGNC Symbol;Acc:HGNC:18043]	3.14E-08
ENSG00000168411	*RFWD3*	ring finger and WD repeat domain 3 [Source:HGNC Symbol;Acc:HGNC:25539]	3.66E-08
ENSG00000094804	*CDC6*	cell division cycle 6 [Source:HGNC Symbol;Acc:HGNC:1744]	4.97E-08
ENSG00000100297	*MCM5*	minichromosome maintenance complex component 5 [Source:HGNC Symbol;Acc:HGNC:6948]	8.74E-08
ENSG00000167670	*CHAF1A*	chromatin assembly factor 1 subunit A [Source:HGNC Symbol;Acc:HGNC:1910]	1.15E-07
ENSG00000276043	*UHRF1*	ubiquitin like with PHD and ring finger domains 1 [Source:HGNC Symbol;Acc:HGNC:12556]	3.72E-07
ENSG00000118655	*DCLRE1B*	DNA cross-link repair 1B [Source:HGNC Symbol;Acc:HGNC:17641]	5.78E-07
ENSG00000277157	*H4C4*	H4 clustered histone 4 [Source:HGNC Symbol;Acc:HGNC:4782]	8.05E-07
ENSG00000197312	*DDI2*	DNA damage inducible 1 homolog 2 [Source:HGNC Symbol;Acc:HGNC:24578]	1.06E-06
ENSG00000140534	*TICRR*	TOPBP1 interacting checkpoint and replication regulator [Source:HGNC Symbol;Acc:HGNC:28704]	1.36E-06
ENSG00000286522	*H3C2*	H3 clustered histone 2 [Source:HGNC Symbol;Acc:HGNC:4776]	1.65E-06
ENSG00000196787	*H2AC11*	H2A clustered histone 11 [Source:HGNC Symbol;Acc:HGNC:4737]	1.95E-06
ENSG00000147526	*TACC1*	transforming acidic coiled-coil containing protein 1 [Source:HGNC Symbol;Acc:HGNC:11522]	2.62E-06
ENSG00000161547	*SRSF2*	serine and arginine rich splicing factor 2 [Source:HGNC Symbol;Acc:HGNC:10783]	3.53E-06
ENSG00000180596	*H2BC4*	H2B clustered histone 4 [Source:HGNC Symbol;Acc:HGNC:4757]	6.48E-06

Table 6. Top biological processes from over-representation analyses on up-regulated genes from the comparison between X-ray irradiated cells collected 3 hrs post-irradiation and sham-irradiated ones under 1G.

Gene Set	Description	P Value	FDR
GO:0072331	signal transduction by p53 class mediator	2.42E-09	2.94E-05
GO:0033554	cellular response to stress	1.70E-08	0.000104
GO:0006950	response to stress	4.97E-08	0.000181
GO:0006974	cellular response to DNA damage stimulus	5.93E-08	0.000181
GO:0050896	response to stimulus	4.03E-07	0.000981
GO:0030330	DNA damage response, signal transduction by p53 class mediator	5.52E-07	0.001119
GO:0035556	intracellular signal transduction	1.12E-06	0.001944
GO:0009628	response to abiotic stimulus	1.57E-06	0.002386
GO:0097193	intrinsic apoptotic signaling pathway	1.99E-06	0.002686
GO:0042770	signal transduction in response to DNA damage	2.88E-06	0.003104
GO:0071214	cellular response to abiotic stimulus	3.06E-06	0.003104
GO:0104004	cellular response to environmental stimulus	3.06E-06	0.003104
GO:0051716	cellular response to stimulus	8.22E-06	0.007698
GO:0045862	positive regulation of proteolysis	9.03E-06	0.00785

GO:0072332	intrinsic apoptotic signaling pathway by p53 class mediator	1.21E-05	0.009809
GO:0031331	positive regulation of cellular catabolic process	1.41E-05	0.010737
GO:0006915	apoptotic process	1.73E-05	0.012388
GO:0034644	cellular response to UV	2.04E-05	0.013774
GO:0012501	programmed cell death	3.3E-05	0.021132
GO:0008219	cell death	3.58E-05	0.021395

Table 7. Top biological processes from over-representation analyses on down-regulated genes from the comparison between X-ray irradiated cells collected 3 hrs post-irradiation and sham-irradiated ones under 1G.

Gene Set	Description	P Value	FDR
GO:0007049	cell cycle	<2.2e-16	<2.2e-16
GO:1903047	mitotic cell cycle process	5.55E-16	3.38E-12
GO:0006270	DNA replication initiation	3.33E-15	1.25E-11
GO:0000278	mitotic cell cycle	4.11E-15	1.25E-11
GO:0000082	G1/S transition of mitotic cell cycle	2.51E-14	6.11E-11
GO:0051276	chromosome organization	5.26E-14	1.07E-10
GO:0044843	cell cycle G1/S phase transition	6.97E-14	1.21E-10
GO:0022402	cell cycle process	1.50E-13	2.28E-10
GO:0006261	DNA-dependent DNA replication	3.26E-13	4.19E-10
GO:0006259	DNA metabolic process	3.44E-13	4.19E-10
GO:0006260	DNA replication	4.21E-13	4.66E-10
GO:0044772	mitotic cell cycle phase transition	7.36E-13	7.47E-10
GO:0044770	cell cycle phase transition	2.85E-12	2.66E-09
GO:0071103	DNA conformation change	9.89E-11	8.60E-08
GO:0031497	chromatin assembly	1.14E-10	9.23E-08
GO:0065004	protein-DNA complex assembly	1.91E-10	1.45E-07
GO:0051726	regulation of cell cycle	3.38E-10	2.42E-07
GO:0006334	nucleosome assembly	4.29E-10	2.90E-07
GO:0006333	chromatin assembly or disassembly	9.17E-10	5.88E-07
GO:0071824	protein-DNA complex subunit organization	1.16E-09	7.05E-07

Table 8. Top molecular functions from over-representation analyses on down-regulated genes from the comparison between X-ray irradiated cells collected 3 hrs post-irradiation and sham-irradiated ones under 1G.

Gene Set	Description	P Value	FDR
GO:0003677	DNA binding	6.01E-09	1.78E-05
GO:0003676	nucleic acid binding	4.30E-07	0.000636
GO:0003688	DNA replication origin binding	3.22E-06	0.003174
GO:0005515	protein binding	5.28E-06	0.003902
GO:1901363	heterocyclic compound binding	1.15E-05	0.006811
GO:0097159	organic cyclic compound binding	1.64E-05	0.007075
GO:0019899	enzyme binding	1.68E-05	0.007075
GO:0003682	chromatin binding	2.72E-05	0.010035
GO:0003690	double-stranded DNA binding	5.79E-05	0.019004
GO:0046982	protein heterodimerization activity	0.000114	0.033772
GO:0019900	kinase binding	0.000163	0.042404
GO:0046983	protein dimerization activity	0.000172	0.042404

Table 9. Top cellular component from over-representation analyses on down-regulated genes from the comparison between X-ray irradiated cells collected 3 hrs post-irradiation and sham-irradiated ones under 1G.

Gene Set	Description	P Value	FDR
GO:0005694	chromosome	<2.2e-16	<2.2e-16
GO:0044427	chromosomal part	<2.2e-16	<2.2e-16
GO:0000785	chromatin	4.27E-13	2.29E-10
GO:0031981	nuclear lumen	5.50E-13	2.29E-10
GO:0044454	nuclear chromosome part	8.93E-13	2.53E-10
GO:0000786	nucleosome	9.12E-13	2.53E-10
GO:0005654	nucleoplasm	2.98E-12	6.56E-10
GO:0000228	nuclear chromosome	3.31E-12	6.56E-10
GO:0044428	nuclear part	3.76E-12	6.56E-10
GO:0044815	DNA packaging complex	3.94E-12	6.56E-10
GO:0005634	nucleus	4.13E-11	6.25E-09
GO:0032993	protein-DNA complex	8.18E-11	1.14E-08
GO:0031974	membrane-enclosed lumen	5.24E-10	5.82E-08
GO:0043233	organelle lumen	5.24E-10	5.82E-08
GO:0070013	intracellular organelle lumen	5.24E-10	5.82E-08
GO:0098687	chromosomal region	7.67E-10	7.98E-08
GO:0043232	intracellular non-membrane-bounded organelle	1.14E-09	1.12E-07
GO:0043228	non-membrane-bounded organelle	1.24E-09	1.15E-07
GO:0042555	MCM complex	3.61E-09	3.17E-07
GO:0000781	chromosome, telomeric region	1.34E-07	1.12E-05

Table 10. Top KEGG pathways from over-representation analyses on up-regulated genes from the comparison between X-ray irradiated cells collected 3 hrs post-irradiation and sham-irradiated ones under 1G.

Gene Set	Description	P Value	FDR
hsa04115	p53 signaling pathway	1.11E-15	3.65E-13
hsa01524	Platinum drug resistance	4.07E-08	6.7E-06

Table 11. Top KEGG pathways from over-representation analyses on down-regulated genes from the comparison between X-ray irradiated cells collected 3 hrs post-irradiation and sham-irradiated ones under 1G.

Gene Set	Description	P Value	FDR
hsa05034	Alcoholism	<2.2e-16	<2.2e-16
hsa05322	Systemic lupus erythematosus	<2.2e-16	<2.2e-16
hsa05203	Viral carcinogenesis	1.98E-09	2.17E-07
hsa04110	Cell cycle	8.97E-07	0.00007377
hsa03030	DNA replication	0.000057062	0.0037547
hsa05206	MicroRNAs in cancer	0.00021987	0.012056
hsa05202	Transcriptional misregulation in cancer	0.00040318	0.018949

3.2. Late response genes to X-ray irradiation under 1G

From the comparison between X-ray irradiated cells collected 24 hrs post-irradiation (late response) and sham-irradiated ones under 1G (X24G-X0G), 571 up- and 1026 down-regulated genes were found. Over-expressed genes *PURPL*, *PTCHD4* and *PAPPA* were found to be predominant. *PURPL* for

example suppresses basal p53 levels and promotes tumorigenicity in colorectal cancer (X. L. Li et al., 2017). Enrichment analyses in all Gene Ontology aspects highlighted terms related to cell proliferation and cardiovascular system development, such as angiogenesis. The main KEGG pathway identified was as rather expected the p53 signaling pathway indicating the response to varying types of stresses like radiation, hypoxia, oxidative attack (Pflaum, Schlosser, & Müller, 2014) and even simulated µG (Shi et al., 2021). FOXO4 was identified as transcription factor controlling the expression of up-regulated genes. Among the down-regulated genes, many stood out. A few were *MKI67*, *ASPM*, *CENPF*, *ANLN*, *CDC20*, *DLGAP5*, *CCNB1*, *CEP55* and *PLK1*. Enrichment analyses in all Gene Ontology domains, as well as in KEGG pathways, highlighted cell cycle and DNA repair related terms. E2F was found to control the expression of down-regulated genes.

Table 12. Top up-regulated genes from the comparison between X-ray irradiated cells collected 24 hrs post-irradiation and sham-irradiated ones under 1G.

Gene Id	Gene Name	Description	svalue
ENSG00000250337	*PURPL*	p53 upregulated regulator of p53 levels [Source:HGNC Symbol;Acc:HGNC:48995]	1.49E-25
ENSG00000127241	*MASP1*	MBL associated serine protease 1 [Source:HGNC Symbol;Acc:HGNC:6901]	1.16E-22
ENSG00000244694	*PTCHD4*	patched domain containing 4 [Source:HGNC Symbol;Acc:HGNC:21345]	9.09E-22
ENSG00000182752	*PAPPA*	pappalysin 1 [Source:HGNC Symbol;Acc:HGNC:8602]	6.53E-20
ENSG00000124762	*CDKN1A*	cyclin dependent kinase inhibitor 1A [Source:HGNC Symbol;Acc:HGNC:1784]	1.73E-17
ENSG00000048392	*RRM2B*	ribonucleotide reductase regulatory TP53 inducible subunit M2B [Source:HGNC Symbol;Acc:HGNC:17296]	3.64E-17
ENSG00000170581	*STAT2*	signal transducer and activator of transcription 2 [Source:HGNC Symbol;Acc:HGNC:11363]	4.81E-15
ENSG00000255248	*MIR100HG*	mir-100-let-7a-2-mir-125b-1 cluster host gene [Source:HGNC Symbol;Acc:HGNC:39522]	9.98E-15
ENSG00000135919	*SERPINE2*	serpin family E member 2 [Source:HGNC Symbol;Acc:HGNC:8951]	2.03E-13
ENSG00000136542	*GALNT5*	polypeptide N-acetylgalactosaminyltransferase 5 [Source:HGNC Symbol;Acc:HGNC:4127]	4.77E-13
ENSG00000172667	*ZMAT3*	zinc finger matrin-type 3 [Source:HGNC Symbol;Acc:HGNC:29983]	6.67E-12
ENSG00000135679	*MDM2*	MDM2 proto-oncogene [Source:HGNC Symbol;Acc:HGNC:6973]	8.69E-12
ENSG00000132274	*TRIM22*	tripartite motif containing 22 [Source:HGNC Symbol;Acc:HGNC:16379]	1.67E-11
ENSG00000142089	*IFITM3*	interferon induced transmembrane protein 3 [Source:HGNC Symbol;Acc:HGNC:5414]	4.15E-11
ENSG00000140443	*IGF1R*	insulin like growth factor 1 receptor [Source:HGNC Symbol;Acc:HGNC:5465]	6.88E-11
ENSG00000185088	*RPS27L*	ribosomal protein S27 like [Source:HGNC Symbol;Acc:HGNC:18476]	1.96E-10
ENSG00000119938	*PPP1R3C*	protein phosphatase 1 regulatory subunit 3C [Source:HGNC Symbol;Acc:HGNC:9293]	2.10E-10
ENSG00000164938	*TP53INP1*	tumor protein p53 inducible nuclear protein 1 [Source:HGNC Symbol;Acc:HGNC:18022]	3.32E-10
ENSG00000105270	*CLIP3*	CAP-Gly domain containing linker protein 3 [Source:HGNC Symbol;Acc:HGNC:24314]	3.52E-10
ENSG00000154736	*ADAMTS5*	ADAM metallopeptidase with thrombospondin type 1 motif 5 [Source:HGNC Symbol;Acc:HGNC:221]	5.10E-10

Table 13. Top down-regulated genes from the comparison between X-ray irradiated cells collected 24 hrs post-irradiation and sham-irradiated ones under 1G.

Gene Id	Gene Name	description	svalue
ENSG00000148773	*MKI67*	marker of proliferation Ki-67 [Source:HGNC Symbol;Acc:HGNC:7107]	5.26E-88
ENSG00000066279	*ASPM*	assembly factor for spindle microtubules [Source:HGNC Symbol;Acc:HGNC:19048]	1.90E-78
ENSG00000117724	*CENPF*	centromere protein F [Source:HGNC Symbol;Acc:HGNC:1857]	7.24E-78
ENSG00000011426	*ANLN*	anillin actin binding protein [Source:HGNC Symbol;Acc:HGNC:14082]	8.75E-75
ENSG00000117399	*CDC20*	cell division cycle 20 [Source:HGNC Symbol;Acc:HGNC:1723]	1.13E-63
ENSG00000131747	*TOP2A*	DNA topoisomerase II alpha [Source:HGNC Symbol;Acc:HGNC:11989]	2.80E-62
ENSG00000126787	*DLGAP5*	DLG associated protein 5 [Source:HGNC Symbol;Acc:HGNC:16864]	8.34E-62
ENSG00000183856	*IQGAP3*	IQ motif containing GTPase activating protein 3 [Source:HGNC Symbol;Acc:HGNC:20669]	8.95E-60
ENSG00000088325	*TPX2*	TPX2 microtubule nucleation factor [Source:HGNC Symbol;Acc:HGNC:1249]	3.74E-58
ENSG00000134057	*CCNB1*	cyclin B1 [Source:HGNC Symbol;Acc:HGNC:1579]	1.46E-53
ENSG00000138180	*CEP55*	centrosomal protein 55 [Source:HGNC Symbol;Acc:HGNC:1161]	3.01E-53
ENSG00000198901	*PRC1*	protein regulator of cytokinesis 1 [Source:HGNC Symbol;Acc:HGNC:9341]	5.49E-53
ENSG00000136108	*CKAP2*	cytoskeleton associated protein 2 [Source:HGNC Symbol;Acc:HGNC:1990]	2.55E-52
ENSG00000166851	*PLK1*	polo like kinase 1 [Source:HGNC Symbol;Acc:HGNC:9077]	1.04E-50
ENSG00000182481	*KPNA2*	karyopherin subunit alpha 2 [Source:HGNC Symbol;Acc:HGNC:6395]	3.88E-49
ENSG00000120802	*TMPO*	thymopoietin [Source:HGNC Symbol;Acc:HGNC:11875]	1.72E-48
ENSG00000138778	*CENPE*	centromere protein E [Source:HGNC Symbol;Acc:HGNC:1856]	6.35E-48
ENSG00000013810	*TACC3*	transforming acidic coiled-coil containing protein 3 [Source:HGNC Symbol;Acc:HGNC:11524]	1.09E-47
ENSG00000184357	*H1-5*	H1.5 linker histone, cluster member [Source:HGNC Symbol;Acc:HGNC:4719]	2.48E-47
ENSG00000286522	*H3C2*	H3 clustered histone 2 [Source:HGNC Symbol;Acc:HGNC:4776]	6.66E-47

Table 14. Top biological processes from over-representation analyses on up-regulated genes from the comparison between X-ray irradiated cells collected 24 hrs post-irradiation and sham-irradiated ones under 1G.

Gene Set	Description	P Value	FDR
GO:0030198	extracellular matrix organization	<2.2e-16	<2.2e-16
GO:0043062	extracellular structure organization	3.33E-16	2.03E-12
GO:0072358	cardiovascular system development	1.15E-12	4.68E-09
GO:0001944	vasculature development	2.19E-12	6.48E-09
GO:0009888	tissue development	2.70E-12	6.48E-09
GO:0001568	blood vessel development	3.20E-12	6.48E-09
GO:0042127	regulation of cell proliferation	5.25E-12	9.14E-09
GO:0008283	cell proliferation	8.47E-12	1.29E-08
GO:0048514	blood vessel morphogenesis	1.73E-11	2.35E-08
GO:0035295	tube development	4.00E-11	4.87E-08
GO:0035239	tube morphogenesis	6.33E-11	7.01E-08
GO:0050896	response to stimulus	1.94E-10	1.97E-07
GO:0072359	circulatory system development	3.14E-10	2.94E-07
GO:0008285	negative regulation of cell proliferation	6.06E-10	5.27E-07
GO:0030199	collagen fibril organization	1.53E-09	1.24E-06
GO:0048519	negative regulation of biological process	3.27E-09	2.49E-06
GO:0016477	cell migration	5.88E-09	4.21E-06

GO:0001525	angiogenesis	6.51E-09	4.41E-06
GO:0048870	cell motility	9.60E-09	5.85E-06
GO:0051674	localization of cell	9.60E-09	5.85E-06

Table 15. Top biological processes from over-representation analyses on down-regulated genes from the comparison between X-ray irradiated cells collected 24 hrs post-irradiation and sham-irradiated ones under 1G.

Gene Set	Description	P Value	FDR
GO:0071840	cellular component organization or biogenesis	<2.2e-16	<2.2e-16
GO:0016043	cellular component organization	<2.2e-16	<2.2e-16
GO:0090304	nucleic acid metabolic process	<2.2e-16	<2.2e-16
GO:0006996	organelle organization	<2.2e-16	<2.2e-16
GO:0033554	cellular response to stress	<2.2e-16	<2.2e-16
GO:0007049	cell cycle	<2.2e-16	<2.2e-16
GO:0022402	cell cycle process	<2.2e-16	<2.2e-16
GO:0033043	regulation of organelle organization	<2.2e-16	<2.2e-16
GO:0051276	chromosome organization	<2.2e-16	<2.2e-16
GO:0051726	regulation of cell cycle	<2.2e-16	<2.2e-16
GO:0006259	DNA metabolic process	<2.2e-16	<2.2e-16
GO:0000278	mitotic cell cycle	<2.2e-16	<2.2e-16
GO:0006974	cellular response to DNA damage stimulus	<2.2e-16	<2.2e-16
GO:1903047	mitotic cell cycle process	<2.2e-16	<2.2e-16
GO:0007017	microtubule-based process	<2.2e-16	<2.2e-16
GO:0006325	chromatin organization	<2.2e-16	<2.2e-16
GO:0010564	regulation of cell cycle process	<2.2e-16	<2.2e-16
GO:0007346	regulation of mitotic cell cycle	<2.2e-16	<2.2e-16
GO:0051301	cell division	<2.2e-16	<2.2e-16
GO:0045786	negative regulation of cell cycle	<2.2e-16	<2.2e-16

Table 16. Top molecular functions from over-representation analyses on up-regulated genes from the comparison between X-ray irradiated cells collected 24 hrs post-irradiation and sham-irradiated ones under 1G.

Gene Set	Description	P Value	FDR
GO:0005201	extracellular matrix structural constituent	6.66E-16	1.97E-12
GO:0019838	growth factor binding	6.16E-14	9.10E-11
GO:0005539	glycosaminoglycan binding	6.36E-10	6.27E-07
GO:0005178	integrin binding	3.60E-09	2.66E-06
GO:0005509	calcium ion binding	5.73E-09	3.39E-06
GO:0048407	platelet-derived growth factor binding	2.24E-07	0.000103
GO:0030020	extracellular matrix structural constituent conferring tensile strength	2.44E-07	0.000103
GO:0005102	signaling receptor binding	9.41E-07	0.000347
GO:0008201	heparin binding	1.36E-06	0.000431
GO:0005198	structural molecule activity	1.46E-06	0.000431
GO:0005518	collagen binding	1.76E-06	0.000473
GO:0050840	extracellular matrix binding	2.1E-06	0.000508
GO:0031994	insulin-like growth factor I binding	2.23E-06	0.000508
GO:1901681	sulfur compound binding	3.28E-06	0.000692
GO:0005520	insulin-like growth factor binding	3.53E-06	0.000696

GO:0043394	proteoglycan binding	8.77E-06	0.00162
GO:0050431	transforming growth factor beta binding	7.22E-05	0.012555
GO:0043167	ion binding	0.00011	0.01802
GO:0031995	insulin-like growth factor II binding	0.000128	0.019932
GO:0002020	protease binding	0.000154	0.022793

Table 17. Top molecular functions from over-representation analyses on down-regulated genes from the comparison between X-ray irradiated cells collected 24 hrs post-irradiation and sham-irradiated ones under 1G.

Gene Set	Description	P Value	FDR
GO:0005515	protein binding	<2.2e-16	<2.2e-16
GO:0097159	organic cyclic compound binding	<2.2e-16	<2.2e-16
GO:1901363	heterocyclic compound binding	<2.2e-16	<2.2e-16
GO:0003676	nucleic acid binding	<2.2e-16	<2.2e-16
GO:0003677	DNA binding	<2.2e-16	<2.2e-16
GO:0003723	RNA binding	<2.2e-16	<2.2e-16
GO:0003682	chromatin binding	<2.2e-16	<2.2e-16
GO:0140097	catalytic activity, acting on DNA	<2.2e-16	<2.2e-16
GO:0008094	DNA-dependent ATPase activity	<2.2e-16	<2.2e-16
GO:0005524	ATP binding	1.11E-15	3.28E-13
GO:0008144	drug binding	1.22E-15	3.28E-13
GO:0003697	single-stranded DNA binding	6.77E-15	1.67E-12
GO:0032559	adenyl ribonucleotide binding	7.55E-15	1.72E-12
GO:0030554	adenyl nucleotide binding	8.55E-15	1.80E-12
GO:0000166	nucleotide binding	2.58E-14	5.04E-12
GO:1901265	nucleoside phosphate binding	2.73E-14	5.04E-12
GO:0035639	purine ribonucleoside triphosphate binding	1.22E-13	2.12E-11
GO:0017076	purine nucleotide binding	4.39E-13	7.21E-11
GO:0032553	ribonucleotide binding	6.76E-13	1.03E-10
GO:0032555	purine ribonucleotide binding	6.98E-13	1.03E-10

Table 18. Top cellular components from over-representation analyses on up-regulated genes from the comparison between X-ray irradiated cells collected 24 hrs post-irradiation and sham-irradiated ones under 1G.

Gene Set	Description	P Value	FDR
GO:0031012	extracellular matrix	<2.2e-16	<2.2e-16
GO:0062023	collagen-containing extracellular matrix	<2.2e-16	<2.2e-16
GO:0005615	extracellular space	3.55E-14	1.79E-11
GO:0044421	extracellular region part	4.31E-14	1.79E-11
GO:0005576	extracellular region	1.82E-13	6.07E-11
GO:0044420	extracellular matrix component	8.32E-11	2.31E-08
GO:0005788	endoplasmic reticulum lumen	4.37E-10	1.04E-07
GO:0005604	basement membrane	5.04E-08	1.05E-05
GO:1903561	extracellular vesicle	1.18E-07	2.03E-05
GO:0043230	extracellular organelle	1.22E-07	2.03E-05
GO:0098644	complex of collagen trimers	1.41E-07	2.14E-05
GO:0070062	extracellular exosome	2.57E-07	3.57E-05
GO:0031982	vesicle	3.36E-07	4.3E-05

GO:0005583	fibrillar collagen trimer	5.79E-07	6.44E-05
GO:0098643	banded collagen fibril	5.79E-07	6.44E-05
GO:0005581	collagen trimer	1.64E-06	0.000171
GO:0012505	endomembrane system	4.04E-06	0.000395
GO:0005773	vacuole	1.85E-05	0.001712
GO:0005764	lysosome	3.16E-05	0.002744
GO:0000323	lytic vacuole	3.29E-05	0.002744

Table 19. Top cellular components from over-representation analyses on down-regulated genes from the comparison between X-ray irradiated cells collected 24 hrs post-irradiation and sham-irradiated ones under 1G.

Gene Set	Description	P Value	FDR
GO:0005622	intracellular	<2.2e-16	<2.2e-16
GO:0044424	intracellular part	<2.2e-16	<2.2e-16
GO:0043226	organelle	<2.2e-16	<2.2e-16
GO:0043229	intracellular organelle	<2.2e-16	<2.2e-16
GO:0043231	intracellular membrane-bounded organelle	<2.2e-16	<2.2e-16
GO:0044422	organelle part	<2.2e-16	<2.2e-16
GO:0044446	intracellular organelle part	<2.2e-16	<2.2e-16
GO:0005634	nucleus	<2.2e-16	<2.2e-16
GO:0031974	membrane-enclosed lumen	<2.2e-16	<2.2e-16
GO:0043233	organelle lumen	<2.2e-16	<2.2e-16
GO:0070013	intracellular organelle lumen	<2.2e-16	<2.2e-16
GO:0032991	protein-containing complex	<2.2e-16	<2.2e-16
GO:0005829	cytosol	<2.2e-16	<2.2e-16
GO:0044428	nuclear part	<2.2e-16	<2.2e-16
GO:0031981	nuclear lumen	<2.2e-16	<2.2e-16
GO:0043228	non-membrane-bounded organelle	<2.2e-16	<2.2e-16
GO:0043232	intracellular non-membrane-bounded organelle	<2.2e-16	<2.2e-16
GO:0005654	nucleoplasm	<2.2e-16	<2.2e-16
GO:0005856	cytoskeleton	<2.2e-16	<2.2e-16
GO:0044430	cytoskeletal part	<2.2e-16	<2.2e-16

Table 20. Top KEGG pathways from over-representation analyses on up-regulated genes from the comparison between X-ray irradiated cells collected 24 hrs post-irradiation and sham-irradiated ones under 1G.

Gene Set	Description	P Value	FDR
hsa04115	p53 signaling pathway	2.02E-06	0.000666
hsa04512	ECM-receptor interaction	1.94E-05	0.003188
hsa04510	Focal adhesion	3.54E-05	0.00388
hsa04151	PI3K-Akt signaling pathway	0.000152	0.009819
hsa04974	Protein digestion and absorption	0.000162	0.009819
hsa05206	MicroRNAs in cancer	0.000179	0.009819
hsa05214	Glioma	0.000245	0.0115
hsa05218	Melanoma	0.000772	0.031735
hsa05165	Human papillomavirus infection	0.000997	0.036435

Table 21. Top KEGG pathways from over-representation analyses on down-regulated genes from the comparison between X-ray irradiated cells collected 24 hrs post-irradiation and sham-irradiated ones under 1G.

Gene Set	Description	P Value	FDR
hsa05034	Alcoholism	<2.2e-16	<2.2e-16
hsa04110	Cell cycle	<2.2e-16	<2.2e-16
hsa05322	Systemic lupus erythematosus	<2.2e-16	<2.2e-16
hsa03030	DNA replication	<2.2e-16	<2.2e-16
hsa05203	Viral carcinogenesis	1.05E-11	6.91E-10
hsa03440	Homologous recombination	1.78E-11	8.44E-10
hsa03460	Fanconi anemia pathway	1.80E-11	8.44E-10
hsa03430	Mismatch repair	2.33E-11	9.58E-10
hsa04114	Oocyte meiosis	2.06E-08	7.54E-07
hsa03040	Spliceosome	5.28E-07	1.74E-05
hsa03410	Base excision repair	1.46E-06	4.36E-05
hsa04218	Cellular senescence	1.65E-06	4.52E-05
hsa03013	RNA transport	5.03E-06	0.000118
hsa03420	Nucleotide excision repair	5.03E-06	0.000118
hsa00240	Pyrimidine metabolism	3.62E-05	0.000795
hsa04217	Necroptosis	5.28E-05	0.001087
hsa04914	Progesterone-mediated oocyte maturation	0.000138	0.002673
hsa05130	Pathogenic Escherichia coli infection	0.000184	0.003354
hsa05166	Human T-cell leukemia virus 1 infection	0.002876	0.049803

3.3. Late vs early response genes to X-ray irradiation under 1G

From the comparison between X-ray irradiated cells collected 3 (early) and 24 (late) hrs post-irradiation under 1G (X24G-X3G), 255 up- and 619 down-regulated genes were identified. For up-regulated genes, enrichment analyses concerning Gene Ontology aspects highlighted anatomical morphogenesis and response to stimulus related terms. The predominant KEGG pathway identified was mitophagy. FOXO4 was identified as an up-regulated gene targeting transcription factor. Among the down-regulated genes, *MKI67*, *ASPM*, *CENPF*, *TOP2A* and *PRC1* stood out. Over-representation analyses in all Gene Ontology categories, as well as in KEGG pathways, highlighted cell cycle and DNA repair related terms. E2F was identified as a under-expressed gene-targeting transcription factor.

Table 22. Top up-regulated genes from the comparison between X-ray irradiated cells collected 3 and 24 hrs post-irradiation under 1G.

Gene Id	Gene Name	Description	svalue
ENSG00000146674	*IGFBP3*	insulin like growth factor binding protein 3 [Source:HGNC Symbol;Acc:HGNC:5472]	1.01E-13
ENSG00000144810	*COL8A1*	collagen type VIII alpha 1 chain [Source:HGNC Symbol;Acc:HGNC:2215]	3.35E-13
ENSG00000170581	*STAT2*	signal transducer and activator of transcription 2 [Source:HGNC Symbol;Acc:HGNC:11363]	8.59E-13
ENSG00000152661	*GJA1*	gap junction protein alpha 1 [Source:HGNC Symbol;Acc:HGNC:4274]	9.89E-13
ENSG00000137573	*SULF1*	sulfatase 1 [Source:HGNC Symbol;Acc:HGNC:20391]	4.25E-12
ENSG00000138061	*CYP1B1*	cytochrome P450 family 1 subfamily B member 1 [Source:HGNC Symbol;Acc:HGNC:2597]	4.64E-12
ENSG00000103888	*CEMIP*	cell migration inducing hyaluronidase 1 [Source:HGNC Symbol;Acc:HGNC:29213]	8.59E-12
ENSG00000164761	*TNFRSF11B*	TNF receptor superfamily member 11b [Source:HGNC Symbol;Acc:HGNC:11909]	6.55E-11

ENSG00000198796	*ALPK2*	alpha kinase 2 [Source:HGNC Symbol;Acc:HGNC:20565]	1.02E-10
ENSG00000221852	*KRTAP1-5*	keratin associated protein 1-5 [Source:HGNC Symbol;Acc:HGNC:16777]	1.56E-10
ENSG00000173706	*HEG1*	heart development protein with EGF like domains 1 [Source:HGNC Symbol;Acc:HGNC:29227]	1.98E-10
ENSG00000101825	*MXRA5*	matrix remodeling associated 5 [Source:HGNC Symbol;Acc:HGNC:7539]	9.68E-10
ENSG00000140323	*DISP2*	dispatched RND transporter family member 2 [Source:HGNC Symbol;Acc:HGNC:19712]	1.99E-09
ENSG00000174807	*CD248*	CD248 molecule [Source:HGNC Symbol;Acc:HGNC:18219]	1.09E-08
ENSG00000115504	*EHBP1*	EH domain binding protein 1 [Source:HGNC Symbol;Acc:HGNC:29144]	1.60E-08
ENSG00000173559	*NABP1*	nucleic acid binding protein 1 [Source:HGNC Symbol;Acc:HGNC:26232]	1.79E-08
ENSG00000013016	*EHD3*	EH domain containing 3 [Source:HGNC Symbol;Acc:HGNC:3244]	1.89E-08
ENSG00000112769	*LAMA4*	laminin subunit alpha 4 [Source:HGNC Symbol;Acc:HGNC:6484]	2.11E-08
ENSG00000141753	*IGFBP4*	insulin like growth factor binding protein 4 [Source:HGNC Symbol;Acc:HGNC:5473]	2.36E-08
ENSG00000135919	*SERPINE2*	serpin family E member 2 [Source:HGNC Symbol;Acc:HGNC:8951]	3.58E-08

Table 23. Top down-regulated genes from the comparison between X-ray irradiated cells collected 3 and 24 hrs post-irradiation under 1G.

Gene Id	Gene Name	description	svalue
ENSG00000148773	*MKI67*	marker of proliferation Ki-67 [Source:HGNC Symbol;Acc:HGNC:7107]	1.66E-96
ENSG00000117724	*CENPF*	centromere protein F [Source:HGNC Symbol;Acc:HGNC:1857]	3.99E-63
ENSG00000066279	*ASPM*	assembly factor for spindle microtubules [Source:HGNC Symbol;Acc:HGNC:19048]	4.84E-62
ENSG00000183856	*IQGAP3*	IQ motif containing GTPase activating protein 3 [Source:HGNC Symbol;Acc:HGNC:20669]	7.28E-61
ENSG00000131747	*TOP2A*	DNA topoisomerase II alpha [Source:HGNC Symbol;Acc:HGNC:11989]	4.73E-60
ENSG00000198901	*PRC1*	protein regulator of cytokinesis 1 [Source:HGNC Symbol;Acc:HGNC:9341]	5.26E-56
ENSG00000182481	*KPNA2*	karyopherin subunit alpha 2 [Source:HGNC Symbol;Acc:HGNC:6395]	1.22E-55
ENSG00000136108	*CKAP2*	cytoskeleton associated protein 2 [Source:HGNC Symbol;Acc:HGNC:1990]	5.62E-52
ENSG00000112984	*KIF20A*	kinesin family member 20A [Source:HGNC Symbol;Acc:HGNC:9787]	3.33E-50
ENSG00000134057	*CCNB1*	cyclin B1 [Source:HGNC Symbol;Acc:HGNC:1579]	3.00E-49
ENSG00000013810	*TACC3*	transforming acidic coiled-coil containing protein 3 [Source:HGNC Symbol;Acc:HGNC:11524]	2.43E-46
ENSG00000088325	*TPX2*	TPX2 microtubule nucleation factor [Source:HGNC Symbol;Acc:HGNC:1249]	1.10E-45
ENSG00000117399	*CDC20*	cell division cycle 20 [Source:HGNC Symbol;Acc:HGNC:1723]	2.64E-44
ENSG00000124762	*CDKN1A*	cyclin dependent kinase inhibitor 1A [Source:HGNC Symbol;Acc:HGNC:1784]	7.47E-44
ENSG00000167553	*TUBA1C*	tubulin alpha 1c [Source:HGNC Symbol;Acc:HGNC:20768]	1.96E-43
ENSG00000075218	*GTSE1*	G2 and S-phase expressed 1 [Source:HGNC Symbol;Acc:HGNC:13698]	3.29E-43
ENSG00000184357	*H1-5*	H1.5 linker histone, cluster member [Source:HGNC Symbol;Acc:HGNC:4719]	4.28E-42
ENSG00000126787	*DLGAP5*	DLG associated protein 5 [Source:HGNC Symbol;Acc:HGNC:16864]	5.24E-41
ENSG00000166851	*PLK1*	polo like kinase 1 [Source:HGNC Symbol;Acc:HGNC:9077]	1.76E-40
ENSG00000138180	*CEP55*	centrosomal protein 55 [Source:HGNC Symbol;Acc:HGNC:1161]	1.51E-39

Table 24. Top biological processes from over-representation analyses on up-regulated genes from the comparison between X-ray irradiated cells collected 3 and 24 hrs post-irradiation under 1G.

Gene Set	Description	P Value	FDR
GO:0030198	extracellular matrix organization	1.34E-10	1.63E-06
GO:0032502	developmental process	5.37E-10	2.48E-06
GO:0048856	anatomical structure development	6.10E-10	2.48E-06
GO:0072359	circulatory system development	1.05E-09	2.72E-06
GO:0009653	anatomical structure morphogenesis	1.17E-09	2.72E-06
GO:0032501	multicellular organismal process	1.34E-09	2.72E-06
GO:0043062	extracellular structure organization	1.63E-09	2.83E-06
GO:0050896	response to stimulus	9.34E-09	1.21E-05
GO:0035295	tube development	9.58E-09	1.21E-05
GO:0007275	multicellular organism development	9.93E-09	1.21E-05
GO:0035239	tube morphogenesis	2.03E-08	2.25E-05
GO:0009887	animal organ morphogenesis	2.23E-08	2.26E-05
GO:0048513	animal organ development	2.68E-08	2.51E-05
GO:0051239	regulation of multicellular organismal process	3.86E-08	3.36E-05
GO:0001501	skeletal system development	6.06E-08	4.91E-05
GO:0050793	regulation of developmental process	6.55E-08	4.98E-05
GO:0007166	cell surface receptor signaling pathway	7.72E-08	5.53E-05
GO:0007167	enzyme linked receptor protein signaling pathway	9.45E-08	6.19E-05
GO:0007154	cell communication	1.01E-07	6.19E-05
GO:0010033	response to organic substance	1.05E-07	6.19E-05

Table 25. Top biological processes from over-representation analyses on down-regulated genes from the comparison between X-ray irradiated cells collected 3 and 24 hrs post-irradiation under 1G.

Gene Set	Description	P Value	FDR
GO:0071840	cellular component organization or biogenesis	<2.2e-16	<2.2e-16
GO:0016043	cellular component organization	<2.2e-16	<2.2e-16
GO:0006996	organelle organization	<2.2e-16	<2.2e-16
GO:0033554	cellular response to stress	<2.2e-16	<2.2e-16
GO:0007049	cell cycle	<2.2e-16	<2.2e-16
GO:0022402	cell cycle process	<2.2e-16	<2.2e-16
GO:0051276	chromosome organization	<2.2e-16	<2.2e-16
GO:0051726	regulation of cell cycle	<2.2e-16	<2.2e-16
GO:0006259	DNA metabolic process	<2.2e-16	<2.2e-16
GO:0000278	mitotic cell cycle	<2.2e-16	<2.2e-16
GO:0006974	cellular response to DNA damage stimulus	<2.2e-16	<2.2e-16
GO:1903047	mitotic cell cycle process	<2.2e-16	<2.2e-16
GO:0007017	microtubule-based process	<2.2e-16	<2.2e-16
GO:0006325	chromatin organization	<2.2e-16	<2.2e-16
GO:0010564	regulation of cell cycle process	<2.2e-16	<2.2e-16
GO:0007346	regulation of mitotic cell cycle	<2.2e-16	<2.2e-16
GO:0051301	cell division	<2.2e-16	<2.2e-16
GO:0045786	negative regulation of cell cycle	<2.2e-16	<2.2e-16

GO:0044770	cell cycle phase transition	<2.2e-16	<2.2e-16
GO:0006281	DNA repair	<2.2e-16	<2.2e-16

Table 26. Top molecular functions from over-representation analyses on up-regulated genes from the comparison between X-ray irradiated cells collected 3 and 24 hrs post-irradiation under 1G.

Gene Set	Description	P Value	FDR
GO:0005201	extracellular matrix structural constituent	1.32E-11	3.89E-08
GO:0005539	glycosaminoglycan binding	1.37E-08	2.03E-05
GO:0005102	signaling receptor binding	3.97E-08	3.91E-05
GO:0005509	calcium ion binding	1.17E-07	8.67E-05
GO:0005520	insulin-like growth factor binding	5.15E-06	0.002891
GO:0008201	heparin binding	5.87E-06	0.002891
GO:0005198	structural molecule activity	1.29E-05	0.005433
GO:0005178	integrin binding	2.25E-05	0.008324
GO:0050840	extracellular matrix binding	2.72E-05	0.008947
GO:0019838	growth factor binding	3.1E-05	0.009147
GO:0031994	insulin-like growth factor I binding	4.36E-05	0.011711
GO:0004720	protein-lysine 6-oxidase activity	5.45E-05	0.013426
GO:0005515	protein binding	9.57E-05	0.021199
GO:0004322	ferroxidase activity	0.000108	0.021199
GO:0016724	oxidoreductase activity, oxidizing metal ions, oxygen as acceptor	0.000108	0.021199
GO:1901681	sulfur compound binding	0.000154	0.028528

Table 27. Top molecular functions from over-representation analyses on down-regulated genes from the comparison between X-ray irradiated cells collected 3 and 24 hrs post-irradiation under 1G.

Gene Set	Description	P Value	FDR
GO:0005515	protein binding	<2.2e-16	<2.2e-16
GO:0097159	organic cyclic compound binding	<2.2e-16	<2.2e-16
GO:1901363	heterocyclic compound binding	<2.2e-16	<2.2e-16
GO:0003676	nucleic acid binding	<2.2e-16	<2.2e-16
GO:0003677	DNA binding	<2.2e-16	<2.2e-16
GO:0003682	chromatin binding	<2.2e-16	<2.2e-16
GO:0140097	catalytic activity, acting on DNA	1.33E-15	5.62E-13
GO:0015631	tubulin binding	5.82E-14	2.15E-11
GO:0008017	microtubule binding	9.77E-13	3.21E-10
GO:0005524	ATP binding	1.20E-12	3.56E-10
GO:0008094	DNA-dependent ATPase activity	3.40E-12	9.12E-10
GO:0032559	adenyl ribonucleotide binding	1.27E-11	3.13E-09
GO:0008144	drug binding	1.80E-11	4.09E-09
GO:0030554	adenyl nucleotide binding	2.28E-11	4.80E-09
GO:0016887	ATPase activity	2.43E-11	4.80E-09
GO:0031491	nucleosome binding	7.63E-11	1.37E-08
GO:0035639	purine ribonucleoside triphosphate binding	8.07E-11	1.37E-08
GO:0016462	pyrophosphatase activity	8.68E-11	1.37E-08
GO:0017111	nucleoside-triphosphatase activity	9.24E-11	1.37E-08
GO:0016817	hydrolase activity, acting on acid anhydrides	9.73E-11	1.37E-08

Table 28. Top cellular components from over-representation analyses on up-regulated genes from the comparison between X-ray irradiated cells collected 3 and 24 hrs post-irradiation under 1G.

Gene Set	Description	P Value	FDR
GO:0031012	extracellular matrix	<2.2e-16	<2.2e-16
GO:0062023	collagen-containing extracellular matrix	<2.2e-16	<2.2e-16
GO:0005576	extracellular region	1.69E-12	9.38E-10
GO:0044421	extracellular region part	1.47E-11	6.13E-09
GO:0005615	extracellular space	1.56E-10	5.20E-08
GO:0005604	basement membrane	1.78E-08	4.94E-06
GO:0005788	endoplasmic reticulum lumen	2.18E-08	5.19E-06
GO:0005886	plasma membrane	2.66E-07	5.53E-05
GO:0031982	vesicle	7.97E-07	0.000148
GO:0071944	cell periphery	9.52E-07	0.000159
GO:0012505	endomembrane system	1.21E-05	0.001834
GO:0031410	cytoplasmic vesicle	2.18E-05	0.002885
GO:0097708	intracellular vesicle	2.25E-05	0.002885
GO:0044433	cytoplasmic vesicle part	4.54E-05	0.005398
GO:1903561	extracellular vesicle	0.000145	0.01532
GO:0043230	extracellular organelle	0.000147	0.01532
GO:0030662	coated vesicle membrane	0.000274	0.026869
GO:0008043	intracellular ferritin complex	0.000322	0.027112
GO:0070288	ferritin complex	0.000322	0.027112
GO:0005783	endoplasmic reticulum	0.000338	0.027112

Table 29. Top cellular components from over-representation analyses on down-regulated genes from the comparison between X-ray irradiated cells collected 3 and 24 hrs post-irradiation under 1G.

Gene Set	Description	P Value	FDR
GO:0005622	intracellular	<2.2e-16	<2.2e-16
GO:0044424	intracellular part	<2.2e-16	<2.2e-16
GO:0043229	intracellular organelle	<2.2e-16	<2.2e-16
GO:0044422	organelle part	<2.2e-16	<2.2e-16
GO:0044446	intracellular organelle part	<2.2e-16	<2.2e-16
GO:0005634	nucleus	<2.2e-16	<2.2e-16
GO:0031974	membrane-enclosed lumen	<2.2e-16	<2.2e-16
GO:0043233	organelle lumen	<2.2e-16	<2.2e-16
GO:0070013	intracellular organelle lumen	<2.2e-16	<2.2e-16
GO:0032991	protein-containing complex	<2.2e-16	<2.2e-16
GO:0005829	cytosol	<2.2e-16	<2.2e-16
GO:0044428	nuclear part	<2.2e-16	<2.2e-16
GO:0031981	nuclear lumen	<2.2e-16	<2.2e-16
GO:0043228	non-membrane-bounded organelle	<2.2e-16	<2.2e-16
GO:0043232	intracellular non-membrane-bounded organelle	<2.2e-16	<2.2e-16
GO:0005654	nucleoplasm	<2.2e-16	<2.2e-16
GO:0005856	cytoskeleton	<2.2e-16	<2.2e-16
GO:0044430	cytoskeletal part	<2.2e-16	<2.2e-16
GO:0015630	microtubule cytoskeleton	<2.2e-16	<2.2e-16

GO:0005694	chromosome	<2.2e-16	<2.2e-16

Table 30. Top KEGG pathway from over-representation analyses on up-regulated genes from the comparison between X-ray irradiated cells collected 3 and 24 hrs post-irradiation under 1G.

Gene Set	Description	P Value	FDR
hsa04137	Mitophagy	1.97E-05	0.006469

Table 31. Top KEGG pathways from over-representation analyses on down-regulated genes from the comparison between X-ray irradiated cells collected 3 and 24 hrs post-irradiation under 1G.

Gene Set	Description	P Value	FDR
hsa05034	Alcoholism	<2.2e-16	<2.2e-16
hsa04110	Cell cycle	<2.2e-16	<2.2e-16
hsa05322	Systemic lupus erythematosus	<2.2e-16	<2.2e-16
hsa03030	DNA replication	1.44E-14	1.19E-12
hsa05203	Viral carcinogenesis	1.98E-13	1.30E-11
hsa04114	Oocyte meiosis	7.02E-10	3.85E-08
hsa04217	Necroptosis	4.59E-08	2.15E-06
hsa03430	Mismatch repair	1.1E-05	0.000452
hsa03460	Fanconi anemia pathway	1.32E-05	0.000483
hsa04115	p53 signaling pathway	2.32E-05	0.000762
hsa03410	Base excision repair	2.85E-05	0.000814
hsa03440	Homologous recombination	2.97E-05	0.000814
hsa04914	Progesterone-mediated oocyte maturation	3.37E-05	0.000852
hsa03420	Nucleotide excision repair	0.000104	0.002449
hsa04218	Cellular senescence	0.000149	0.003276

3.4. Early response genes to C-ion irradiation under 1G

The high LET of C-ions is expected to elicit quantitatively and qualitatively different responses compared to low-LET including not only the DNA damage response (DDR) pathways but also inflammatory and immune system activation and systemic effects (Nikitaki et al., 2022). From the comparison between C-ion irradiated cells collected 3 hrs post-irradiation and sham-irradiated ones under 1G (C3G-C0G), 159 over-expressed genes were identified in total. Among those ones, *CDKN1A*, *MDM2*, *PAPPA*, *TNFRSF10B*, *BTG2*, *TP53INP1*, *PTCHD4* and *PURPL* stood out. In particular, the expression of CDKN1A (p21) and *MDM2* had log2 fold change of 2.5 and 2.2. *CDKN1A* is a downstream gene to *TP53* and often showed to act as a negative regulator of the cellular levels of *TP53* (Broude et al., 2007). Likewise, 114 genes were found to be under-expressed at a statistically significant manner. Down-regulated genes *PLK1*, *MKI67*, *BUB1B* and *DTL* were most prominent. Concerning the over-expressed genes, enrichment analyses in all Gene Ontology aspects highlighted apoptosis and type I interferon signaling pathway related terms. KEGG pathways identified the p53 signaling pathway. LEF1 was identified as a gene-targeting transcription factor. Concentrating on under-expressed genes, biological term over-representation analyses in all Gene Ontology domains, as well as in KEGG pathways, highlighted cell cycle related terms. E2F was identified as a targeting transcription factor for under-expressed genes.

Table 32. Top up-regulated genes from the comparison between C-ion irradiated cells collected 3 hrs post-irradiation and sham-irradiated ones under 1G.

Gene Id	Gene Name	description	svalue
ENSG00000124762	*CDKN1A*	cyclin dependent kinase inhibitor 1A [Source:HGNC Symbol;Acc:HGNC:1784]	1.03E-152

ENSG00000135679	*MDM2*	MDM2 proto-oncogene [Source:HGNC Symbol;Acc:HGNC:6973]	8.19E-69
ENSG00000182752	*PAPPA*	pappalysin 1 [Source:HGNC Symbol;Acc:HGNC:8602]	9.50E-34
ENSG00000120889	*TNFRSF10B*	TNF receptor superfamily member 10b [Source:HGNC Symbol;Acc:HGNC:11905]	1.28E-25
ENSG00000159388	*BTG2*	BTG anti-proliferation factor 2 [Source:HGNC Symbol;Acc:HGNC:1131]	9.65E-25
ENSG00000256664	*NA*	ribosomal L24 domain containing 1 (RSL24D1) pseudogene	1.04E-23
ENSG00000164938	*TP53INP1*	tumor protein p53 inducible nuclear protein 1 [Source:HGNC Symbol;Acc:HGNC:18022]	1.15E-22
ENSG00000244694	*PTCHD4*	patched domain containing 4 [Source:HGNC Symbol;Acc:HGNC:21345]	2.23E-22
ENSG00000250337	*PURPL*	p53 upregulated regulator of p53 levels [Source:HGNC Symbol;Acc:HGNC:48995]	4.41E-20
ENSG00000172667	*ZMAT3*	zinc finger matrin-type 3 [Source:HGNC Symbol;Acc:HGNC:29983]	1.72E-17
ENSG00000161513	*FDXR*	ferredoxin reductase [Source:HGNC Symbol;Acc:HGNC:3642]	4.91E-16
ENSG00000164070	*HSPA4L*	heat shock protein family A (Hsp70) member 4 like [Source:HGNC Symbol;Acc:HGNC:17041]	1.25E-15
ENSG00000026103	*FAS*	Fas cell surface death receptor [Source:HGNC Symbol;Acc:HGNC:11920]	9.53E-15
ENSG00000164125	*GASK1B*	golgi associated kinase 1B [Source:HGNC Symbol;Acc:HGNC:25312]	2.16E-14
ENSG00000164236	*ANKRD33B*	ankyrin repeat domain 33B [Source:HGNC Symbol;Acc:HGNC:35240]	3.25E-14
ENSG00000028277	*POU2F2*	POU class 2 homeobox 2 [Source:HGNC Symbol;Acc:HGNC:9213]	4.59E-14
ENSG00000134363	*FST*	follistatin [Source:HGNC Symbol;Acc:HGNC:3971]	9.35E-13
ENSG00000130513	*GDF15*	growth differentiation factor 15 [Source:HGNC Symbol;Acc:HGNC:30142]	1.33E-12
ENSG00000055163	*CYFIP2*	cytoplasmic FMR1 interacting protein 2 [Source:HGNC Symbol;Acc:HGNC:13760]	1.93E-12
ENSG00000167196	*FBXO22*	F-box protein 22 [Source:HGNC Symbol;Acc:HGNC:13593]	2.86E-12

Table 33. Top down-regulated genes from the comparison between C-ion irradiated cells collected 3 hrs post-irradiation and sham-irradiated ones under 1G.

Gene Id	Gene Name	description	svalue
ENSG00000148773	*MKI67*	marker of proliferation Ki-67 [Source:HGNC Symbol;Acc:HGNC:7107]	6.02E-17
ENSG00000166851	*PLK1*	polo like kinase 1 [Source:HGNC Symbol;Acc:HGNC:9077]	4.82E-15
ENSG00000156970	*BUB1B*	BUB1 mitotic checkpoint serine/threonine kinase B [Source:HGNC Symbol;Acc:HGNC:1149]	1.40E-14
ENSG00000143476	*DTL*	denticleless E3 ubiquitin protein ligase homolog [Source:HGNC Symbol;Acc:HGNC:30288]	1.36E-13
ENSG00000123473	*STIL*	STIL centriolar assembly protein [Source:HGNC Symbol;Acc:HGNC:10879]	2.28E-13
ENSG00000162063	*CCNF*	cyclin F [Source:HGNC Symbol;Acc:HGNC:1591]	3.53E-13
ENSG00000087586	*AURKA*	aurora kinase A [Source:HGNC Symbol;Acc:HGNC:11393]	4.95E-13
ENSG00000134690	*CDCA8*	cell division cycle associated 8 [Source:HGNC Symbol;Acc:HGNC:14629]	6.65E-13
ENSG00000113368	*LMNB1*	lamin B1 [Source:HGNC Symbol;Acc:HGNC:6637]	2.81E-11
ENSG00000112984	*KIF20A*	kinesin family member 20A [Source:HGNC Symbol;Acc:HGNC:9787]	8.87E-10
ENSG00000165244	*ZNF367*	zinc finger protein 367 [Source:HGNC Symbol;Acc:HGNC:18320]	1.42E-09
ENSG00000137807	*KIF23*	kinesin family member 23 [Source:HGNC Symbol;Acc:HGNC:6392]	2.52E-09
ENSG00000276043	*UHRF1*	ubiquitin like with PHD and ring finger domains 1 [Source:HGNC Symbol;Acc:HGNC:12556]	3.04E-09
ENSG00000101447	*FAM83D*	family with sequence similarity 83 member D [Source:HGNC Symbol;Acc:HGNC:16122]	5.27E-09
ENSG00000186185	*KIF18B*	kinesin family member 18B [Source:HGNC Symbol;Acc:HGNC:27102]	7.09E-09
ENSG00000168411	*RFWD3*	ring finger and WD repeat domain 3 [Source:HGNC Symbol;Acc:HGNC:25539]	8.92E-09
ENSG00000013810	*TACC3*	transforming acidic coiled-coil containing protein 3 [Source:HGNC Symbol;Acc:HGNC:11524]	1.16E-08

ENSG00000198826	*ARHGAP11A*	Rho GTPase activating protein 11A [Source:HGNC Symbol;Acc:HGNC:15783]	1.68E-08
ENSG00000164104	*HMGB2*	high mobility group box 2 [Source:HGNC Symbol;Acc:HGNC:5000]	2.23E-08
ENSG00000177084	*POLE*	DNA polymerase epsilon, catalytic subunit [Source:HGNC Symbol;Acc:HGNC:9177]	3.43E-08

Table 34. Top biological processes from over-representation analyses on up-regulated genes from the comparison between C-ion irradiated cells collected 3 hrs post-irradiation and sham-irradiated ones under 1G.

Gene Set	Description	P Value	FDR
GO:0006950	response to stress	3.47E-12	4.53E-08
GO:0035556	intracellular signal transduction	9.55E-12	6.22E-08
GO:1902531	regulation of intracellular signal transduction	9.61E-11	3.96E-07
GO:0006915	apoptotic process	1.21E-10	3.96E-07
GO:0060337	type I interferon signaling pathway	2.05E-10	4.06E-07
GO:0071357	cellular response to type I interferon	2.05E-10	4.06E-07
GO:0008219	cell death	2.18E-10	4.06E-07
GO:0012501	programmed cell death	3.19E-10	5.20E-07
GO:0034340	response to type I interferon	3.87E-10	5.61E-07
GO:0009605	response to external stimulus	1.29E-09	1.58E-06
GO:0050896	response to stimulus	1.33E-09	1.58E-06
GO:0048519	negative regulation of biological process	1.97E-09	2.14E-06
GO:0042981	regulation of apoptotic process	2.73E-09	2.74E-06
GO:0043067	regulation of programmed cell death	3.53E-09	3.16E-06
GO:0060333	interferon-gamma-mediated signaling pathway	3.64E-09	3.16E-06
GO:0010941	regulation of cell death	8.05E-09	6.56E-06
GO:0072331	signal transduction by p53 class mediator	9.21E-09	7.07E-06
GO:0009968	negative regulation of signal transduction	1.64E-08	1.19E-05
GO:0007166	cell surface receptor signaling pathway	1.79E-08	1.23E-05
GO:0010942	positive regulation of cell death	1.95E-08	1.23E-05

Table 35. Top biological processes from over-representation analyses on down-regulated genes from the comparison between C-ion irradiated cells collected 3 hrs post-irradiation and sham-irradiated ones under 1G.

Gene Set	Description	P Value	FDR
GO:0006996	organelle organization	<2.2e-16	<2.2e-16
GO:0007049	cell cycle	<2.2e-16	<2.2e-16
GO:0022402	cell cycle process	<2.2e-16	<2.2e-16
GO:0051276	chromosome organization	<2.2e-16	<2.2e-16
GO:0051726	regulation of cell cycle	<2.2e-16	<2.2e-16
GO:0000278	mitotic cell cycle	<2.2e-16	<2.2e-16
GO:1903047	mitotic cell cycle process	<2.2e-16	<2.2e-16
GO:0007017	microtubule-based process	<2.2e-16	<2.2e-16
GO:0010564	regulation of cell cycle process	<2.2e-16	<2.2e-16
GO:0051301	cell division	<2.2e-16	<2.2e-16
GO:0007346	regulation of mitotic cell cycle	<2.2e-16	<2.2e-16
GO:0045786	negative regulation of cell cycle	<2.2e-16	<2.2e-16
GO:0000226	microtubule cytoskeleton organization	<2.2e-16	<2.2e-16
GO:0044770	cell cycle phase transition	<2.2e-16	<2.2e-16

GO:0044772	mitotic cell cycle phase transition	<2.2e-16	<2.2e-16
GO:0048285	organelle fission	<2.2e-16	<2.2e-16
GO:0000280	nuclear division	<2.2e-16	<2.2e-16
GO:1901987	regulation of cell cycle phase transition	<2.2e-16	<2.2e-16
GO:1901990	regulation of mitotic cell cycle phase transition	<2.2e-16	<2.2e-16
GO:0007059	chromosome segregation	<2.2e-16	<2.2e-16

Table 36. Top molecular functions from over-representation analyses on up-regulated genes from the comparison between C-ion irradiated cells collected 3 hrs post-irradiation and sham-irradiated ones under 1G.

Gene Set	Description	P Value	FDR
GO:0001730	2'-5'-oligoadenylate synthetase activity	2.8E-06	0.009128
GO:0004331	fructose-2,6-bisphosphate 2-phosphatase activity	6.96E-06	0.011335

Table 37. Top molecular functions from over-representation analyses on down-regulated genes from the comparison between C-ion irradiated cells collected 3 hrs post-irradiation and sham-irradiated ones under 1G.

Gene Set	Description	P Value	FDR
GO:0015631	tubulin binding	6.13E-14	2.00E-10
GO:0008017	microtubule binding	1.08E-12	1.77E-09
GO:0003777	microtubule motor activity	2.67E-12	2.90E-09
GO:0005524	ATP binding	2.55E-10	2.08E-07
GO:0005515	protein binding	3.37E-10	2.19E-07
GO:0003774	motor activity	5.71E-10	3.03E-07
GO:0032559	adenyl ribonucleotide binding	6.50E-10	3.03E-07
GO:0030554	adenyl nucleotide binding	8.03E-10	3.27E-07
GO:0008144	drug binding	3.01E-09	1.09E-06
GO:0016887	ATPase activity	8.40E-09	2.74E-06
GO:0003682	chromatin binding	1.42E-08	4.21E-06
GO:0035639	purine ribonucleoside triphosphate binding	3.67E-08	9.96E-06
GO:0019900	kinase binding	4.63E-08	1.16E-05
GO:0032555	purine ribonucleotide binding	8.25E-08	1.9E-05
GO:0010997	anaphase-promoting complex binding	8.81E-08	1.9E-05
GO:0017076	purine nucleotide binding	9.93E-08	1.9E-05
GO:0032553	ribonucleotide binding	9.93E-08	1.9E-05
GO:0000166	nucleotide binding	1.22E-07	2.1E-05
GO:1901265	nucleoside phosphate binding	1.23E-07	2.1E-05
GO:0017111	nucleoside-triphosphatase activity	1.29E-07	2.1E-05

Table 38. Top cellular components from over-representation analyses on down-regulated genes from the comparison between C-ion irradiated cells collected 3 hrs post-irradiation and sham-irradiated ones under 1G.

Gene Set	Description	P Value	FDR
GO:0044422	organelle part	<2.2e-16	<2.2e-16
GO:0044446	intracellular organelle part	<2.2e-16	<2.2e-16
GO:0005634	nucleus	<2.2e-16	<2.2e-16
GO:0044428	nuclear part	<2.2e-16	<2.2e-16
GO:0043228	non-membrane-bounded organelle	<2.2e-16	<2.2e-16
GO:0043232	intracellular non-membrane-bounded organelle	<2.2e-16	<2.2e-16

GO:0031981	nuclear lumen	<2.2e-16	<2.2e-16
GO:0005654	nucleoplasm	<2.2e-16	<2.2e-16
GO:0005856	cytoskeleton	<2.2e-16	<2.2e-16
GO:0044430	cytoskeletal part	<2.2e-16	<2.2e-16
GO:0015630	microtubule cytoskeleton	<2.2e-16	<2.2e-16
GO:0005694	chromosome	<2.2e-16	<2.2e-16
GO:0044427	chromosomal part	<2.2e-16	<2.2e-16
GO:0005819	spindle	<2.2e-16	<2.2e-16
GO:0000793	condensed chromosome	<2.2e-16	<2.2e-16
GO:0000775	chromosome, centromeric region	<2.2e-16	<2.2e-16
GO:0098687	chromosomal region	2.22E-16	2.13E-14
GO:0000779	condensed chromosome, centromeric region	2.22E-16	2.13E-14
GO:0000922	spindle pole	4.44E-16	3.83E-14
GO:0072686	mitotic spindle	4.44E-16	3.83E-14

Table 39. Top KEGG pathways from over-representation analyses on up-regulated genes from the comparison between C-ion irradiated cells collected 3 hrs post-irradiation and sham-irradiated ones under 1G.

Gene Set	Description	P Value	FDR
hsa04115	p53 signaling pathway	7.01E-13	2.31E-10
hsa05162	Measles	2.07E-08	3.41E-06
hsa05169	Epstein-Barr virus infection	2.63E-07	2.89E-05
hsa05164	Influenza A	2.48E-06	0.000204
hsa05168	Herpes simplex infection	3.4E-05	0.00224
hsa05160	Hepatitis C	0.000101	0.005526
hsa01524	Platinum drug resistance	0.000144	0.005905
hsa05218	Melanoma	0.000144	0.005905
hsa05165	Human papillomavirus infection	0.000361	0.012784
hsa05205	Proteoglycans in cancer	0.000389	0.012784
hsa04621	NOD-like receptor signaling pathway	0.000532	0.015921
hsa05222	Small cell lung cancer	0.000581	0.01593
hsa05200	Pathways in cancer	0.000638	0.016136
hsa04625	C-type lectin receptor signaling pathway	0.001049	0.024648
hsa05212	Pancreatic cancer	0.001467	0.032018
hsa05220	Chronic myeloid leukemia	0.001557	0.032018
hsa04217	Necroptosis	0.002029	0.039273

Table 40. Top KEGG pathways from over-representation analyses on down-regulated genes from the comparison between C-ion irradiated cells collected 3 hrs post-irradiation and sham-irradiated ones under 1G.

Gene Set	Description	P Value	FDR
hsa04110	Cell cycle	2.69E-14	8.84E-12
hsa04114	Oocyte meiosis	9.09E-08	1.5E-05
hsa03460	Fanconi anemia pathway	2.56E-05	0.002808
hsa04914	Progesterone-mediated oocyte maturation	4.32E-05	0.003557
hsa04115	p53 signaling pathway	0.000104	0.006816

3.5. Late response genes to C-ion irradiation under 1G

From the comparison between C-ion irradiated collected 24 hrs post-irradiation and sham-irradiated cells under 1G (C24G-C0G), 620 up- and 1022 down-regulated genes were found. Over-expressed genes *PTCHD4*, *PURPL*, *BTG2* and *CDKN1A* were found to be predominant. Biological term enrichment analyses in all Gene Ontology categories highlighted terms related to cell proliferation and cardiovascular system development, such as angiogenesis. The predominant KEGG pathway identified was the p53 signaling pathway. The transcription factor Forkhead Box O4 was also identified. Among the down-regulated genes, many stood out. A few were *MKI67*, *ASPM*, *CENPF*, *ANLN*, *CDC20*, *DLGAP5*, *CCNB1*, *CEP55* and *PLK1*. Enrichment analyses in all Gene Ontology aspects, as well as in KEGG pathways, highlighted cell cycle and DNA repair related terms. E2F was identified as a gene-targeting transcription factor.

Table 41. Top up-regulated genes from the comparison between C-ion irradiated cells collected 24 hrs post-irradiation and sham-irradiated ones under 1G.

Gene Id	Gene Name	Description	svalue
ENSG00000124762	*CDKN1A*	cyclin dependent kinase inhibitor 1A [Source:HGNC Symbol;Acc:HGNC:1784]	5.52E-84
ENSG00000244694	*PTCHD4*	patched domain containing 4 [Source:HGNC Symbol;Acc:HGNC:21345]	2.62E-43
ENSG00000250337	*PURPL*	p53 upregulated regulator of p53 levels [Source:HGNC Symbol;Acc:HGNC:48995]	6.95E-43
ENSG00000135679	*MDM2*	MDM2 proto-oncogene [Source:HGNC Symbol;Acc:HGNC:6973]	1.65E-33
ENSG00000136542	*GALNT5*	polypeptide N-acetylgalactosaminyltransferase 5 [Source:HGNC Symbol;Acc:HGNC:4127]	5.34E-28
ENSG00000172667	*ZMAT3*	zinc finger matrin-type 3 [Source:HGNC Symbol;Acc:HGNC:29983]	1.72E-24
ENSG00000185088	*RPS27L*	ribosomal protein S27 like [Source:HGNC Symbol;Acc:HGNC:18476]	1.73E-23
ENSG00000159388	*BTG2*	BTG anti-proliferation factor 2 [Source:HGNC Symbol;Acc:HGNC:1131]	7.89E-23
ENSG00000135919	*SERPINE2*	serpin family E member 2 [Source:HGNC Symbol;Acc:HGNC:8951]	2.83E-22
ENSG00000182752	*PAPPA*	pappalysin 1 [Source:HGNC Symbol;Acc:HGNC:8602]	8.48E-22
ENSG00000164938	*TP53INP1*	tumor protein p53 inducible nuclear protein 1 [Source:HGNC Symbol;Acc:HGNC:18022]	1.02E-21
ENSG00000214548	*MEG3*	maternally expressed 3 [Source:HGNC Symbol;Acc:HGNC:14575]	1.20E-21
ENSG00000244509	*APOBEC3C*	apolipoprotein B mRNA editing enzyme catalytic subunit 3C [Source:HGNC Symbol;Acc:HGNC:17353]	2.70E-20
ENSG00000245532	*NEAT1*	nuclear paraspeckle assembly transcript 1 [Source:HGNC Symbol;Acc:HGNC:30815]	1.28E-19
ENSG00000107984	*DKK1*	dickkopf WNT signaling pathway inhibitor 1 [Source:HGNC Symbol;Acc:HGNC:2891]	1.32E-17
ENSG00000055163	*CYFIP2*	cytoplasmic FMR1 interacting protein 2 [Source:HGNC Symbol;Acc:HGNC:13760]	6.96E-17
ENSG00000171451	*DSEL*	dermatan sulfate epimerase like [Source:HGNC Symbol;Acc:HGNC:18144]	2.90E-16
ENSG00000163071	*SPATA18*	spermatogenesis associated 18 [Source:HGNC Symbol;Acc:HGNC:29579]	3.21E-16
ENSG00000164125	*GASK1B*	golgi associated kinase 1B [Source:HGNC Symbol;Acc:HGNC:25312]	9.33E-16
ENSG00000138685	*FGF2*	fibroblast growth factor 2 [Source:HGNC Symbol;Acc:HGNC:3676]	6.79E-15

Table 42. Top down-regulated genes from the comparison between C-ion irradiated cells collected 24 hrs post-irradiation and sham-irradiated ones under 1G.

Gene Id	Gene Name	description	svalue
ENSG00000148773	*MKI67*	marker of proliferation Ki-67 [Source:HGNC Symbol;Acc:HGNC:7107]	8.08E-139
ENSG00000120802	*TMPO*	thymopoietin [Source:HGNC Symbol;Acc:HGNC:11875]	1.01E-86
ENSG00000203814	*H2BC18*	H2B clustered histone 18 [Source:HGNC Symbol;Acc:HGNC:24700]	1.96E-86
ENSG00000288825	*H2AC18*	H2A clustered histone 18 [Source:HGNC Symbol;Acc:HGNC:4736]	1.31E-82

ENSG00000277157	*H4C4*	H4 clustered histone 4 [Source:HGNC Symbol;Acc:HGNC:4782]	1.24E-75
ENSG00000124575	*H1-3*	H1.3 linker histone, cluster member [Source:HGNC Symbol;Acc:HGNC:4717]	7.58E-73
ENSG00000196787	*H2AC11*	H2A clustered histone 11 [Source:HGNC Symbol;Acc:HGNC:4737]	1.93E-66
ENSG00000176619	*LMNB2*	lamin B2 [Source:HGNC Symbol;Acc:HGNC:6638]	1.46E-64
ENSG00000278828	*H3C10*	H3 clustered histone 10 [Source:HGNC Symbol;Acc:HGNC:4775]	1.45E-63
ENSG00000092853	*CLSPN*	claspin [Source:HGNC Symbol;Acc:HGNC:19715]	7.19E-61
ENSG00000143476	*DTL*	denticleless E3 ubiquitin protein ligase homolog [Source:HGNC Symbol;Acc:HGNC:30288]	1.58E-59
ENSG00000274997	*H2AC12*	H2A clustered histone 12 [Source:HGNC Symbol;Acc:HGNC:13671]	8.78E-58
ENSG00000187837	*H1-2*	H1.2 linker histone, cluster member [Source:HGNC Symbol;Acc:HGNC:4716]	1.95E-57
ENSG00000197903	*H2BC12*	H2B clustered histone 12 [Source:HGNC Symbol;Acc:HGNC:13954]	3.07E-57
ENSG00000276043	*UHRF1*	ubiquitin like with PHD and ring finger domains 1 [Source:HGNC Symbol;Acc:HGNC:12556]	3.24E-56
ENSG00000203852	*H3C15*	H3 clustered histone 15 [Source:HGNC Symbol;Acc:HGNC:20505]	1.20E-54
ENSG00000277075	*H2AC8*	H2A clustered histone 8 [Source:HGNC Symbol;Acc:HGNC:4724]	7.35E-54
ENSG00000113368	*LMNB1*	lamin B1 [Source:HGNC Symbol;Acc:HGNC:6637]	1.45E-53
ENSG00000273983	*H3C8*	H3 clustered histone 8 [Source:HGNC Symbol;Acc:HGNC:4772]	3.27E-53
ENSG00000138160	*KIF11*	kinesin family member 11 [Source:HGNC Symbol;Acc:HGNC:6388]	7.17E-53

Table 43. Top biological processes from over-representation analyses on up-regulated genes from the comparison between C-ion irradiated cells collected 24 hrs post-irradiation and sham-irradiated ones under 1G.

Gene Set	Description	P Value	FDR
GO:0050896	response to stimulus	5.81E-08	0.000391
GO:0009605	response to external stimulus	8.81E-08	0.000391
GO:0032501	multicellular organismal process	9.63E-08	0.000391
GO:0051179	localization	2.29E-07	0.000477
GO:0009888	tissue development	2.74E-07	0.000477
GO:0009653	anatomical structure morphogenesis	2.89E-07	0.000477
GO:0006928	movement of cell or subcellular component	3.98E-07	0.000477
GO:0032502	developmental process	4.04E-07	0.000477
GO:2000045	regulation of G1/S transition of mitotic cell cycle	4.56E-07	0.000477
GO:0048870	cell motility	5.10E-07	0.000477
GO:0051674	localization of cell	5.10E-07	0.000477
GO:0019538	protein metabolic process	5.53E-07	0.000477
GO:0006915	apoptotic process	5.59E-07	0.000477
GO:1902806	regulation of cell cycle G1/S phase transition	5.83E-07	0.000477
GO:0016477	cell migration	5.87E-07	0.000477
GO:0008219	cell death	7.69E-07	0.000585
GO:0048513	animal organ development	9.35E-07	0.000644
GO:0048856	anatomical structure development	9.72E-07	0.000644
GO:0012501	programmed cell death	1.01E-06	0.000644
GO:0050673	epithelial cell proliferation	1.07E-06	0.000653

Table 44. Top biological processes from over-representation analyses on down-regulated genes from the comparison between C-ion irradiated cells collected 24 hrs post-irradiation and sham-irradiated ones under 1G.

Gene Set	Description	P Value	FDR
GO:0071840	cellular component organization or biogenesis	<2.2e-16	<2.2e-16
GO:0016043	cellular component organization	<2.2e-16	<2.2e-16
GO:0006725	cellular aromatic compound metabolic process	<2.2e-16	<2.2e-16
GO:0046483	heterocycle metabolic process	<2.2e-16	<2.2e-16
GO:0006139	nucleobase-containing compound metabolic process	<2.2e-16	<2.2e-16
GO:0090304	nucleic acid metabolic process	<2.2e-16	<2.2e-16
GO:0006996	organelle organization	<2.2e-16	<2.2e-16
GO:0033554	cellular response to stress	<2.2e-16	<2.2e-16
GO:0007049	cell cycle	<2.2e-16	<2.2e-16
GO:0022402	cell cycle process	<2.2e-16	<2.2e-16
GO:0033043	regulation of organelle organization	<2.2e-16	<2.2e-16
GO:0051276	chromosome organization	<2.2e-16	<2.2e-16
GO:0051726	regulation of cell cycle	<2.2e-16	<2.2e-16
GO:0006259	DNA metabolic process	<2.2e-16	<2.2e-16
GO:0000278	mitotic cell cycle	<2.2e-16	<2.2e-16
GO:0006974	cellular response to DNA damage stimulus	<2.2e-16	<2.2e-16
GO:1903047	mitotic cell cycle process	<2.2e-16	<2.2e-16
GO:0007017	microtubule-based process	<2.2e-16	<2.2e-16
GO:0006325	chromatin organization	<2.2e-16	<2.2e-16
GO:0010564	regulation of cell cycle process	<2.2e-16	<2.2e-16

Table 45. Top molecular function from over-representation analyses on up-regulated genes from the comparison between C-ion irradiated cells collected 24 hrs post-irradiation and sham-irradiated ones under 1G.

Gene Set	Description	P Value	FDR
GO:0005509	calcium ion binding	5.22E-06	0.015434

Table 46. Top molecular functions from over-representation analyses on down-regulated genes from the comparison between C-ion irradiated cells collected 24 hrs post-irradiation and sham-irradiated ones under 1G.

Gene Set	Description	P Value	FDR
GO:0005515	protein binding	<2.2e-16	<2.2e-16
GO:0097159	organic cyclic compound binding	<2.2e-16	<2.2e-16
GO:1901363	heterocyclic compound binding	<2.2e-16	<2.2e-16
GO:0003676	nucleic acid binding	<2.2e-16	<2.2e-16
GO:0003677	DNA binding	<2.2e-16	<2.2e-16
GO:0003723	RNA binding	<2.2e-16	<2.2e-16
GO:0008144	drug binding	<2.2e-16	<2.2e-16
GO:0032559	adenyl ribonucleotide binding	<2.2e-16	<2.2e-16
GO:0005524	ATP binding	<2.2e-16	<2.2e-16
GO:0003682	chromatin binding	<2.2e-16	<2.2e-16
GO:0140097	catalytic activity, acting on DNA	<2.2e-16	<2.2e-16
GO:0003697	single-stranded DNA binding	<2.2e-16	<2.2e-16
GO:0008094	DNA-dependent ATPase activity	1.11E-16	2.52E-14
GO:0030554	adenyl nucleotide binding	2.22E-16	4.69E-14

GO:0031491	nucleosome binding	5.66E-15	1.12E-12
GO:0035639	purine ribonucleoside triphosphate binding	9.10E-15	1.68E-12
GO:0005488	binding	2.13E-14	3.71E-12
GO:0000166	nucleotide binding	6.74E-14	1.11E-11
GO:1901265	nucleoside phosphate binding	7.13E-14	1.11E-11
GO:0032553	ribonucleotide binding	1.13E-13	1.63E-11

Table 47. Top cellular components from over-representation analyses on up-regulated genes from the comparison between C-ion irradiated cells collected 24 hrs post-irradiation and sham-irradiated ones under 1G.

Gene Set	Description	P Value	FDR
GO:0031982	vesicle	2.41E-11	4.02E-08
GO:0005576	extracellular region	2.09E-10	1.74E-07
GO:0062023	collagen-containing extracellular matrix	5.17E-10	2.87E-07
GO:0005615	extracellular space	8.83E-10	3.65E-07
GO:0044421	extracellular region part	1.09E-09	3.65E-07
GO:0098805	whole membrane	6.17E-09	1.71E-06
GO:0031012	extracellular matrix	1.53E-08	3.65E-06
GO:0005925	focal adhesion	1.02E-07	1.65E-05
GO:0005912	adherens junction	1.03E-07	1.65E-05
GO:0044433	cytoplasmic vesicle part	1.05E-07	1.65E-05
GO:0005924	cell-substrate adherens junction	1.09E-07	1.65E-05
GO:0030055	cell-substrate junction	1.42E-07	1.97E-05
GO:0070161	anchoring junction	1.74E-07	2.1E-05
GO:0097708	intracellular vesicle	1.76E-07	2.1E-05
GO:0031410	cytoplasmic vesicle	3.00E-07	3.33E-05
GO:0030054	cell junction	7.68E-07	7.99E-05
GO:1903561	extracellular vesicle	9.48E-07	8.65E-05
GO:0043230	extracellular organelle	9.76E-07	8.65E-05
GO:0044437	vacuolar part	9.87E-07	8.65E-05
GO:0012505	endomembrane system	1.34E-06	0.000111

Table 48. Top cellular components from over-representation analyses on down-regulated genes from the comparison between C-ion irradiated cells collected 24 hrs post-irradiation and sham-irradiated ones under 1G.

Gene Set	Description	P Value	FDR
GO:0005622	intracellular	<2.2e-16	<2.2e-16
GO:0044424	intracellular part	<2.2e-16	<2.2e-16
GO:0043226	organelle	<2.2e-16	<2.2e-16
GO:0043229	intracellular organelle	<2.2e-16	<2.2e-16
GO:0043231	intracellular membrane-bounded organelle	<2.2e-16	<2.2e-16
GO:0044422	organelle part	<2.2e-16	<2.2e-16
GO:0044446	intracellular organelle part	<2.2e-16	<2.2e-16
GO:0005634	nucleus	<2.2e-16	<2.2e-16
GO:0031974	membrane-enclosed lumen	<2.2e-16	<2.2e-16
GO:0043233	organelle lumen	<2.2e-16	<2.2e-16
GO:0070013	intracellular organelle lumen	<2.2e-16	<2.2e-16
GO:0032991	protein-containing complex	<2.2e-16	<2.2e-16

GO:0005829	cytosol	<2.2e-16	<2.2e-16
GO:0044428	nuclear part	<2.2e-16	<2.2e-16
GO:0031981	nuclear lumen	<2.2e-16	<2.2e-16
GO:0043228	non-membrane-bounded organelle	<2.2e-16	<2.2e-16
GO:0043232	intracellular non-membrane-bounded organelle	<2.2e-16	<2.2e-16
GO:0005654	nucleoplasm	<2.2e-16	<2.2e-16
GO:0005856	cytoskeleton	<2.2e-16	<2.2e-16
GO:0044430	cytoskeletal part	<2.2e-16	<2.2e-16

Table 49. Top KEGG pathways from over-representation analyses on up-regulated genes from the comparison between C-ion irradiated cells collected 24 hrs post-irradiation and sham-irradiated ones under 1G.

Gene Set	Description	P Value	FDR
C0023893	Liver Cirrhosis, Experimental	5.18E-08	0.000413
GO:0030198	extracellular matrix organization	1.74E-05	0.064552
GO:0043062	extracellular structure organization	2.43E-05	0.064552
GO:0001503	ossification	4.24E-05	0.084528
C0003504	Aortic Valve Insufficiency	6.99E-05	0.11154
C2973725	Pulmonary arterial hypertension	0.000164	0.15077
C3203102	Idiopathic pulmonary arterial hypertension	0.000164	0.15077
C0018772	Hearing Loss, Partial	0.000194	0.15077
C0339789	Congenital deafness	0.000194	0.15077
GO:0009887	animal organ morphogenesis	0.000206	0.15077

Table 50. Top KEGG pathways from over-representation analyses on down-regulated genes from the comparison between C-ion irradiated cells collected 24 hrs post-irradiation and sham-irradiated ones under 1G.

Gene Set	Description	P Value	FDR
hsa05034	Alcoholism	<2.2e-16	<2.2e-16
hsa04110	Cell cycle	<2.2e-16	<2.2e-16
hsa05322	Systemic lupus erythematosus	<2.2e-16	<2.2e-16
hsa03030	DNA replication	<2.2e-16	<2.2e-16
hsa05203	Viral carcinogenesis	4.52E-12	2.98E-10
hsa03440	Homologous recombination	2.33E-11	1.14E-09
hsa03460	Fanconi anemia pathway	2.42E-11	1.14E-09
hsa03430	Mismatch repair	5.17E-10	2.13E-08
hsa03040	Spliceosome	1.67E-08	6.11E-07
hsa03410	Base excision repair	1.72E-06	5.65E-05
hsa03013	RNA transport	6.84E-06	0.000205
hsa04114	Oocyte meiosis	5.15E-05	0.001413
hsa03420	Nucleotide excision repair	0.000134	0.003295
hsa00240	Pyrimidine metabolism	0.00014	0.003295
hsa04914	Progesterone-mediated oocyte maturation	0.000167	0.003667
hsa04217	Necroptosis	0.000179	0.003691
hsa04218	Cellular senescence	0.00033	0.006387
hsa05166	Human T-cell leukemia virus 1 infection	0.000447	0.008167
hsa05206	MicroRNAs in cancer	0.002217	0.038389
hsa03450	Non-homologous end-joining	0.002388	0.039286

3.6. Late vs early response genes to C-ion irradiation under 1G

From the comparison between C-ion irradiated cells collected 24 and 3 hrs post-irradiation under 1G (C24G-C3G), 147 up- and 563 down-regulated genes were identified. Statistically significant terms were not found after performing over-representation analyses for over-expressed genes. For under-expressed genes, enrichment analyses in all Gene Ontology domains, as well as in KEGG pathways, highlighted cell cycle related terms. Biological processes related to response to stimulus and DNA repair were identified. E2F was found as a gene-targeting transcription factor. Down-regulated genes, whose expression was found to be expressed 3-5 times less, were *MKI67*, *H2BC18*, *H1-3*, *H2AC18*, *TMPO*, *H4C4* and *H3C3*.

Table 51. Top up-regulated genes from the comparison between C-ion irradiated cells collected 24 and 3 hrs post-irradiation under 1G.

Gene Id	Gene Name	Description	svalue
ENSG00000230590	*FTX*	FTX transcript, XIST regulator [Source:HGNC Symbol;Acc:HGNC:37190]	8.50E-12
ENSG00000128641	*MYO1B*	myosin IB [Source:HGNC Symbol;Acc:HGNC:7596]	2.11E-11
ENSG00000153944	*MSI2*	musashi RNA binding protein 2 [Source:HGNC Symbol;Acc:HGNC:18585]	4.66E-09
ENSG00000214548	*MEG3*	maternally expressed 3 [Source:HGNC Symbol;Acc:HGNC:14575]	8.59E-09
ENSG00000225830	*ERCC6*	ERCC excision repair 6, chromatin remodeling factor [Source:HGNC Symbol;Acc:HGNC:3438]	1.04E-08
ENSG00000204941	*PSG5*	pregnancy specific beta-1-glycoprotein 5 [Source:HGNC Symbol;Acc:HGNC:9522]	5.47E-08
ENSG00000148634	*HERC4*	HECT and RLD domain containing E3 ubiquitin protein ligase 4 [Source:HGNC Symbol;Acc:HGNC:24521]	5.77E-08
ENSG00000221852	*KRTAP1-5*	keratin associated protein 1-5 [Source:HGNC Symbol;Acc:HGNC:16777]	8.10E-08
ENSG00000185742	*C11orf87*	chromosome 11 open reading frame 87 [Source:HGNC Symbol;Acc:HGNC:33788]	1.01E-07
ENSG00000171451	*DSEL*	dermatan sulfate epimerase like [Source:HGNC Symbol;Acc:HGNC:18144]	1.31E-07
ENSG00000164663	*USP49*	ubiquitin specific peptidase 49 [Source:HGNC Symbol;Acc:HGNC:20078]	2.71E-07
ENSG00000101333	*PLCB4*	phospholipase C beta 4 [Source:HGNC Symbol;Acc:HGNC:9059]	3.25E-07
ENSG00000103888	*CEMIP*	cell migration inducing hyaluronidase 1 [Source:HGNC Symbol;Acc:HGNC:29213]	3.38E-07
ENSG00000198796	*ALPK2*	alpha kinase 2 [Source:HGNC Symbol;Acc:HGNC:20565]	6.56E-07
ENSG00000033867	*SLC4A7*	solute carrier family 4 member 7 [Source:HGNC Symbol;Acc:HGNC:11033]	7.70E-07
ENSG00000152661	*GJA1*	gap junction protein alpha 1 [Source:HGNC Symbol;Acc:HGNC:4274]	1.10E-06
ENSG00000146463	*ZMYM4*	zinc finger MYM-type containing 4 [Source:HGNC Symbol;Acc:HGNC:13055]	1.78E-06
ENSG00000113328	*CCNG1*	cyclin G1 [Source:HGNC Symbol;Acc:HGNC:1592]	2.26E-06
ENSG00000185088	*RPS27L*	ribosomal protein S27 like [Source:HGNC Symbol;Acc:HGNC:18476]	2.61E-06
ENSG00000138061	*CYP1B1*	cytochrome P450 family 1 subfamily B member 1 [Source:HGNC Symbol;Acc:HGNC:2597]	2.71E-06

Table 52. Top down-regulated genes from the comparison between C-ion irradiated cells collected 24 and 3 hrs post-irradiation under 1G.

Gene Id	Gene Name	Description	svalue
ENSG00000148773	*MKI67*	marker of proliferation Ki-67 [Source:HGNC Symbol;Acc:HGNC:7107]	7.82E-51
ENSG00000203814	*H2BC18*	H2B clustered histone 18 [Source:HGNC Symbol;Acc:HGNC:24700]	9.19E-51
ENSG00000124575	*H1-3*	H1.3 linker histone, cluster member [Source:HGNC Symbol;Acc:HGNC:4717]	2.25E-41
ENSG00000288825	*H2AC18*	H2A clustered histone 18 [Source:HGNC Symbol;Acc:HGNC:4736]	2.24E-40
ENSG00000120802	*TMPO*	thymopoietin [Source:HGNC Symbol;Acc:HGNC:11875]	4.46E-40
ENSG00000277157	*H4C4*	H4 clustered histone 4 [Source:HGNC Symbol;Acc:HGNC:4782]	1.12E-39

ENSG00000287080	*H3C3*	H3 clustered histone 3 [Source:HGNC Symbol;Acc:HGNC:4768]	4.13E-39
ENSG00000176619	*LMNB2*	lamin B2 [Source:HGNC Symbol;Acc:HGNC:6638]	3.92E-38
ENSG00000187837	*H1-2*	H1.2 linker histone, cluster member [Source:HGNC Symbol;Acc:HGNC:4716]	2.64E-37
ENSG00000196787	*H2AC11*	H2A clustered histone 11 [Source:HGNC Symbol;Acc:HGNC:4737]	3.90E-36
ENSG00000184357	*H1-5*	H1.5 linker histone, cluster member [Source:HGNC Symbol;Acc:HGNC:4719]	1.52E-35
ENSG00000203852	*H3C15*	H3 clustered histone 15 [Source:HGNC Symbol;Acc:HGNC:20505]	3.27E-35
ENSG00000278828	*H3C10*	H3 clustered histone 10 [Source:HGNC Symbol;Acc:HGNC:4775]	6.89E-34
ENSG00000274997	*H2AC12*	H2A clustered histone 12 [Source:HGNC Symbol;Acc:HGNC:13671]	7.87E-33
ENSG00000277075	*H2AC8*	H2A clustered histone 8 [Source:HGNC Symbol;Acc:HGNC:4724]	1.83E-32
ENSG00000183856	*IQGAP3*	IQ motif containing GTPase activating protein 3 [Source:HGNC Symbol;Acc:HGNC:20669]	1.27E-31
ENSG00000158373	*H2BC5*	H2B clustered histone 5 [Source:HGNC Symbol;Acc:HGNC:4747]	1.19E-30
ENSG00000054654	*SYNE2*	spectrin repeat containing nuclear envelope protein 2 [Source:HGNC Symbol;Acc:HGNC:17084]	3.52E-30
ENSG00000273983	*H3C8*	H3 clustered histone 8 [Source:HGNC Symbol;Acc:HGNC:4772]	5.66E-30
ENSG00000197903	*H2BC12*	H2B clustered histone 12 [Source:HGNC Symbol;Acc:HGNC:13954]	7.77E-30

Table 53. Top biological processes from over-representation on up-regulated genes from the comparison between C-ion irradiated cells collected 24 and 3 hrs post-irradiation under 1G.

Gene Set	Description	P Value	FDR
GO:0071840	cellular component organization or biogenesis	<2.2e-16	<2.2e-16
GO:0016043	cellular component organization	<2.2e-16	<2.2e-16
GO:0006996	organelle organization	<2.2e-16	<2.2e-16
GO:0007049	cell cycle	<2.2e-16	<2.2e-16
GO:0022402	cell cycle process	<2.2e-16	<2.2e-16
GO:0051276	chromosome organization	<2.2e-16	<2.2e-16
GO:0051726	regulation of cell cycle	<2.2e-16	<2.2e-16
GO:0006259	DNA metabolic process	<2.2e-16	<2.2e-16
GO:0000278	mitotic cell cycle	<2.2e-16	<2.2e-16
GO:0006974	cellular response to DNA damage stimulus	<2.2e-16	<2.2e-16
GO:1903047	mitotic cell cycle process	<2.2e-16	<2.2e-16
GO:0007017	microtubule-based process	<2.2e-16	<2.2e-16
GO:0006325	chromatin organization	<2.2e-16	<2.2e-16
GO:0010564	regulation of cell cycle process	<2.2e-16	<2.2e-16
GO:0007346	regulation of mitotic cell cycle	<2.2e-16	<2.2e-16
GO:0051301	cell division	<2.2e-16	<2.2e-16
GO:0045786	negative regulation of cell cycle	<2.2e-16	<2.2e-16
GO:0044770	cell cycle phase transition	<2.2e-16	<2.2e-16
GO:0006281	DNA repair	<2.2e-16	<2.2e-16
GO:0000226	microtubule cytoskeleton organization	<2.2e-16	<2.2e-16

Table 54. Top molecular functions from over-representation on down-regulated genes from the comparison between C-ion irradiated cells collected 24 and 3 hrs post-irradiation under 1G.

Gene Set	Description	P Value	FDR
GO:0005515	protein binding	<2.2e-16	<2.2e-16

GO:0003676	nucleic acid binding	<2.2e-16	<2.2e-16
GO:0003677	DNA binding	<2.2e-16	<2.2e-16
GO:0003682	chromatin binding	<2.2e-16	<2.2e-16
GO:1901363	heterocyclic compound binding	2.22E-16	1.31E-13
GO:0097159	organic cyclic compound binding	3.33E-16	1.64E-13
GO:0140097	catalytic activity, acting on DNA	4.54E-12	1.92E-09
GO:0046982	protein heterodimerization activity	5.27E-12	1.95E-09
GO:0005524	ATP binding	9.78E-12	2.90E-09
GO:0035639	purine ribonucleoside triphosphate binding	9.81E-12	2.90E-09
GO:0000166	nucleotide binding	1.34E-11	3.42E-09
GO:1901265	nucleoside phosphate binding	1.39E-11	3.42E-09
GO:0008017	microtubule binding	4.39E-11	9.98E-09
GO:0017076	purine nucleotide binding	6.29E-11	1.33E-08
GO:0032555	purine ribonucleotide binding	7.72E-11	1.39E-08
GO:0017111	nucleoside-triphosphatase activity	8.32E-11	1.39E-08
GO:0015631	tubulin binding	8.38E-11	1.39E-08
GO:0032559	adenyl ribonucleotide binding	8.45E-11	1.39E-08
GO:0032553	ribonucleotide binding	1.17E-10	1.81E-08
GO:0030554	adenyl nucleotide binding	1.44E-10	2.13E-08

Table 55. Top cellular components from over-representation on down-regulated genes from the comparison between C-ion irradiated cells collected 24 and 3 hrs post-irradiation under 1G.

Gene Set	Description	P Value	FDR
GO:0043226	organelle	<2.2e-16	<2.2e-16
GO:0043229	intracellular organelle	<2.2e-16	<2.2e-16
GO:0043231	intracellular membrane-bounded organelle	<2.2e-16	<2.2e-16
GO:0044422	organelle part	<2.2e-16	<2.2e-16
GO:0044446	intracellular organelle part	<2.2e-16	<2.2e-16
GO:0005634	nucleus	<2.2e-16	<2.2e-16
GO:0031974	membrane-enclosed lumen	<2.2e-16	<2.2e-16
GO:0043233	organelle lumen	<2.2e-16	<2.2e-16
GO:0070013	intracellular organelle lumen	<2.2e-16	<2.2e-16
GO:0032991	protein-containing complex	<2.2e-16	<2.2e-16
GO:0044428	nuclear part	<2.2e-16	<2.2e-16
GO:0031981	nuclear lumen	<2.2e-16	<2.2e-16
GO:0043228	non-membrane-bounded organelle	<2.2e-16	<2.2e-16
GO:0043232	intracellular non-membrane-bounded organelle	<2.2e-16	<2.2e-16
GO:0005654	nucleoplasm	<2.2e-16	<2.2e-16
GO:0044430	cytoskeletal part	<2.2e-16	<2.2e-16
GO:0015630	microtubule cytoskeleton	<2.2e-16	<2.2e-16
GO:0005694	chromosome	<2.2e-16	<2.2e-16
GO:0044427	chromosomal part	<2.2e-16	<2.2e-16
GO:0000228	nuclear chromosome	<2.2e-16	<2.2e-16

Table 56. Top KEGG pathways from over-representation on down-regulated genes from the comparison between C-ion irradiated cells collected 24 and 3 hrs post-irradiation under 1G.

Gene Set	Description	P Value	FDR
hsa05034	Alcoholism	<2.2e-16	<2.2e-16
hsa04110	Cell cycle	<2.2e-16	<2.2e-16
hsa05322	Systemic lupus erythematosus	<2.2e-16	<2.2e-16
hsa03030	DNA replication	8.88E-16	7.31E-14
hsa05203	Viral carcinogenesis	1.55E-15	1.02E-13
hsa04217	Necroptosis	2.41E-07	1.32E-05
hsa03440	Homologous recombination	6.22E-07	2.93E-05
hsa03430	Mismatch repair	1.04E-06	4.28E-05
hsa03410	Base excision repair	3.89E-06	0.000142
hsa04114	Oocyte meiosis	3.83E-05	0.001262
hsa03460	Fanconi anemia pathway	0.00038	0.011378
hsa04914	Progesterone-mediated oocyte maturation	0.000542	0.014568
hsa03420	Nucleotide excision repair	0.000576	0.014568
hsa05206	MicroRNAs in cancer	0.000847	0.019906
hsa04218	Cellular senescence	0.001361	0.029844
hsa05166	Human T-cell leukemia virus 1 infection	0.001615	0.033206
hsa04115	p53 signaling pathway	0.001932	0.037384

3.7. Effects of simulated µG on sham-irradiated cells

From the comparison of sham-irradiated cells under simulated µG and 1G (X0µG-X0G and C0µG-C0G), up-regulated genes were identified and among those *PCDHGC4* and *PCLO* were prominent. After performing over-representation analyses for over-expressed genes, statistically significant terms were not found. Down-regulated genes were also identified and genes *TTN* and *MSTN* were found to be predominant based on their log2 fold changes. For under-expressed genes, enrichment analyses in all Gene Ontology aspects highlighted response to oxygen levels, muscle contraction and regulation of blood circulation related terms. The prevalent KEGG pathway identified was Pathogenic Escherichia coli infection. SRF was identified as a gene-targeting transcription factor for down-regulated genes.

Table 57. Top up-regulated genes from the comparison of sham-irradiated cells under simulated µG and 1G.

Gene Id	Gene Name	Description	svalue
ENSG00000013297	*CLDN11*	claudin 11 [Source:HGNC Symbol;Acc:HGNC:8514]	2.70E-09
ENSG00000167325	*RRM1*	ribonucleotide reductase catalytic subunit M1 [Source:HGNC Symbol;Acc:HGNC:10451]	1.25E-05
ENSG00000173852	*DPY19L1*	dpy-19 like C-mannosyltransferase 1 [Source:HGNC Symbol;Acc:HGNC:22205]	1.47E-05
ENSG00000242419	*PCDHGC4*	protocadherin gamma subfamily C, 4 [Source:HGNC Symbol;Acc:HGNC:8717]	2.20E-05
ENSG00000272333	*KMT2B*	lysine methyltransferase 2B [Source:HGNC Symbol;Acc:HGNC:15840]	2.52E-05
ENSG00000182580	*EPHB3*	EPH receptor B3 [Source:HGNC Symbol;Acc:HGNC:3394]	3.16E-05
ENSG00000155761	*SPAG17*	sperm associated antigen 17 [Source:HGNC Symbol;Acc:HGNC:26620]	6.90E-05
ENSG00000129226	*CD68*	CD68 molecule [Source:HGNC Symbol;Acc:HGNC:1693]	7.78E-05
ENSG00000177706	*FAM20C*	FAM20C golgi associated secretory pathway kinase [Source:HGNC Symbol;Acc:HGNC:22140]	9.67E-05
ENSG00000186472	*PCLO*	piccolo presynaptic cytomatrix protein [Source:HGNC Symbol;Acc:HGNC:13406]	0.000107
ENSG00000100393	*EP300*	E1A binding protein p300 [Source:HGNC Symbol;Acc:HGNC:3373]	0.000193

ENSG00000185760	*KCNQ5*	potassium voltage-gated channel subfamily Q member 5 [Source:HGNC Symbol;Acc:HGNC:6299]	0.000211
ENSG00000009830	*POMT2*	protein O-mannosyltransferase 2 [Source:HGNC Symbol;Acc:HGNC:19743]	0.000311
ENSG00000079931	*MOXD1*	monooxygenase DBH like 1 [Source:HGNC Symbol;Acc:HGNC:21063]	0.000336
ENSG00000161800	*RACGAP1*	Rac GTPase activating protein 1 [Source:HGNC Symbol;Acc:HGNC:9804]	0.000363
ENSG00000148700	*ADD3*	adducin 3 [Source:HGNC Symbol;Acc:HGNC:245]	0.000517
ENSG00000134802	*SLC43A3*	solute carrier family 43 member 3 [Source:HGNC Symbol;Acc:HGNC:17466]	0.00057
ENSG00000011426	*ANLN*	anillin actin binding protein [Source:HGNC Symbol;Acc:HGNC:14082]	0.000663
ENSG00000147536	*GINS4*	GINS complex subunit 4 [Source:HGNC Symbol;Acc:HGNC:28226]	0.000757
ENSG00000135919	*SERPINE2*	serpin family E member 2 [Source:HGNC Symbol;Acc:HGNC:8951]	0.000827

Table 58. Top down-regulated genes from the comparison of sham-irradiated cells under simulated µG and 1G.

Gene Id	Gene Name	Description	svalue
ENSG00000128534	*LSM8*	LSM8 homolog, U6 small nuclear RNA associated [Source:HGNC Symbol;Acc:HGNC:20471]	2.89E-09
ENSG00000155657	*TTN*	titin [Source:HGNC Symbol;Acc:HGNC:12403]	5.15E-09
ENSG00000138771	*SHROOM3*	shroom family member 3 [Source:HGNC Symbol;Acc:HGNC:30422]	7.88E-09
ENSG00000140416	*TPM1*	tropomyosin 1 [Source:HGNC Symbol;Acc:HGNC:12010]	1.15E-08
ENSG00000173641	*HSPB7*	heat shock protein family B (small) member 7 [Source:HGNC Symbol;Acc:HGNC:5249]	1.47E-08
ENSG00000198467	*TPM2*	tropomyosin 2 [Source:HGNC Symbol;Acc:HGNC:12011]	8.34E-08
ENSG00000118523	*CCN2*	cellular communication network factor 2 [Source:HGNC Symbol;Acc:HGNC:2500]	2.26E-07
ENSG00000138379	*MSTN*	myostatin [Source:HGNC Symbol;Acc:HGNC:4223]	3.56E-07
ENSG00000140443	*IGF1R*	insulin like growth factor 1 receptor [Source:HGNC Symbol;Acc:HGNC:5465]	4.86E-07
ENSG00000107796	*ACTA2*	actin alpha 2, smooth muscle [Source:HGNC Symbol;Acc:HGNC:130]	7.51E-07
ENSG00000172403	*SYNPO2*	synaptopodin 2 [Source:HGNC Symbol;Acc:HGNC:17732]	1.03E-06
ENSG00000180914	*OXTR*	oxytocin receptor [Source:HGNC Symbol;Acc:HGNC:8529]	1.74E-06
ENSG00000116016	*EPAS1*	endothelial PAS domain protein 1 [Source:HGNC Symbol;Acc:HGNC:3374]	3.01E-06
ENSG00000096696	*DSP*	desmoplakin [Source:HGNC Symbol;Acc:HGNC:3052]	4.69E-06
ENSG00000132530	*XAF1*	XIAP associated factor 1 [Source:HGNC Symbol;Acc:HGNC:30932]	6.54E-06
ENSG00000115419	*GLS*	glutaminase [Source:HGNC Symbol;Acc:HGNC:4331]	8.51E-06
ENSG00000137801	*THBS1*	thrombospondin 1 [Source:HGNC Symbol;Acc:HGNC:11785]	1.05E-05
ENSG00000163431	*LMOD1*	leiomodin 1 [Source:HGNC Symbol;Acc:HGNC:6647]	1.70E-05
ENSG00000157601	*MX1*	MX dynamin like GTPase 1 [Source:HGNC Symbol;Acc:HGNC:7532]	1.93E-05
ENSG00000142149	*HUNK*	hormonally up-regulated Neu-associated kinase [Source:HGNC Symbol;Acc:HGNC:13326]	2.84E-05

Table 59. Top biological processes from over-representation analyses on down-regulated genes from the comparison of sham-irradiated cells under simulated µG and 1G.

Gene Set	Description	P Value	FDR
GO:0034059	response to anoxia	0.000035361	0.0192
GO:0030049	muscle filament sliding	0.000057698	0.023412
GO:0033275	actin-myosin filament sliding	0.000057698	0.023412
GO:0071675	regulation of mononuclear cell migration	0.00018137	0.045996
GO:0032233	positive regulation of actin filament bundle assembly	0.00004099	0.019959
GO:0070252	actin-mediated cell contraction	7.5112E-06	0.0060956
GO:0060337	type I interferon signaling pathway	0.000083191	0.028934

GO:0071357	cellular response to type I interferon	0.000083191	0.028934
GO:0060048	cardiac muscle contraction	0.000013482	0.0091173
GO:0034340	response to type I interferon	0.00011026	0.031241
GO:0030048	actin filament-based movement	0.00002264	0.014447
GO:0032231	regulation of actin filament bundle assembly	0.00020061	0.049837
GO:0006936	muscle contraction	6.91E-10	4.2589E-06
GO:0006941	striated muscle contraction	0.000046619	0.021018
GO:0060047	heart contraction	1.8437E-06	0.0032062
GO:0003015	heart process	2.5012E-06	0.003383
GO:0003012	muscle system process	7.00E-10	4.2589E-06
GO:1902905	positive regulation of supramolecular fiber organization	0.000030402	0.017623
GO:0008016	regulation of heart contraction	0.00016421	0.042531
GO:1903522	regulation of blood circulation	0.000037853	0.0192

Table 60. Top molecular functions from over-representation analyses on down-regulated genes from the comparison of sham-irradiated cells under simulated µG and 1G.

Gene Set	Description	P Value	FDR
GO:0003779	actin binding	3.65E-07	0.00108
GO:0008092	cytoskeletal protein binding	2.96E-06	0.004373

Table 61. Top cellular components from over-representation analyses on down-regulated genes from the comparison of sham-irradiated cells under simulated µG and 1G.

Gene Set	Description	P Value	FDR
GO:0015629	actin cytoskeleton	1.19E-08	1.98E-05
GO:0043292	contractile fiber	1.28E-07	0.000106
GO:0099512	supramolecular fiber	3.11E-07	0.000118
GO:0099081	supramolecular polymer	3.49E-07	0.000118
GO:0099080	supramolecular complex	3.54E-07	0.000118
GO:0005865	striated muscle thin filament	4.31E-07	0.00012
GO:0036379	myofilament	5.38E-07	0.000128
GO:0044449	contractile fiber part	1.19E-06	0.000248
GO:0030016	myofibril	1.4E-06	0.000259
GO:0030017	sarcomere	9.94E-06	0.001655
GO:0032432	actin filament bundle	5.58E-05	0.008454
GO:0005862	muscle thin filament tropomyosin	6.72E-05	0.009323
GO:0005856	cytoskeleton	0.000177	0.022622

3.8. Response to simulated µG in cells collected 3 hrs after C-ion irradiation

In the comparison referring to the response to simulated µG in cells collected 3 hrs after C-ion-irradiation (C3µG-C3G), cell cycle promoting terms, such as cell division, were over-represented in up-regulated genes. In comparisons involving the response to simulated µG in cells collected 3 hrs after X-ray-irradiation (X3µG-X3G), 24 hrs after X-ray-irradiation (X24µG-X24G), or 24 hrs after C-ion-irradiation (C24µG-C24G), no enriched biological terms were identified.

3.9. Early response genes to X-ray irradiation and simulated µG combined effect

From the comparison between X-ray irradiated cells collected 3 hrs post-irradiation under simulated µG and sham-irradiated under 1G (X3µG-X0G), 76 over-expressed genes were found and among

those *CDKN1A*, *MDM2*, *FDXR*, *PTCHD4*, *TP53INP1*, *BTG2* and *GDF15* stood out. Likewise, 21 under-expressed genes were found to be statistically significant. Down-regulated genes *FAM111B*, *ZNF367* and *VIM-AS1* stood out. Concerning the over-expressed genes, enrichment analyses for Gene Ontology biological processes and KEGG pathways highlighted the p53 signaling pathway. Biological processes related to response to stimulus and apoptosis were also identified. Focusing on under-expressed genes, biological term over-representation analyses highlighted cell cycle related biological processes.

Table 62. Top up -regulated genes from the comparison between X-ray irradiated cells collected 3 hrs post-irradiation under simulated µG and sham-irradiated under 1G.

Gene Id	Gene Name	Description	svalue
ENSG00000124762	*CDKN1A*	cyclin dependent kinase inhibitor 1A [Source:HGNC Symbol;Acc:HGNC:1784]	7.92E-63
ENSG00000135679	*MDM2*	MDM2 proto-oncogene [Source:HGNC Symbol;Acc:HGNC:6973]	2.10E-44
ENSG00000256664	*NA*	ribosomal L24 domain containing 1 (RSL24D1) pseudogene	1.14E-22
ENSG00000174307	*PHLDA3*	pleckstrin homology like domain family A member 3 [Source:HGNC Symbol;Acc:HGNC:8934]	3.20E-18
ENSG00000161513	*FDXR*	ferredoxin reductase [Source:HGNC Symbol;Acc:HGNC:3642]	7.94E-17
ENSG00000168497	*CAVIN2*	caveolae associated protein 2 [Source:HGNC Symbol;Acc:HGNC:10690]	3.34E-16
ENSG00000172667	*ZMAT3*	zinc finger matrin-type 3 [Source:HGNC Symbol;Acc:HGNC:29983]	3.05E-15
ENSG00000244694	*PTCHD4*	patched domain containing 4 [Source:HGNC Symbol;Acc:HGNC:21345]	5.46E-15
ENSG00000026103	*FAS*	Fas cell surface death receptor [Source:HGNC Symbol;Acc:HGNC:11920]	1.27E-14
ENSG00000080546	*SESN1*	sestrin 1 [Source:HGNC Symbol;Acc:HGNC:21595]	2.09E-13
ENSG00000159388	*BTG2*	BTG anti-proliferation factor 2 [Source:HGNC Symbol;Acc:HGNC:1131]	3.79E-13
ENSG00000170734	*POLH*	DNA polymerase eta [Source:HGNC Symbol;Acc:HGNC:9181]	1.06E-12
ENSG00000028277	*POU2F2*	POU class 2 homeobox 2 [Source:HGNC Symbol;Acc:HGNC:9213]	2.66E-12
ENSG00000164938	*TP53INP1*	tumor protein p53 inducible nuclear protein 1 [Source:HGNC Symbol;Acc:HGNC:18022]	6.06E-12
ENSG00000148400	*NOTCH1*	notch receptor 1 [Source:HGNC Symbol;Acc:HGNC:7881]	1.41E-11
ENSG00000130513	*GDF15*	growth differentiation factor 15 [Source:HGNC Symbol;Acc:HGNC:30142]	2.80E-11
ENSG00000250337	*PURPL*	p53 upregulated regulator of p53 levels [Source:HGNC Symbol;Acc:HGNC:48995]	4.20E-11
ENSG00000182752	*PAPPA*	pappalysin 1 [Source:HGNC Symbol;Acc:HGNC:8602]	1.42E-10
ENSG00000048392	*RRM2B*	ribonucleotide reductase regulatory TP53 inducible subunit M2B [Source:HGNC Symbol;Acc:HGNC:17296]	2.90E-10
ENSG00000167196	*FBXO22*	F-box protein 22 [Source:HGNC Symbol;Acc:HGNC:13593]	6.18E-10

Table 63. Top down -regulated genes from the comparison between X-ray irradiated cells collected 3 hrs post-irradiation under simulated µG and sham-irradiated under 1G.

Gene Id	Gene Name	Description	svalue
ENSG00000254681	*PKD1P5*	polycystin 1, transient receptor potential channel interacting pseudogene 5 [Source:HGNC Symbol;Acc:HGNC:30069]	3.91E-07
ENSG00000229124	*VIM-AS1*	VIM antisense RNA 1 [Source:HGNC Symbol;Acc:HGNC:44879]	1.85E-06
ENSG00000165244	*ZNF367*	zinc finger protein 367 [Source:HGNC Symbol;Acc:HGNC:18320]	4.96E-06
ENSG00000013573	*DDX11*	DEAD/H-box helicase 11 [Source:HGNC Symbol;Acc:HGNC:2736]	5.62E-06
ENSG00000206588	*RNU1-28P*	RNA, U1 small nuclear 28, pseudogene [Source:HGNC Symbol;Acc:HGNC:37498]	1.31E-05
ENSG00000075303	*SLC25A40*	solute carrier family 25 member 40 [Source:HGNC Symbol;Acc:HGNC:29680]	1.76E-05
ENSG00000135362	*PRR5L*	proline rich 5 like [Source:HGNC Symbol;Acc:HGNC:25878]	2.32E-05
ENSG00000189057	*FAM111B*	FAM111 trypsin like peptidase B [Source:HGNC Symbol;Acc:HGNC:24200]	2.88E-05
ENSG00000198824	*CHAMP1*	chromosome alignment maintaining phosphoprotein 1 [Source:HGNC Symbol;Acc:HGNC:20311]	4.63E-05

ENSG00000187741	*FANCA*	FA complementation group A [Source:HGNC Symbol;Acc:HGNC:3582]	5.18E-05
ENSG00000167670	*CHAF1A*	chromatin assembly factor 1 subunit A [Source:HGNC Symbol;Acc:HGNC:1910]	7.98E-05
ENSG00000183598	*H3C13*	H3 clustered histone 13 [Source:HGNC Symbol;Acc:HGNC:25311]	8.78E-05
ENSG00000288894	*NA*	novel protein	9.56E-05
ENSG00000119969	*HELLS*	helicase, lymphoid specific [Source:HGNC Symbol;Acc:HGNC:4861]	0.000134
ENSG00000138346	*DNA2*	DNA replication helicase/nuclease 2 [Source:HGNC Symbol;Acc:HGNC:2939]	0.000237
ENSG00000175305	*CCNE2*	cyclin E2 [Source:HGNC Symbol;Acc:HGNC:1590]	0.000327
ENSG00000115421	*PAPOLG*	poly(A) polymerase gamma [Source:HGNC Symbol;Acc:HGNC:14982]	0.000377
ENSG00000210082	*MT-RNR2*	mitochondrially encoded 16S rRNA [Source:HGNC Symbol;Acc:HGNC:7471]	0.000404
ENSG00000164045	*CDC25A*	cell division cycle 25A [Source:HGNC Symbol;Acc:HGNC:1725]	0.000516
ENSG00000102317	*RBM3*	RNA binding motif protein 3 [Source:HGNC Symbol;Acc:HGNC:9900]	0.000733

Table 64. Top biological processes from over-representation analyses on up -regulated genes from the comparison between X-ray irradiated cells collected 3 hrs post-irradiation under simulated µG and sham-irradiated under 1G.

Gene Set	Description	P Value	FDR
GO:0033554	cellular response to stress	9.23E-13	1.20E-08
GO:0006974	cellular response to DNA damage stimulus	9.61E-11	6.26E-07
GO:0006950	response to stress	7.03E-10	3.06E-06
GO:0044774	mitotic DNA integrity checkpoint	6.91E-09	2.25E-05
GO:0072331	signal transduction by p53 class mediator	1.00E-08	2.62E-05
GO:0007093	mitotic cell cycle checkpoint	1.30E-08	2.83E-05
GO:0034644	cellular response to UV	2.49E-08	4.65E-05
GO:0044773	mitotic DNA damage checkpoint	8.78E-08	0.000143
GO:0097193	intrinsic apoptotic signaling pathway	1.26E-07	0.000173
GO:0000075	cell cycle checkpoint	1.33E-07	0.000173
GO:0031570	DNA integrity checkpoint	1.58E-07	0.000187
GO:0071214	cellular response to abiotic stimulus	3.68E-07	0.000369
GO:0104004	cellular response to environmental stimulus	3.68E-07	0.000369
GO:0072332	intrinsic apoptotic signaling pathway by p53 class mediator	4.55E-07	0.000414
GO:0071482	cellular response to light stimulus	5.01E-07	0.000414
GO:0051716	cellular response to stimulus	5.08E-07	0.000414
GO:0045930	negative regulation of mitotic cell cycle	5.59E-07	0.000414
GO:0071478	cellular response to radiation	5.72E-07	0.000414
GO:0050896	response to stimulus	7.78E-07	0.000534
GO:0009411	response to UV	1.08E-06	0.000673

Table 65. Top molecular functions from over-representation analyses on down -regulated genes from the comparison between X-ray irradiated cells collected 3 hrs post-irradiation under simulated µG and sham-irradiated under 1G.

Gene Set	Description	P Value	FDR
GO:0007049	cell cycle	1.81E-06	0.023608
GO:0006259	DNA metabolic process	5.36E-06	0.03496

Table 66. Top cellular components from over-representation analyses on down -regulated genes from the comparison between X-ray irradiated cells collected 3 hrs post-irradiation under simulated µG and sham-irradiated under 1G.

Gene Set	Description	P Value	FDR
GO:0031981	nuclear lumen	1.6E-05	0.016806
GO:0044427	chromosomal part	3.43E-05	0.016806
GO:0005654	nucleoplasm	3.68E-05	0.016806
GO:0044428	nuclear part	3.89E-05	0.016806
GO:0005694	chromosome	7.35E-05	0.025361
GO:0098687	chromosomal region	0.000107	0.030872
GO:0031974	membrane-enclosed lumen	0.000198	0.037891
GO:0043233	organelle lumen	0.000198	0.037891
GO:0070013	intracellular organelle lumen	0.000198	0.037891

Table 67. Top KEGG pathways from over-representation analyses on up -regulated genes from the comparison between X-ray irradiated cells collected 3 hrs post-irradiation under simulated µG and sham-irradiated under 1G.

Gene Set	Description	P Value	FDR
hsa04115	p53 signaling pathway	2.22E-16	7.31E-14
hsa01524	Platinum drug resistance	1.31E-09	2.16E-07
hsa05220	Chronic myeloid leukemia	2.94E-05	0.003226
hsa05202	Transcriptional misregulation in cancer	0.000228	0.01875
hsa05214	Glioma	0.000364	0.019079
hsa05218	Melanoma	0.000384	0.019079
hsa05212	Pancreatic cancer	0.000448	0.019079
hsa04210	Apoptosis	0.000464	0.019079
hsa04215	Apoptosis	0.000522	0.019079
hsa05216	Thyroid cancer	0.000733	0.022561
hsa05210	Colorectal cancer	0.000754	0.022561
hsa05222	Small cell lung cancer	0.001012	0.027755
hsa01522	Endocrine resistance	0.00114	0.028849

3.10. Late response genes to X-ray irradiation and simulated µG combined effect

From the comparison between X-ray irradiated cells collected 24 hrs post-irradiation under simulated µG and sham-irradiated cells under 1G (X24µG-X0G), 877 up- and 1429 down-regulated genes were found. Over-expressed genes *PTCHD4*, *PURPL* and *PAPPA* were found to be predominant. Enrichment analyses in all Gene Ontology aspects highlighted terms related to cell proliferation and cardiovascular system development. The main KEGG pathway identified was the p53 signaling pathway. The transcription factor FOXO4 was also identified as a trans-activator of up-regulated genes. Furthermore, from over-expressed microRNAs: MIR-17, MIR-20A and MIR-106A were discovered. Among the down-regulated genes, many stood out. A few were *MKI67*, *ASPM*, *TPX2*, *IQGAP3*, *CENPF*, *KIF20B*, *CCNB1* and *CEP55*. Enrichment analyses in all Gene Ontology domains highlighted cell cycle and DNA repair related terms. The predominant KEGG pathway was found to be carcinogenesis. E2F was identified as a gene-targeting transcription factor for under-expressed genes.

Table 68. Top up -regulated genes from the comparison between X-ray irradiated cells collected 24 hrs post-irradiation under simulated µG and sham-irradiated under 1G.

Gene Id	Gene Name	Description	svalue
ENSG00000182752	*PAPPA*	pappalysin 1 [Source:HGNC Symbol;Acc:HGNC:8602]	8.94E-35

ENSG00000244694	*PTCHD4*	patched domain containing 4 [Source:HGNC Symbol;Acc:HGNC:21345]	1.27E-29
ENSG00000250337	*PURPL*	p53 upregulated regulator of p53 levels [Source:HGNC Symbol;Acc:HGNC:48995]	3.66E-29
ENSG00000127241	*MASP1*	MBL associated serine protease 1 [Source:HGNC Symbol;Acc:HGNC:6901]	5.50E-26
ENSG00000124762	*CDKN1A*	cyclin dependent kinase inhibitor 1A [Source:HGNC Symbol;Acc:HGNC:1784]	4.96E-23
ENSG00000172667	*ZMAT3*	zinc finger matrin-type 3 [Source:HGNC Symbol;Acc:HGNC:29983]	9.49E-19
ENSG00000136542	*GALNT5*	polypeptide N-acetylgalactosaminyltransferase 5 [Source:HGNC Symbol;Acc:HGNC:4127]	2.43E-18
ENSG00000101825	*MXRA5*	matrix remodeling associated 5 [Source:HGNC Symbol;Acc:HGNC:7539]	1.19E-16
ENSG00000105270	*CLIP3*	CAP-Gly domain containing linker protein 3 [Source:HGNC Symbol;Acc:HGNC:24314]	2.17E-16
ENSG00000135919	*SERPINE2*	serpin family E member 2 [Source:HGNC Symbol;Acc:HGNC:8951]	2.46E-16
ENSG00000123933	*MXD4*	MAX dimerization protein 4 [Source:HGNC Symbol;Acc:HGNC:13906]	1.29E-15
ENSG00000113328	*CCNG1*	cyclin G1 [Source:HGNC Symbol;Acc:HGNC:1592]	3.90E-15
ENSG00000072201	*LNX1*	ligand of numb-protein X 1 [Source:HGNC Symbol;Acc:HGNC:6657]	4.89E-15
ENSG00000132386	*SERPINF1*	serpin family F member 1 [Source:HGNC Symbol;Acc:HGNC:8824]	6.28E-15
ENSG00000168542	*COL3A1*	collagen type III alpha 1 chain [Source:HGNC Symbol;Acc:HGNC:2201]	1.69E-14
ENSG00000196576	*PLXNB2*	plexin B2 [Source:HGNC Symbol;Acc:HGNC:9104]	1.88E-14
ENSG00000168477	*TNXB*	tenascin XB [Source:HGNC Symbol;Acc:HGNC:11976]	2.08E-14
ENSG00000144810	*COL8A1*	collagen type VIII alpha 1 chain [Source:HGNC Symbol;Acc:HGNC:2215]	6.38E-14
ENSG00000149451	*ADAM33*	ADAM metallopeptidase domain 33 [Source:HGNC Symbol;Acc:HGNC:15478]	4.94E-13
ENSG00000184347	*SLIT3*	slit guidance ligand 3 [Source:HGNC Symbol;Acc:HGNC:11087]	6.46E-13

Table 69. Top down -regulated genes from the comparison between X-ray irradiated cells collected 24 hrs post-irradiation under simulated μG and sham-irradiated under 1G.

Gene Id	Gene Name	description	svalue
ENSG00000066279	*ASPM*	assembly factor for spindle microtubules [Source:HGNC Symbol;Acc:HGNC:19048]	2.81E-122
ENSG00000148773	*MKI67*	marker of proliferation Ki-67 [Source:HGNC Symbol;Acc:HGNC:7107]	7.41E-108
ENSG00000088325	*TPX2*	TPX2 microtubule nucleation factor [Source:HGNC Symbol;Acc:HGNC:1249]	3.32E-89
ENSG00000183856	*IQGAP3*	IQ motif containing GTPase activating protein 3 [Source:HGNC Symbol;Acc:HGNC:20669]	1.16E-85
ENSG00000188229	*TUBB4B*	tubulin beta 4B class IVb [Source:HGNC Symbol;Acc:HGNC:20771]	1.36E-80
ENSG00000182481	*KPNA2*	karyopherin subunit alpha 2 [Source:HGNC Symbol;Acc:HGNC:6395]	2.67E-80
ENSG00000117724	*CENPF*	centromere protein F [Source:HGNC Symbol;Acc:HGNC:1857]	1.94E-74
ENSG00000184357	*H1-5*	H1.5 linker histone, cluster member [Source:HGNC Symbol;Acc:HGNC:4719]	3.53E-72
ENSG00000138182	*KIF20B*	kinesin family member 20B [Source:HGNC Symbol;Acc:HGNC:7212]	1.95E-71
ENSG00000138778	*CENPE*	centromere protein E [Source:HGNC Symbol;Acc:HGNC:1856]	6.75E-71
ENSG00000138160	*KIF11*	kinesin family member 11 [Source:HGNC Symbol;Acc:HGNC:6388]	1.29E-69
ENSG00000134057	*CCNB1*	cyclin B1 [Source:HGNC Symbol;Acc:HGNC:1579]	2.82E-69
ENSG00000203852	*H3C15*	H3 clustered histone 15 [Source:HGNC Symbol;Acc:HGNC:20505]	1.10E-66
ENSG00000138180	*CEP55*	centrosomal protein 55 [Source:HGNC Symbol;Acc:HGNC:1161]	4.86E-66
ENSG00000131747	*TOP2A*	DNA topoisomerase II alpha [Source:HGNC Symbol;Acc:HGNC:11989]	7.21E-65
ENSG00000120802	*TMPO*	thymopoietin [Source:HGNC Symbol;Acc:HGNC:11875]	3.21E-64
ENSG00000136108	*CKAP2*	cytoskeleton associated protein 2 [Source:HGNC Symbol;Acc:HGNC:1990]	1.76E-62
ENSG00000123485	*HJURP*	Holliday junction recognition protein [Source:HGNC Symbol;Acc:HGNC:25444]	4.28E-62
ENSG00000286522	*H3C2*	H3 clustered histone 2 [Source:HGNC Symbol;Acc:HGNC:4776]	2.05E-60
ENSG00000013810	*TACC3*	transforming acidic coiled-coil containing protein 3 [Source:HGNC Symbol;Acc:HGNC:11524]	5.78E-58

Table 70. Top biological processes from over-representation analyses on up -regulated genes from the comparison between X-ray irradiated cells collected 24 hrs post-irradiation under simulated μG and sham-irradiated under 1G.

Gene Set	Description	P Value	FDR
GO:0048519	negative regulation of biological process	<2.2e-16	<2.2e-16
GO:0043062	extracellular structure organization	<2.2e-16	<2.2e-16
GO:0030198	extracellular matrix organization	<2.2e-16	<2.2e-16
GO:0070972	protein localization to endoplasmic reticulum	<2.2e-16	<2.2e-16
GO:0000184	nuclear-transcribed mRNA catabolic process, nonsense-mediated decay	<2.2e-16	<2.2e-16
GO:0072599	establishment of protein localization to endoplasmic reticulum	<2.2e-16	<2.2e-16
GO:0045047	protein targeting to ER	<2.2e-16	<2.2e-16
GO:0006613	cotranslational protein targeting to membrane	<2.2e-16	<2.2e-16
GO:0006614	SRP-dependent cotranslational protein targeting to membrane	<2.2e-16	<2.2e-16
GO:0006612	protein targeting to membrane	8.40E-14	1.10E-10
GO:0009888	tissue development	1.60E-13	1.90E-10
GO:0000956	nuclear-transcribed mRNA catabolic process	3.57E-13	3.88E-10
GO:0048523	negative regulation of cellular process	3.94E-13	3.95E-10
GO:0006413	translational initiation	9.97E-13	9.29E-10
GO:0009056	catabolic process	1.40E-12	1.22E-09
GO:0009057	macromolecule catabolic process	1.87E-12	1.53E-09
GO:0072358	cardiovascular system development	2.11E-12	1.62E-09
GO:0008285	negative regulation of cell proliferation	2.94E-12	2.12E-09
GO:0001944	vasculature development	3.09E-12	2.12E-09
GO:0019538	protein metabolic process	8.26E-12	5.30E-09

Table 71. Top biological processes from over-representation analyses on down -regulated genes from the comparison between X-ray irradiated cells collected 24 hrs post-irradiation under simulated μG and sham-irradiated under 1G.

Gene Set	Description	P Value	FDR
GO:0071840	cellular component organization or biogenesis	<2.2e-16	<2.2e-16
GO:0034641	cellular nitrogen compound metabolic process	<2.2e-16	<2.2e-16
GO:0016043	cellular component organization	<2.2e-16	<2.2e-16
GO:1901360	organic cyclic compound metabolic process	<2.2e-16	<2.2e-16
GO:0006725	cellular aromatic compound metabolic process	<2.2e-16	<2.2e-16
GO:0046483	heterocycle metabolic process	<2.2e-16	<2.2e-16
GO:0006139	nucleobase-containing compound metabolic process	<2.2e-16	<2.2e-16
GO:0090304	nucleic acid metabolic process	<2.2e-16	<2.2e-16
GO:0006996	organelle organization	<2.2e-16	<2.2e-16
GO:0044085	cellular component biogenesis	<2.2e-16	<2.2e-16
GO:0022607	cellular component assembly	<2.2e-16	<2.2e-16
GO:0043933	protein-containing complex subunit organization	<2.2e-16	<2.2e-16
GO:0033554	cellular response to stress	<2.2e-16	<2.2e-16
GO:0065003	protein-containing complex assembly	<2.2e-16	<2.2e-16
GO:0007049	cell cycle	<2.2e-16	<2.2e-16
GO:0007010	cytoskeleton organization	<2.2e-16	<2.2e-16
GO:0022402	cell cycle process	<2.2e-16	<2.2e-16
GO:0033043	regulation of organelle organization	<2.2e-16	<2.2e-16
GO:0051276	chromosome organization	<2.2e-16	<2.2e-16

GO:0051726	regulation of cell cycle	<2.2e-16	<2.2e-16

Table 72. Top molecular functions from over-representation analyses on up -regulated genes from the comparison between X-ray irradiated cells collected 24 hrs post-irradiation under simulated µG and sham-irradiated under 1G.

Gene Set	Description	P Value	FDR
GO:0005198	structural molecule activity	<2.2e-16	<2.2e-16
GO:0005201	extracellular matrix structural constituent	<2.2e-16	<2.2e-16
GO:0003735	structural constituent of ribosome	8.44E-15	9.16E-12
GO:0005518	collagen binding	5.61E-11	4.57E-08
GO:0030020	extracellular matrix structural constituent conferring tensile strength	2.58E-10	1.68E-07
GO:0019838	growth factor binding	1.95E-09	1.06E-06
GO:0005509	calcium ion binding	7.67E-09	3.57E-06
GO:0005539	glycosaminoglycan binding	4.40E-08	1.79E-05
GO:0048407	platelet-derived growth factor binding	9.66E-08	3.5E-05
GO:0005178	integrin binding	1.95E-07	6.34E-05
GO:0044877	protein-containing complex binding	7.02E-07	0.000208
GO:0043394	proteoglycan binding	1.96E-06	0.000532
GO:0008484	sulfuric ester hydrolase activity	4.5E-06	0.001127
GO:0031995	insulin-like growth factor II binding	8.74E-06	0.002033
GO:0005515	protein binding	1.32E-05	0.002868
GO:0005102	signaling receptor binding	2.68E-05	0.004982
GO:0043395	heparan sulfate proteoglycan binding	2.74E-05	0.004982
GO:1901681	sulfur compound binding	2.75E-05	0.004982
GO:0008201	heparin binding	3.04E-05	0.005205
GO:0002020	protease binding	3.62E-05	0.00589

Table 73. Top molecular functions from over-representation analyses on down -regulated genes from the comparison between X-ray irradiated cells collected 24 hrs post-irradiation under simulated µG and sham-irradiated under 1G.

Gene Set	Description	P Value	FDR
GO:0005488	binding	<2.2e-16	<2.2e-16
GO:0005515	protein binding	<2.2e-16	<2.2e-16
GO:0097159	organic cyclic compound binding	<2.2e-16	<2.2e-16
GO:1901363	heterocyclic compound binding	<2.2e-16	<2.2e-16
GO:0003676	nucleic acid binding	<2.2e-16	<2.2e-16
GO:0036094	small molecule binding	<2.2e-16	<2.2e-16
GO:0019899	enzyme binding	<2.2e-16	<2.2e-16
GO:1901265	nucleoside phosphate binding	<2.2e-16	<2.2e-16
GO:0000166	nucleotide binding	<2.2e-16	<2.2e-16
GO:0017076	purine nucleotide binding	<2.2e-16	<2.2e-16
GO:0032553	ribonucleotide binding	<2.2e-16	<2.2e-16
GO:0032555	purine ribonucleotide binding	<2.2e-16	<2.2e-16
GO:0035639	purine ribonucleoside triphosphate binding	<2.2e-16	<2.2e-16
GO:0008144	drug binding	<2.2e-16	<2.2e-16
GO:0003723	RNA binding	<2.2e-16	<2.2e-16
GO:0030554	adenyl nucleotide binding	<2.2e-16	<2.2e-16
GO:0032559	adenyl ribonucleotide binding	<2.2e-16	<2.2e-16

GO:0005524	ATP binding	<2.2e-16	<2.2e-16
GO:0044877	protein-containing complex binding	<2.2e-16	<2.2e-16
GO:0016817	hydrolase activity, acting on acid anhydrides	<2.2e-16	<2.2e-16

Table 74. Top cellular components from over-representation analyses on up -regulated genes from the comparison between X-ray irradiated cells collected 24 hrs post-irradiation under simulated µG and sham-irradiated under 1G.

Gene Set	Description	P Value	FDR
GO:0005576	extracellular region	<2.2e-16	<2.2e-16
GO:0044421	extracellular region part	<2.2e-16	<2.2e-16
GO:0005615	extracellular space	<2.2e-16	<2.2e-16
GO:0043230	extracellular organelle	<2.2e-16	<2.2e-16
GO:1903561	extracellular vesicle	<2.2e-16	<2.2e-16
GO:0070062	extracellular exosome	<2.2e-16	<2.2e-16
GO:0031012	extracellular matrix	<2.2e-16	<2.2e-16
GO:0062023	collagen-containing extracellular matrix	<2.2e-16	<2.2e-16
GO:0022626	cytosolic ribosome	<2.2e-16	<2.2e-16
GO:0005788	endoplasmic reticulum lumen	6.66E-16	1.15E-13
GO:0031982	vesicle	1.33E-15	2.09E-13
GO:0022625	cytosolic large ribosomal subunit	5.92E-14	8.51E-12
GO:0044391	ribosomal subunit	2.55E-13	3.38E-11
GO:0044420	extracellular matrix component	1.03E-12	1.27E-10
GO:0044445	cytosolic part	1.07E-11	1.23E-09
GO:0043202	lysosomal lumen	1.21E-11	1.30E-09
GO:0005840	ribosome	2.84E-11	2.89E-09
GO:0005604	basement membrane	4.36E-11	4.18E-09
GO:0005925	focal adhesion	1.23E-09	1.11E-07
GO:0005924	cell-substrate adherens junction	1.56E-09	1.35E-07

Table 75. Top cellular components from over-representation analyses on down -regulated genes from the comparison between X-ray irradiated cells collected 24 hrs post-irradiation under simulated µG and sham-irradiated under 1G.

Gene Set	Description	P Value	FDR
GO:0005623	cell	<2.2e-16	<2.2e-16
GO:0044464	cell part	<2.2e-16	<2.2e-16
GO:0005622	intracellular	<2.2e-16	<2.2e-16
GO:0044424	intracellular part	<2.2e-16	<2.2e-16
GO:0043226	organelle	<2.2e-16	<2.2e-16
GO:0043229	intracellular organelle	<2.2e-16	<2.2e-16
GO:0043227	membrane-bounded organelle	<2.2e-16	<2.2e-16
GO:0005737	cytoplasm	<2.2e-16	<2.2e-16
GO:0043231	intracellular membrane-bounded organelle	<2.2e-16	<2.2e-16
GO:0044444	cytoplasmic part	<2.2e-16	<2.2e-16
GO:0044422	organelle part	<2.2e-16	<2.2e-16
GO:0044446	intracellular organelle part	<2.2e-16	<2.2e-16
GO:0005634	nucleus	<2.2e-16	<2.2e-16
GO:0031974	membrane-enclosed lumen	<2.2e-16	<2.2e-16
GO:0043233	organelle lumen	<2.2e-16	<2.2e-16

GO:0070013	intracellular organelle lumen	<2.2e-16	<2.2e-16
GO:0032991	protein-containing complex	<2.2e-16	<2.2e-16
GO:0005829	cytosol	<2.2e-16	<2.2e-16
GO:0044428	nuclear part	<2.2e-16	<2.2e-16
GO:0043228	non-membrane-bounded organelle	<2.2e-16	<2.2e-16

Table 76. Top KEGG pathways from over-representation analyses on up -regulated genes from the comparison between X-ray irradiated cells collected 24 hrs post-irradiation under simulated µG and sham-irradiated under 1G.

Gene Set	Description	P Value	FDR
hsa03010	Ribosome	8.88E-16	2.92E-13
hsa04512	ECM-receptor interaction	2.77E-08	4.56E-06
hsa04115	p53 signaling pathway	8.36E-07	9.17E-05
hsa04510	Focal adhesion	1.65E-06	0.000135
hsa04142	Lysosome	5.25E-05	0.003454

Table 77. Top KEGG pathways from over-representation analyses on down -regulated genes from the comparison between X-ray irradiated cells collected 24 hrs post-irradiation under simulated µG and sham-irradiated under 1G.

Gene Set	Description	P Value	FDR
hsa05203	Viral carcinogenesis	<2.2e-16	<2.2e-16
hsa05034	Alcoholism	<2.2e-16	<2.2e-16
hsa05322	Systemic lupus erythematosus	<2.2e-16	<2.2e-16
hsa04110	Cell cycle	<2.2e-16	<2.2e-16
hsa03030	DNA replication	<2.2e-16	<2.2e-16
hsa03460	Fanconi anemia pathway	7.33E-15	4.02E-13
hsa03040	Spliceosome	3.26E-14	1.53E-12
hsa03440	Homologous recombination	4.21E-12	1.73E-10
hsa03430	Mismatch repair	4.68E-11	1.71E-09
hsa04114	Oocyte meiosis	1.09E-10	3.58E-09
hsa04218	Cellular senescence	2.60E-10	7.77E-09
hsa03013	RNA transport	9.93E-10	2.72E-08
hsa05130	Pathogenic Escherichia coli infection	1.42E-07	3.4E-06
hsa03050	Proteasome	1.45E-07	3.4E-06
hsa00240	Pyrimidine metabolism	6.11E-07	1.34E-05
hsa03410	Base excision repair	2.5E-06	5.14E-05
hsa04914	Progesterone-mediated oocyte maturation	1.73E-05	0.000334
hsa03420	Nucleotide excision repair	4.31E-05	0.000788
hsa05170	Human immunodeficiency virus 1 infection	0.000142	0.002462
hsa03450	Non-homologous end-joining	0.000526	0.008479

3.11. Early response genes to C-ion irradiation and simulated µG combined effect

From the comparison between C-ion irradiated cells collected 3 hrs post-irradiation under simulated µG and sham-irradiated under 1G (C3µG-C0G), 184 over-expressed genes were found and among those *CDKN1A*, *MDM2*, *PTCHD4*, *BTG2*, *PAPPA*, *TP53INP1*, and *PURPL* stood out. Likewise, 136 under-expressed genes were found to be statistically significant. Down-regulated genes *MKI67* and *DTL* were found to be prominent. Concerning the over-expressed genes, enrichment analyses in all Gene Ontology aspects, as well as KEGG pathways, highlighted the p53 signaling pathway. LEF1 was identified as a gene-targeting transcription factor for up-regulated genes. Concentrating on under-

expressed genes, biological term over-representation analyses in all Gene Ontology domains, as well as KEGG pathway, highlighted cell cycle, circulatory system development and protein digestion and absorption related terms. E2F was identified as a gene-targeting transcription factor.

Table 78. Top up -regulated genes from the comparison between C-ion irradiated cells collected 3 hrs post-irradiation under simulated µG and sham-irradiated under 1G.

Gene Id	Gene Name	Description	svalue
ENSG00000124762	*CDKN1A*	cyclin dependent kinase inhibitor 1A [Source:HGNC Symbol;Acc:HGNC:1784]	1.45E-157
ENSG00000135679	*MDM2*	MDM2 proto-oncogene [Source:HGNC Symbol;Acc:HGNC:6973]	2.75E-74
ENSG00000182752	*PAPPA*	pappalysin 1 [Source:HGNC Symbol;Acc:HGNC:8602]	4.91E-44
ENSG00000244694	*PTCHD4*	patched domain containing 4 [Source:HGNC Symbol;Acc:HGNC:21345]	2.29E-31
ENSG00000256664	*NA*	ribosomal L24 domain containing 1 (RSL24D1) pseudogene	2.01E-29
ENSG00000159388	*BTG2*	BTG anti-proliferation factor 2 [Source:HGNC Symbol;Acc:HGNC:1131]	3.82E-27
ENSG00000164070	*HSPA4L*	heat shock protein family A (Hsp70) member 4 like [Source:HGNC Symbol;Acc:HGNC:17041]	3.02E-24
ENSG00000164938	*TP53INP1*	tumor protein p53 inducible nuclear protein 1 [Source:HGNC Symbol;Acc:HGNC:18022]	6.35E-24
ENSG00000026103	*FAS*	Fas cell surface death receptor [Source:HGNC Symbol;Acc:HGNC:11920]	2.98E-23
ENSG00000250337	*PURPL*	p53 upregulated regulator of p53 levels [Source:HGNC Symbol;Acc:HGNC:48995]	1.08E-20
ENSG00000112249	*ASCC3*	activating signal cointegrator 1 complex subunit 3 [Source:HGNC Symbol;Acc:HGNC:18697]	4.18E-18
ENSG00000120889	*TNFRSF10B*	TNF receptor superfamily member 10b [Source:HGNC Symbol;Acc:HGNC:11905]	8.09E-18
ENSG00000167196	*FBXO22*	F-box protein 22 [Source:HGNC Symbol;Acc:HGNC:13593]	1.66E-17
ENSG00000172667	*ZMAT3*	zinc finger matrin-type 3 [Source:HGNC Symbol;Acc:HGNC:29983]	2.97E-17
ENSG00000028277	*POU2F2*	POU class 2 homeobox 2 [Source:HGNC Symbol;Acc:HGNC:9213]	8.24E-16
ENSG00000168497	*CAVIN2*	caveolae associated protein 2 [Source:HGNC Symbol;Acc:HGNC:10690]	5.07E-15
ENSG00000161513	*FDXR*	ferredoxin reductase [Source:HGNC Symbol;Acc:HGNC:3642]	1.18E-14
ENSG00000080546	*SESN1*	sestrin 1 [Source:HGNC Symbol;Acc:HGNC:21595]	3.36E-14
ENSG00000134574	*DDB2*	damage specific DNA binding protein 2 [Source:HGNC Symbol;Acc:HGNC:2718]	1.19E-13
ENSG00000078237	*TIGAR*	TP53 induced glycolysis regulatory phosphatase [Source:HGNC Symbol;Acc:HGNC:1185]	1.85E-13

Table 79. Top down -regulated genes from the comparison between C-ion irradiated cells collected 3 hrs post-irradiation under simulated µG and sham-irradiated under 1G.

Gene Id	Gene Name	Description	svalue
ENSG00000143476	*DTL*	denticleless E3 ubiquitin protein ligase homolog [Source:HGNC Symbol;Acc:HGNC:30288]	1.17E-17
ENSG00000172403	*SYNPO2*	synaptopodin 2 [Source:HGNC Symbol;Acc:HGNC:17732]	6.26E-14
ENSG00000113140	*SPARC*	secreted protein acidic and cysteine rich [Source:HGNC Symbol;Acc:HGNC:11219]	1.33E-11
ENSG00000134030	*CTIF*	cap binding complex dependent translation initiation factor [Source:HGNC Symbol;Acc:HGNC:23925]	4.54E-11
ENSG00000108821	*COL1A1*	collagen type I alpha 1 chain [Source:HGNC Symbol;Acc:HGNC:2197]	5.78E-10
ENSG00000142149	*HUNK*	hormonally up-regulated Neu-associated kinase [Source:HGNC Symbol;Acc:HGNC:13326]	8.56E-10
ENSG00000173641	*HSPB7*	heat shock protein family B (small) member 7 [Source:HGNC Symbol;Acc:HGNC:5249]	1.42E-09
ENSG00000148773	*MKI67*	marker of proliferation Ki-67 [Source:HGNC Symbol;Acc:HGNC:7107]	1.76E-09
ENSG00000213626	*LBH*	LBH regulator of WNT signaling pathway [Source:HGNC	1.29E-08

		Symbol;Acc:HGNC:29532]	
ENSG00000103257	*SLC7A5*	solute carrier family 7 member 5 [Source:HGNC Symbol;Acc:HGNC:11063]	2.52E-08
ENSG00000167513	*CDT1*	chromatin licensing and DNA replication factor 1 [Source:HGNC Symbol;Acc:HGNC:24576]	3.87E-08
ENSG00000250251	*PKD1P6*	polycystin 1, transient receptor potential channel interacting pseudogene 6 [Source:HGNC Symbol;Acc:HGNC:30070]	5.11E-08
ENSG00000139946	*PELI2*	pellino E3 ubiquitin protein ligase family member 2 [Source:HGNC Symbol;Acc:HGNC:8828]	1.28E-07
ENSG00000104635	*SLC39A14*	solute carrier family 39 member 14 [Source:HGNC Symbol;Acc:HGNC:20858]	1.52E-07
ENSG00000087586	*AURKA*	aurora kinase A [Source:HGNC Symbol;Acc:HGNC:11393]	2.67E-07
ENSG00000162849	*KIF26B*	kinesin family member 26B [Source:HGNC Symbol;Acc:HGNC:25484]	4.69E-07
ENSG00000128283	*CDC42EP1*	CDC42 effector protein 1 [Source:HGNC Symbol;Acc:HGNC:17014]	6.09E-07
ENSG00000163431	*LMOD1*	leiomodin 1 [Source:HGNC Symbol;Acc:HGNC:6647]	9.54E-07
ENSG00000204267	*TAP2*	transporter 2, ATP binding cassette subfamily B member [Source:HGNC Symbol;Acc:HGNC:44]	1.12E-06
ENSG00000123485	*HJURP*	Holliday junction recognition protein [Source:HGNC Symbol;Acc:HGNC:25444]	1.42E-06

Table 80. Top biological processes from over-representation analyses on up -regulated genes from the comparison between C-ion irradiated cells collected 3 hrs post-irradiation under simulated µG and sham-irradiated under 1G.

Gene Set	Description	P Value	FDR
GO:0006915	apoptotic process	2.23E-08	0.000291
GO:0044774	mitotic DNA integrity checkpoint	5.51E-08	0.000325
GO:0042981	regulation of apoptotic process	1.15E-07	0.000325
GO:0072331	signal transduction by p53 class mediator	1.32E-07	0.000325
GO:0043067	regulation of programmed cell death	1.45E-07	0.000325
GO:0012501	programmed cell death	1.50E-07	0.000325
GO:0008219	cell death	2.97E-07	0.00044
GO:0044773	mitotic DNA damage checkpoint	3.01E-07	0.00044
GO:0010941	regulation of cell death	3.04E-07	0.00044
GO:0007093	mitotic cell cycle checkpoint	4.18E-07	0.000545
GO:0032270	positive regulation of cellular protein metabolic process	5.59E-07	0.000645
GO:0030330	DNA damage response, signal transduction by p53 class mediator	5.93E-07	0.000645
GO:0035556	intracellular signal transduction	1.01E-06	0.001013
GO:0043069	negative regulation of programmed cell death	1.21E-06	0.001079
GO:0009605	response to external stimulus	1.24E-06	0.001079
GO:0051246	regulation of protein metabolic process	1.4E-06	0.00111
GO:0006974	cellular response to DNA damage stimulus	1.64E-06	0.00111
GO:0048585	negative regulation of response to stimulus	1.66E-06	0.00111
GO:0071214	cellular response to abiotic stimulus	1.83E-06	0.00111
GO:0104004	cellular response to environmental stimulus	1.83E-06	0.00111

Table 81. Top biological processes from over-representation analyses on down -regulated genes from the comparison between C-ion irradiated cells collected 3 hrs post-irradiation under simulated µG and sham-irradiated under 1G.

Gene Set	Description	P Value	FDR
GO:0016043	cellular component organization	9.60E-11	1.25E-06
GO:0071840	cellular component organization or biogenesis	4.67E-10	3.04E-06
GO:0072359	circulatory system development	2.28E-09	9.92E-06

GO:0007049	cell cycle	4.33E-08	0.000141
GO:0010564	regulation of cell cycle process	2.34E-07	0.000515
GO:0009653	anatomical structure morphogenesis	2.37E-07	0.000515
GO:0010948	negative regulation of cell cycle process	1.36E-06	0.001878
GO:1901987	regulation of cell cycle phase transition	1.37E-06	0.001878
GO:0048731	system development	1.47E-06	0.001878
GO:1901988	negative regulation of cell cycle phase transition	1.52E-06	0.001878
GO:0000278	mitotic cell cycle	1.66E-06	0.001878
GO:0007346	regulation of mitotic cell cycle	1.73E-06	0.001878
GO:1903047	mitotic cell cycle process	1.91E-06	0.001915
GO:0022402	cell cycle process	2.77E-06	0.002538
GO:1901990	regulation of mitotic cell cycle phase transition	2.92E-06	0.002538
GO:0048519	negative regulation of biological process	3.55E-06	0.00282
GO:0006996	organelle organization	3.68E-06	0.00282
GO:1902750	negative regulation of cell cycle G2/M phase transition	4.46E-06	0.003074
GO:0007059	chromosome segregation	4.48E-06	0.003074
GO:1901991	negative regulation of mitotic cell cycle phase transition	5.6E-06	0.003649

Table 82. Top molecular functions from over-representation analyses on up -regulated genes from the comparison between C-ion irradiated cells collected 3 hrs post-irradiation under simulated µG and sham-irradiated under 1G.

Gene Set	Description	P Value	FDR
GO:0005515	protein binding	2.02E-06	0.006567
GO:0045569	TRAIL binding	8.3E-06	0.01352

Table 83. Top molecular functions from over-representation analyses on down -regulated genes from the comparison between C-ion irradiated cells collected 3 hrs post-irradiation under simulated µG and sham-irradiated under 1G.

Gene Set	Description	P Value	FDR
GO:0005515	protein binding	3.72E-07	0.001213
GO:0003682	chromatin binding	2.72E-06	0.004433
GO:0030020	extracellular matrix structural constituent conferring tensile strength	9.28E-06	0.008882
GO:0008092	cytoskeletal protein binding	1.09E-05	0.008882
GO:0005201	extracellular matrix structural constituent	3.21E-05	0.020892
GO:0048407	platelet-derived growth factor binding	7.19E-05	0.039047

Table 84. Top cellular components from over-representation analyses on down -regulated genes from the comparison between C-ion irradiated cells collected 3 hrs post-irradiation under simulated µG and sham-irradiated under 1G.

Gene Set	Description	P Value	FDR
GO:0044424	intracellular part	6.29E-08	5.05E-05
GO:0005622	intracellular	7.65E-08	5.05E-05
GO:0043232	intracellular non-membrane-bounded organelle	1.11E-07	5.05E-05
GO:0043228	non-membrane-bounded organelle	1.19E-07	5.05E-05
GO:0099081	supramolecular polymer	1.92E-07	5.05E-05
GO:0099080	supramolecular complex	1.95E-07	5.05E-05
GO:0098644	complex of collagen trimers	2.05E-07	5.05E-05
GO:0005912	adherens junction	3.86E-07	8.32E-05

GO:0070161	anchoring junction	5.80E-07	0.000111
GO:0043229	intracellular organelle	7.23E-07	0.000125
GO:0044420	extracellular matrix component	1.45E-06	0.000218
GO:0005925	focal adhesion	1.51E-06	0.000218
GO:0005924	cell-substrate adherens junction	1.65E-06	0.000219
GO:0030055	cell-substrate junction	1.85E-06	0.000228
GO:0005737	cytoplasm	2.21E-06	0.000254
GO:0099512	supramolecular fiber	2.66E-06	0.000287
GO:0005694	chromosome	3.85E-06	0.000391
GO:0005856	cytoskeleton	6.32E-06	0.000606
GO:0032432	actin filament bundle	1.01E-05	0.000922
GO:0005788	endoplasmic reticulum lumen	1.51E-05	0.001307

Table 85. Top KEGG pathways from over-representation analyses on up -regulated genes from the comparison between C-ion irradiated cells collected 3 hrs post-irradiation under simulated µG and sham-irradiated under 1G.

Gene Set	Description	P Value	FDR
hsa04115	p53 signaling pathway	2.37E-10	7.81E-08
hsa01524	Platinum drug resistance	0.000125	0.020623
hsa04060	Cytokine-cytokine receptor interaction	0.000327	0.035872

Table 86. Top KEGG pathway from over-representation analyses on down -regulated genes from the comparison between C-ion irradiated cells collected 3 hrs post-irradiation under simulated µG and sham-irradiated under 1G.

Gene Set	Description	P Value	FDR
hsa04974	Protein digestion and absorption	5.65E-06	0.001859

3.12. Late response genes to C-ion irradiation and simulated µG combined effect

From the comparison between C-ion irradiated cells collected 24 hrs post-irradiation under simulated µG and sham-irradiated under 1G (C24µG-C0G), 478 up- and 803 down-regulated genes were found. Over-expressed genes *PTCHD4*, *PURPL*, *BTG2* and *CDKN1A* were found to be predominant. Biological term enrichment analyses in all Gene Ontology categories highlighted terms related to apoptosis and response to stress. The predominant KEGG pathway identified was the p53 signaling pathway. The transcription factor Forkhead Box O4 was also identified. Among the down-regulated genes, many stood out. A few were *MKI67*, *H2BC18*, *H1-3*, *H4C4*, *H3C10*, *H2AC13* and *H3C3*. Enrichment analyses in all Gene Ontology aspects highlighted cell cycle and DNA repair related terms. The predominant KEGG pathways identified are cell cycle and carcinogenesis related. E2F was identified as a gene-targeting transcription factor for under-expressed genes.

Table 87. Top up -regulated genes from the comparison between C-ion irradiated cells collected 24 hrs post-irradiation under simulated µG and sham-irradiated under 1G.

Gene Id	Gene Name	Description	svalue
ENSG00000124762	*CDKN1A*	cyclin dependent kinase inhibitor 1A [Source:HGNC Symbol;Acc:HGNC:1784]	9.73E-38
ENSG00000244694	*PTCHD4*	patched domain containing 4 [Source:HGNC Symbol;Acc:HGNC:21345]	6.66E-34
ENSG00000250337	*PURPL*	p53 upregulated regulator of p53 levels [Source:HGNC Symbol;Acc:HGNC:48995]	1.87E-25
ENSG00000182752	*PAPPA*	pappalysin 1 [Source:HGNC Symbol;Acc:HGNC:8602]	4.44E-24
ENSG00000055163	*CYFIP2*	cytoplasmic FMR1 interacting protein 2 [Source:HGNC Symbol;Acc:HGNC:13760]	1.69E-21
ENSG00000172667	*ZMAT3*	zinc finger matrin-type 3 [Source:HGNC Symbol;Acc:HGNC:29983]	3.35E-21

ENSG00000164938	*TP53INP1*	tumor protein p53 inducible nuclear protein 1 [Source:HGNC Symbol;Acc:HGNC:18022]	4.86E-20
ENSG00000135679	*MDM2*	MDM2 proto-oncogene [Source:HGNC Symbol;Acc:HGNC:6973]	1.52E-19
ENSG00000135919	*SERPINE2*	serpin family E member 2 [Source:HGNC Symbol;Acc:HGNC:8951]	2.99E-19
ENSG00000163071	*SPATA18*	spermatogenesis associated 18 [Source:HGNC Symbol;Acc:HGNC:29579]	2.50E-18
ENSG00000185088	*RPS27L*	ribosomal protein S27 like [Source:HGNC Symbol;Acc:HGNC:18476]	1.44E-17
ENSG00000159388	*BTG2*	BTG anti-proliferation factor 2 [Source:HGNC Symbol;Acc:HGNC:1131]	4.61E-17
ENSG00000136542	*GALNT5*	polypeptide N-acetylgalactosaminyltransferase 5 [Source:HGNC Symbol;Acc:HGNC:4127]	5.72E-17
ENSG00000113328	*CCNG1*	cyclin G1 [Source:HGNC Symbol;Acc:HGNC:1592]	7.58E-16
ENSG00000244509	*APOBEC3C*	apolipoprotein B mRNA editing enzyme catalytic subunit 3C [Source:HGNC Symbol;Acc:HGNC:17353]	1.05E-15
ENSG00000112249	*ASCC3*	activating signal cointegrator 1 complex subunit 3 [Source:HGNC Symbol;Acc:HGNC:18697]	1.38E-14
ENSG00000065357	*DGKA*	diacylglycerol kinase alpha [Source:HGNC Symbol;Acc:HGNC:2849]	1.97E-13
ENSG00000133818	*RRAS2*	RAS related 2 [Source:HGNC Symbol;Acc:HGNC:17271]	2.59E-13
ENSG00000171451	*DSEL*	dermatan sulfate epimerase like [Source:HGNC Symbol;Acc:HGNC:18144]	4.59E-13
ENSG00000107984	*DKK1*	dickkopf WNT signaling pathway inhibitor 1 [Source:HGNC Symbol;Acc:HGNC:2891]	7.07E-13

Table 88. Top down -regulated genes from the comparison between C-ion irradiated cells collected 24 hrs post-irradiation under simulated µG and sham-irradiated under 1G.

Gene Id	Gene Name	Description	svalue
ENSG00000203814	*H2BC18*	H2B clustered histone 18 [Source:HGNC Symbol;Acc:HGNC:24700]	9.36E-70
ENSG00000148773	*MKI67*	marker of proliferation Ki-67 [Source:HGNC Symbol;Acc:HGNC:7107]	1.37E-64
ENSG00000124575	*H1-3*	H1.3 linker histone, cluster member [Source:HGNC Symbol;Acc:HGNC:4717]	2.93E-56
ENSG00000277157	*H4C4*	H4 clustered histone 4 [Source:HGNC Symbol;Acc:HGNC:4782]	7.56E-47
ENSG00000187837	*H1-2*	H1.2 linker histone, cluster member [Source:HGNC Symbol;Acc:HGNC:4716]	1.78E-46
ENSG00000161800	*RACGAP1*	Rac GTPase activating protein 1 [Source:HGNC Symbol;Acc:HGNC:9804]	3.45E-44
ENSG00000273802	*H2BC8*	H2B clustered histone 8 [Source:HGNC Symbol;Acc:HGNC:4746]	3.90E-42
ENSG00000278828	*H3C10*	H3 clustered histone 10 [Source:HGNC Symbol;Acc:HGNC:4775]	1.67E-41
ENSG00000288825	*H2AC18*	H2A clustered histone 18 [Source:HGNC Symbol;Acc:HGNC:4736]	3.41E-41
ENSG00000278588	*H2BC10*	H2B clustered histone 10 [Source:HGNC Symbol;Acc:HGNC:4756]	8.79E-41
ENSG00000196747	*H2AC13*	H2A clustered histone 13 [Source:HGNC Symbol;Acc:HGNC:4725]	1.67E-40
ENSG00000158406	*H4C8*	H4 clustered histone 8 [Source:HGNC Symbol;Acc:HGNC:4788]	3.47E-40
ENSG00000088325	*TPX2*	TPX2 microtubule nucleation factor [Source:HGNC Symbol;Acc:HGNC:1249]	2.16E-39
ENSG00000287080	*H3C3*	H3 clustered histone 3 [Source:HGNC Symbol;Acc:HGNC:4768]	5.53E-39
ENSG00000158373	*H2BC5*	H2B clustered histone 5 [Source:HGNC Symbol;Acc:HGNC:4747]	1.70E-38
ENSG00000286522	*H3C2*	H3 clustered histone 2 [Source:HGNC Symbol;Acc:HGNC:4776]	3.50E-38
ENSG00000196787	*H2AC11*	H2A clustered histone 11 [Source:HGNC Symbol;Acc:HGNC:4737]	8.55E-37
ENSG00000185130	*H2BC13*	H2B clustered histone 13 [Source:HGNC Symbol;Acc:HGNC:4748]	3.22E-36
ENSG00000237649	*KIFC1*	kinesin family member C1 [Source:HGNC Symbol;Acc:HGNC:6389]	1.14E-35
ENSG00000273983	*H3C8*	H3 clustered histone 8 [Source:HGNC Symbol;Acc:HGNC:4772]	2.23E-35

Table 89. Top biological processes from over-representation on up -regulated genes from the comparison between C-ion irradiated cells collected 24 hrs post-irradiation under simulated µG and sham-irradiated under 1G.

Gene Set	Description	P Value	FDR
GO:0033554	cellular response to stress	2.26E-10	2.94E-06

GO:0040012	regulation of locomotion	3.26E-09	1.24E-05
GO:0006915	apoptotic process	3.53E-09	1.24E-05
GO:0051270	regulation of cellular component movement	3.79E-09	1.24E-05
GO:0006950	response to stress	5.56E-09	1.45E-05
GO:0008219	cell death	9.71E-09	1.87E-05
GO:2000145	regulation of cell motility	1.00E-08	1.87E-05
GO:0051246	regulation of protein metabolic process	1.40E-08	2.28E-05
GO:0019538	protein metabolic process	1.75E-08	2.46E-05
GO:0044267	cellular protein metabolic process	1.92E-08	2.46E-05
GO:0030334	regulation of cell migration	2.07E-08	2.46E-05
GO:0012501	programmed cell death	3.96E-08	4.3E-05
GO:0010941	regulation of cell death	4.53E-08	4.54E-05
GO:0043069	negative regulation of programmed cell death	6.64E-08	6.14E-05
GO:0042981	regulation of apoptotic process	7.11E-08	6.14E-05
GO:0035556	intracellular signal transduction	7.90E-08	6.14E-05
GO:0009411	response to UV	8.01E-08	6.14E-05
GO:0043067	regulation of programmed cell death	1.02E-07	7.11E-05
GO:0043066	negative regulation of apoptotic process	1.04E-07	7.11E-05
GO:1902531	regulation of intracellular signal transduction	1.76E-07	0.000115

Table 90. Top biological processes from over-representation on down -regulated genes from the comparison between C-ion irradiated cells collected 24 hrs post-irradiation under simulated µG and sham-irradiated under 1G.

Gene Set	Description	P Value	FDR
GO:0071840	cellular component organization or biogenesis	<2.2e-16	<2.2e-16
GO:0034641	cellular nitrogen compound metabolic process	<2.2e-16	<2.2e-16
GO:0016043	cellular component organization	<2.2e-16	<2.2e-16
GO:1901360	organic cyclic compound metabolic process	<2.2e-16	<2.2e-16
GO:0006725	cellular aromatic compound metabolic process	<2.2e-16	<2.2e-16
GO:0046483	heterocycle metabolic process	<2.2e-16	<2.2e-16
GO:0006139	nucleobase-containing compound metabolic process	<2.2e-16	<2.2e-16
GO:0090304	nucleic acid metabolic process	<2.2e-16	<2.2e-16
GO:0006996	organelle organization	<2.2e-16	<2.2e-16
GO:0033554	cellular response to stress	<2.2e-16	<2.2e-16
GO:0007049	cell cycle	<2.2e-16	<2.2e-16
GO:0007010	cytoskeleton organization	<2.2e-16	<2.2e-16
GO:0022402	cell cycle process	<2.2e-16	<2.2e-16
GO:0033043	regulation of organelle organization	<2.2e-16	<2.2e-16
GO:0051276	chromosome organization	<2.2e-16	<2.2e-16
GO:0051726	regulation of cell cycle	<2.2e-16	<2.2e-16
GO:0006259	DNA metabolic process	<2.2e-16	<2.2e-16
GO:0000278	mitotic cell cycle	<2.2e-16	<2.2e-16
GO:0006974	cellular response to DNA damage stimulus	<2.2e-16	<2.2e-16
GO:1903047	mitotic cell cycle process	<2.2e-16	<2.2e-16

Table 91. Top molecular functions from over-representation on up -regulated genes from the comparison between C-ion irradiated cells collected 24 hrs post-irradiation under simulated μG and sham-irradiated under 1G.

Gene Set	Description	P Value	FDR
GO:0005515	protein binding	1.61E-08	5.25E-05
GO:0019901	protein kinase binding	1E-05	0.016348
GO:0019900	kinase binding	5.2E-05	0.045335
GO:0005488	binding	5.57E-05	0.045335

Table 92. Top molecular functions from over-representation on down -regulated genes from the comparison between C-ion irradiated cells collected 24 hrs post-irradiation under simulated μG and sham-irradiated under 1G.

Gene Set	Description	P Value	FDR
GO:0005488	binding	<2.2e-16	<2.2e-16
GO:0005515	protein binding	<2.2e-16	<2.2e-16
GO:0097159	organic cyclic compound binding	<2.2e-16	<2.2e-16
GO:1901363	heterocyclic compound binding	<2.2e-16	<2.2e-16
GO:0003676	nucleic acid binding	<2.2e-16	<2.2e-16
GO:0003677	DNA binding	<2.2e-16	<2.2e-16
GO:0019899	enzyme binding	<2.2e-16	<2.2e-16
GO:1901265	nucleoside phosphate binding	<2.2e-16	<2.2e-16
GO:0000166	nucleotide binding	<2.2e-16	<2.2e-16
GO:0035639	purine ribonucleoside triphosphate binding	<2.2e-16	<2.2e-16
GO:0008144	drug binding	<2.2e-16	<2.2e-16
GO:0030554	adenyl nucleotide binding	<2.2e-16	<2.2e-16
GO:0032559	adenyl ribonucleotide binding	<2.2e-16	<2.2e-16
GO:0005524	ATP binding	<2.2e-16	<2.2e-16
GO:0003682	chromatin binding	<2.2e-16	<2.2e-16
GO:0140097	catalytic activity, acting on DNA	<2.2e-16	<2.2e-16
GO:0017076	purine nucleotide binding	2.22E-16	3.81E-14
GO:0032553	ribonucleotide binding	2.22E-16	3.81E-14
GO:0032555	purine ribonucleotide binding	2.22E-16	3.81E-14
GO:0031491	nucleosome binding	3.33E-15	5.43E-13

Table 93. Top cellular components from over-representation on up -regulated genes from the comparison between C-ion irradiated cells collected 24 hrs post-irradiation under simulated μG and sham-irradiated under 1G.

Gene Set	Description	P Value	FDR
GO:0031982	vesicle	1.26E-08	2.17E-05
GO:0044444	cytoplasmic part	1.68E-07	0.000145
GO:0005794	Golgi apparatus	3.15E-07	0.000147
GO:0005912	adherens junction	4.57E-07	0.000147
GO:0030054	cell junction	5.83E-07	0.000147
GO:1903561	extracellular vesicle	7.22E-07	0.000147
GO:0043230	extracellular organelle	7.52E-07	0.000147
GO:0005925	focal adhesion	8.06E-07	0.000147
GO:0070161	anchoring junction	8.91E-07	0.000147
GO:0070062	extracellular exosome	9.11E-07	0.000147
GO:0005924	cell-substrate adherens junction	9.34E-07	0.000147

GO:0030055	cell-substrate junction	1.13E-06	0.000163
GO:0005615	extracellular space	1.57E-06	0.000208
GO:0044421	extracellular region part	2.35E-06	0.000288
GO:0044431	Golgi apparatus part	2.6E-06	0.000288
GO:0098791	Golgi subcompartment	2.67E-06	0.000288
GO:0005576	extracellular region	7.37E-06	0.000748
GO:0098805	whole membrane	7.85E-06	0.000753
GO:0009986	cell surface	8.94E-06	0.000812
GO:0005737	cytoplasm	2.74E-05	0.002367

Table 94. Top cellular components from over-representation on down -regulated genes from the comparison between C-ion irradiated cells collected 24 hrs post-irradiation under simulated μG and sham-irradiated under 1G.

Gene Set	Description	P Value	FDR
GO:0005622	intracellular	<2.2e-16	<2.2e-16
GO:0044424	intracellular part	<2.2e-16	<2.2e-16
GO:0043226	organelle	<2.2e-16	<2.2e-16
GO:0043229	intracellular organelle	<2.2e-16	<2.2e-16
GO:0043227	membrane-bounded organelle	<2.2e-16	<2.2e-16
GO:0043231	intracellular membrane-bounded organelle	<2.2e-16	<2.2e-16
GO:0044422	organelle part	<2.2e-16	<2.2e-16
GO:0044446	intracellular organelle part	<2.2e-16	<2.2e-16
GO:0005634	nucleus	<2.2e-16	<2.2e-16
GO:0031974	membrane-enclosed lumen	<2.2e-16	<2.2e-16
GO:0043233	organelle lumen	<2.2e-16	<2.2e-16
GO:0070013	intracellular organelle lumen	<2.2e-16	<2.2e-16
GO:0032991	protein-containing complex	<2.2e-16	<2.2e-16
GO:0005829	cytosol	<2.2e-16	<2.2e-16
GO:0044428	nuclear part	<2.2e-16	<2.2e-16
GO:0043228	non-membrane-bounded organelle	<2.2e-16	<2.2e-16
GO:0043232	intracellular non-membrane-bounded organelle	<2.2e-16	<2.2e-16
GO:0031981	nuclear lumen	<2.2e-16	<2.2e-16
GO:0005654	nucleoplasm	<2.2e-16	<2.2e-16
GO:0005856	cytoskeleton	<2.2e-16	<2.2e-16

Table 95. Top KEGG pathways from over-representation on up -regulated genes from the comparison between C-ion irradiated cells collected 24 hrs post-irradiation under simulated μG and sham-irradiated under 1G.

Gene Set	Description	P Value	FDR
hsa04115	p53 signaling pathway	7.77E-09	2.56E-06
hsa01524	Platinum drug resistance	0.000157	0.02581
hsa05222	Small cell lung cancer	0.000242	0.026558
hsa05205	Proteoglycans in cancer	0.000461	0.03791

Table 96. Top KEGG pathways from over-representation on down -regulated genes from the comparison between C-ion irradiated cells collected 24 hrs post-irradiation under simulated μG and sham-irradiated under 1G.

Gene Set	Description	P Value	FDR
hsa05034	Alcoholism	<2.2e-16	<2.2e-16
hsa05322	Systemic lupus erythematosus	<2.2e-16	<2.2e-16
hsa04110	Cell cycle	<2.2e-16	<2.2e-16
hsa03030	DNA replication	<2.2e-16	<2.2e-16
hsa05203	Viral carcinogenesis	1.11E-16	7.31E-15
hsa03440	Homologous recombination	2.80E-12	1.53E-10
hsa03410	Base excision repair	1.71E-10	7.14E-09
hsa03430	Mismatch repair	1.74E-10	7.14E-09
hsa03460	Fanconi anemia pathway	4.76E-10	1.74E-08
hsa04114	Oocyte meiosis	1.55E-09	5.09E-08
hsa04914	Progesterone-mediated oocyte maturation	1.26E-08	3.78E-07
hsa05166	Human T-cell leukemia virus 1 infection	1.05E-07	2.89E-06
hsa04218	Cellular senescence	3.34E-06	8.45E-05
hsa04217	Necroptosis	4.15E-06	9.76E-05
hsa03040	Spliceosome	1E-05	0.00022
hsa03420	Nucleotide excision repair	1.48E-05	0.000304
hsa00240	Pyrimidine metabolism	0.000137	0.002653
hsa03013	RNA transport	0.002212	0.04043

3.13. Detection of apoptosis-, DNA damage repair- or cell cycle-related genes

From the comparisons between X-ray or C-ion irradiated cells collected 3 or 24 hrs post-irradiation under simulated μG and sham-irradiated under 1G (X3μG-X0G), (X24μG-X0G), (C3μG-C0G) and (C24μG-C0G), apoptosis-related genes *BLOC1S2*, *EDA2R*, *TP53INP1*, *MDM2*, *CDKN1A*, *FAS* and *BCL2L1* were found to be up-regulated, DNA damage repair-related genes *BRCA1*, *POLQ*, *BLM* and *H2AFX* and cell cycle-related genes *MKI67*, *CDT1*, *CDC6*, *MSH6* and *TERT* , were found to down-regulated.

3.14. Overlaps between early and late response genes to X-ray and C-ion radiation under 1G

Venn diagrams were created for up- and down-regulated genes between 4 comparisons under 1G: Early response to C-ion irradiation (C3G-C0G), late response to C-ion irradiation (C24G-C0G), early response to X-ray irradiation (X3G-X0G) and late response to X-ray irradiation (X24G-X0G) (Figure15). 27 up- (Table 97) and 28 down (Table 98)-regulated genes were found to be overlapping in all 4 comparisons. Performing over-representation analyses, focusing on the common over-expressed genes, biological processes highlighted were related to DNA damage response, signal transduction by p53 class mediator, regulation of cell cycle arrest, intrinsic apoptotic signaling pathway and regulation of catabolic process (regulation of autophagy). For both over- and under-expressed genes, biological processes related to regulation of mitotic cell cycle and DNA integrity checkpoint (G1/S phase transition) related terms were identified. Furthermore, for under-expressed genes, the biological process of regulation of G2/M transition of mitotic cell cycle was also identified.

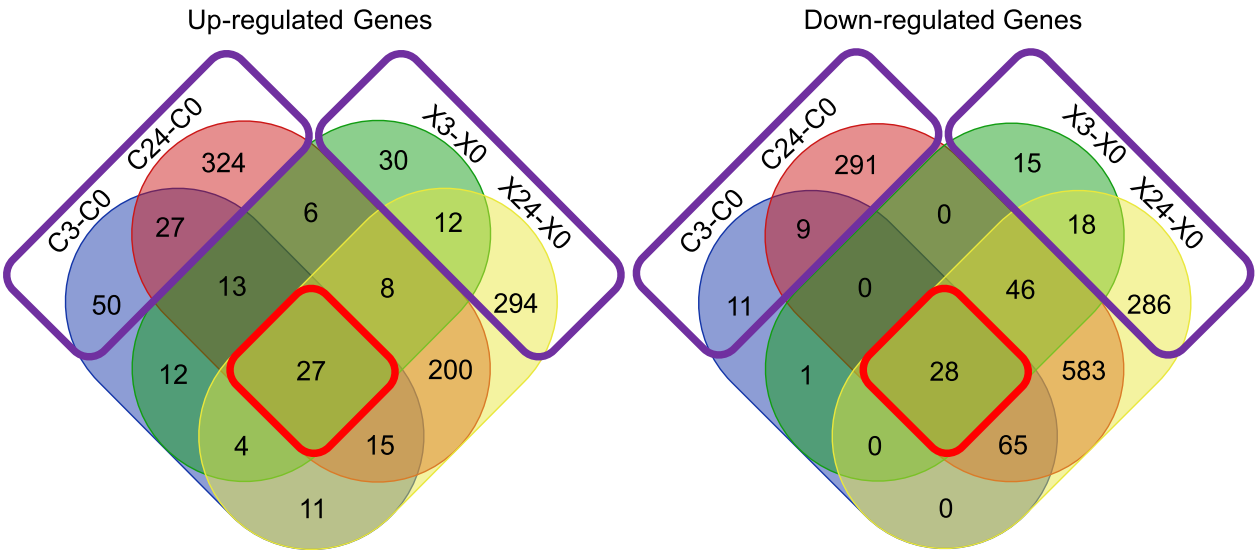

Figure 15. Venn diagrams of up- and down-regulated genes between early and late response genes to X-ray and C-ion radiation under 1G. Common up- and down-regulated genes among all four categories are surrounded in red, while common up- and down-regulated genes between early and late response genes due to only X-ray or C-ion radiation under 1G are surrounded in purple.

Table 97. Common up-regulated genes between early and late response genes to X-ray and C-ion radiation under 1G.

Ensembl Gene ID	Gene Name	Description
ENSG00000136542	*GALNT5*	polypeptide N-acetylgalactosaminyltransferase 5
ENSG00000196576	*PLXNB2*	plexin B2
ENSG00000134574	*DDB2*	damage specific DNA binding protein 2
ENSG00000131080	*EDA2R*	ectodysplasin A2 receptor
ENSG00000163071	*SPATA18*	spermatogenesis associated 18
ENSG00000173846	*PLK3*	polo like kinase
ENSG00000135679	*MDM2*	MDM2 proto-oncogene
ENSG00000244509	*APOBEC3C*	apolipoprotein B mRNA editing enzyme catalytic subunit 3C
ENSG00000120889	*TNFRSF10B*	TNF receptor superfamily member 10b
ENSG00000048392	*RRM2B*	ribonucleotide reductase regulatory TP53 inducible subunit M2B
ENSG00000127241	*MASP1*	MBL associated serine protease 1
ENSG00000182752	*PAPPA*	pappalysin 1
ENSG00000172667	*ZMAT3*	zinc finger matrin-type 3
ENSG00000244694	*PTCHD4*	patched domain containing 4
ENSG00000174307	*PHLDA3*	pleckstrin homology like domain family A member 3
ENSG00000171444	*MCC*	MCC regulator of WNT signaling pathway
ENSG00000124762	*CDKN1A*	cyclin dependent kinase inhibitor 1A
ENSG00000250337	*PURPL*	p53 upregulated regulator of p53
ENSG00000164938	*TP53INP1*	tumor protein p53 inducible nuclear protein 1
ENSG00000132274	*TRIM22*	tripartite motif containing
ENSG00000080546	*SESN1*	sestrin 1
ENSG00000159388	*BTG2*	BTG anti-proliferation factor 2
ENSG00000164125	*GASK1B*	golgi associated kinase 1B
ENSG00000154767	*XPC*	XPC complex subunit, DNA damage recognition and repair factor
ENSG00000167196	*FBXO22*	F-box protein 22
ENSG00000161513	*FDXR*	ferredoxin reductase

Table 98. Common down-regulated genes between early and late response genes to X-ray and C-ion radiation under 1G.

Ensembl Gene ID	Gene Name	Description
ENSG00000156802	*ATAD2*	ATPase family AAA domain containing 2
ENSG00000175305	*CCNE2*	cyclin E2
ENSG00000162063	*CCNF*	cyclin F
ENSG00000094804	*CDC6*	cell division cycle 6
ENSG00000167513	*CDT1*	chromatin licensing and DNA replication factor 1

ENSG00000106462	*EZH2*	enhancer of zeste 2 polycomb repressive complex 2 subunit
ENSG00000189057	*FAM111B*	FAM111 trypsin like peptidase B
ENSG00000184357	*H1-5*	H1.5 linker histone, cluster member
ENSG00000196747	*H2AC13*	H2A clustered histone 13
ENSG00000286522	*H3C2*	H3 clustered histone 2
ENSG00000278828	*H3C10*	H3 clustered histone 10
ENSG00000273983	*H3C8*	H3 clustered histone 8
ENSG00000197061	*H4C3*	H4 clustered histone 3
ENSG00000137807	*KIF23*	kinesin family member 23
ENSG00000065328	*MCM10*	minichromosome maintenance 10 replication initiation factor
ENSG00000112118	*MCM3*	minichromosome maintenance complex component 3
ENSG00000104738	*MCM4*	minichromosome maintenance complex component 4
ENSG00000116062	*MSH6*	mutS homolog 6
ENSG00000085840	*ORC1*	origin recognition complex subunit 1
ENSG00000161800	*RACGAP1*	Rac GTPase activating protein 1
ENSG00000168411	*RFWD3*	ring finger and WD repeat domain 3
ENSG00000171848	*RRM2*	ribonucleotide reductase regulatory subunit M2
ENSG00000140534	*TICRR*	TOPBP1 interacting checkpoint and replication regulator
ENSG00000120802	*TMPO*	thymopoietin
ENSG00000276043	*UHRF1*	ubiquitin like with PHD and ring finger domains 1
ENSG00000162607	*USP1*	ubiquitin specific peptidase 1
ENSG00000092470	*WDR76*	WD repeat domain 76

3.15. Combined effect of radiation and simulated μG on common genes identified between early and late response genes to X-ray and C-ion radiation under 1G

Among the 27 up (Table 97)- and 28 down- regulated (Table 98) genes between early and late response genes to X-ray and C-ion radiation under 1G, 3 up- and 12 down- were found to be statistically significant in at least one of the interactions between early response to X-ray and response to simulated μG ((X3μG-X0μG)-(X3G-X0G)), late response to X-ray and response to simulated μG ((X24μG-X0μG)-(X24G-X0G)), early response to C-ion and response to simulated μG ((C3μG-C0μG)-(C3G-C0G)) or late response to X-ray and response to simulated μG ((C24μG-C0μG)-(C24G-C0G)). Specifically, for over-expressed genes *TNFRSF10B*, *PTCHD4* and *PURPL* (Table 99) that their expression increased with irradiation alone, simulated μG in combination with irradiation resulted in a lower gene expression increase [1]. Furthermore, it was found that in the 12 genes whose expression was decreased with irradiation alone (Table 100), simulated μG in combination with irradiation resulted in a lower gene expression decrease. None the aforementioned 27 up- and 28 down-regulated genes were identified in interactions between late vs early response to X-ray and response to simulated μG ((X24μG-X3μG)-(X24G-X3G)) and in late vs early response to C-ion and response to simulated μG ((C24μG-C3μG)-(C24G-C3G)).

Table 99. 3 up-regulated genes whose expression increased with irradiation alone, while simulated μG in combination with irradiation results in a lower gene expression increase.

Ensembl Gene ID	Gene Name	Description
ENSG00000120889	*TNFRSF10B*	TNF receptor superfamily member 10b
ENSG00000244694	*PTCHD4*	patched domain containing 4
ENSG00000250337	*PURPL*	p53 upregulated regulator of p53

Table 100. 12 down-regulated genes whose expression decreased with irradiation alone, while simulated μG in combination with irradiation results in a lower gene expression decrease.

Ensembl Gene ID	Gene Name	Description
ENSG00000162063	*CCNF*	cyclin F
ENSG00000184357	*H1-5*	H1.5 linker histone, cluster member
ENSG00000196747	*H2AC13*	H2A clustered histone 13
ENSG00000286522	*H3C2*	H3 clustered histone 2
ENSG00000273983	*H3C8*	H3 clustered histone 8
ENSG00000197061	*H4C3*	H4 clustered histone 3

ENSG00000120802	*TMPO*	thymopoietin
ENSG00000137807	*KIF23*	kinesin family member 23
ENSG00000161800	*RACGAP1*	Rac GTPase activating protein 1
ENSG00000168411	*RFWD3*	ring finger and WD repeat domain 3
ENSG00000276043	*UHRF1*	ubiquitin like with PHD and ring finger domains 1
ENSG00000171848	*RRM2*	ribonucleotide reductase regulatory subunit M2
ENSG00000140534	*TICRR*	TOPBP1 interacting checkpoint and replication regulator

3.16. High and Low LET radiation

Venn diagrams were created for up- and down-regulated genes (Figure 15) between 4 comparisons under 1G: Early response to C-ion irradiation (C3G-C0G), late response to C-ion irradiation (C24G-C0G), early response to X-ray irradiation (X3G-X0G) and late response to X-ray irradiation (X24G-X0G). C-ion is high LET (Linear Energy Transfer) radiation, while X-ray is low LET radiation. Genes that were differentially expressed due to only X-ray or C-ion radiation were identified. It was discovered that 401 up- and 311 down-regulated genes were found due to C-ion radiation only, while 336 up- and 319 down – due to X-ray. Performing over-representation analyses for over-expressed genes, in the case of C-ion radiation, biological processes related to defense response (immune effector process and type I interferon signaling pathway) and vesicle-mediated transport between Golgi apparatus and endoplasmic reticulum were highlighted, while for X-ray, the biological process of angiogenesis was identified. Focusing on under-expressed genes, in both types of radiation, the biological process of DNA repair was identified. In C-ion radiation, more specific terms were found, such as double-strand break (DSB) repair, DSB repair via non-homologous end joining and non-recombinational repair relating most probably to the inherent repair difficulty of high-LET radiations and the clustering of ionization and induced damage (Nikitaki et al., 2022). In X-ray, biological processes related to mitotic cell cycle phase transition were more apparent.

3.17. Detection of Oxidase-related genes

From the comparisons between X-ray or C-ion irradiated cells collected 3 or 24 hrs post-irradiation under 1G (X3G-X0G), (X24G-X0G), (C3G-C0G) and (C24G-C0G), the lysyl oxidase (LOX) proteingenes *LOX*, *LOXL1*, *LOXL2*, *LOXL3*, and *LOXL4* were found overexpressed as a response to radiation. All three mitochondrially encoded cytochrome c oxidase subunits (*MT-CO1*, *MT-CO2*, *MT-CO3*) and cytochrome c oxidase subunit 7C (*COX7C*) were also found to be over-expressed. Other oxidases that were discovered to be overexpressed due to IR, were Acyl-CoA oxidase 2 (*ACOX2*), Aldehyde oxidase 1 (AOX1), Quiescin sulfhydryl oxidase 1 (*QSOX1*) and Glutathione peroxidase 1 (*GPX1*).

3.18. Protein-protein interaction networks

Protein-protein interaction networks were made for all DEGs (both up- and down- regulated genes) from the comparison between X-ray irradiated cells collected 24 hrs post-irradiation and sham-irradiated ones under 1G (X24G-X0G) (Figure 16) and between C-ion irradiated cells collected 24 hrs post-irradiation and sham-irradiated ones under 1G (C24G-C0G) (Figure 17). Interactions of each gene were counted and genes with 9 common hub genes, i.e. genes with maximum number of edges, were pinpointed (Table 101). Performing biological term enrichment analyses on those 9 genes, biological processes related to cell cycle G2/M phase transition, histone phosphorylation and DNA integrity checkpoint were identified. The predominant KEGG pathway highlighted was cell cycle.

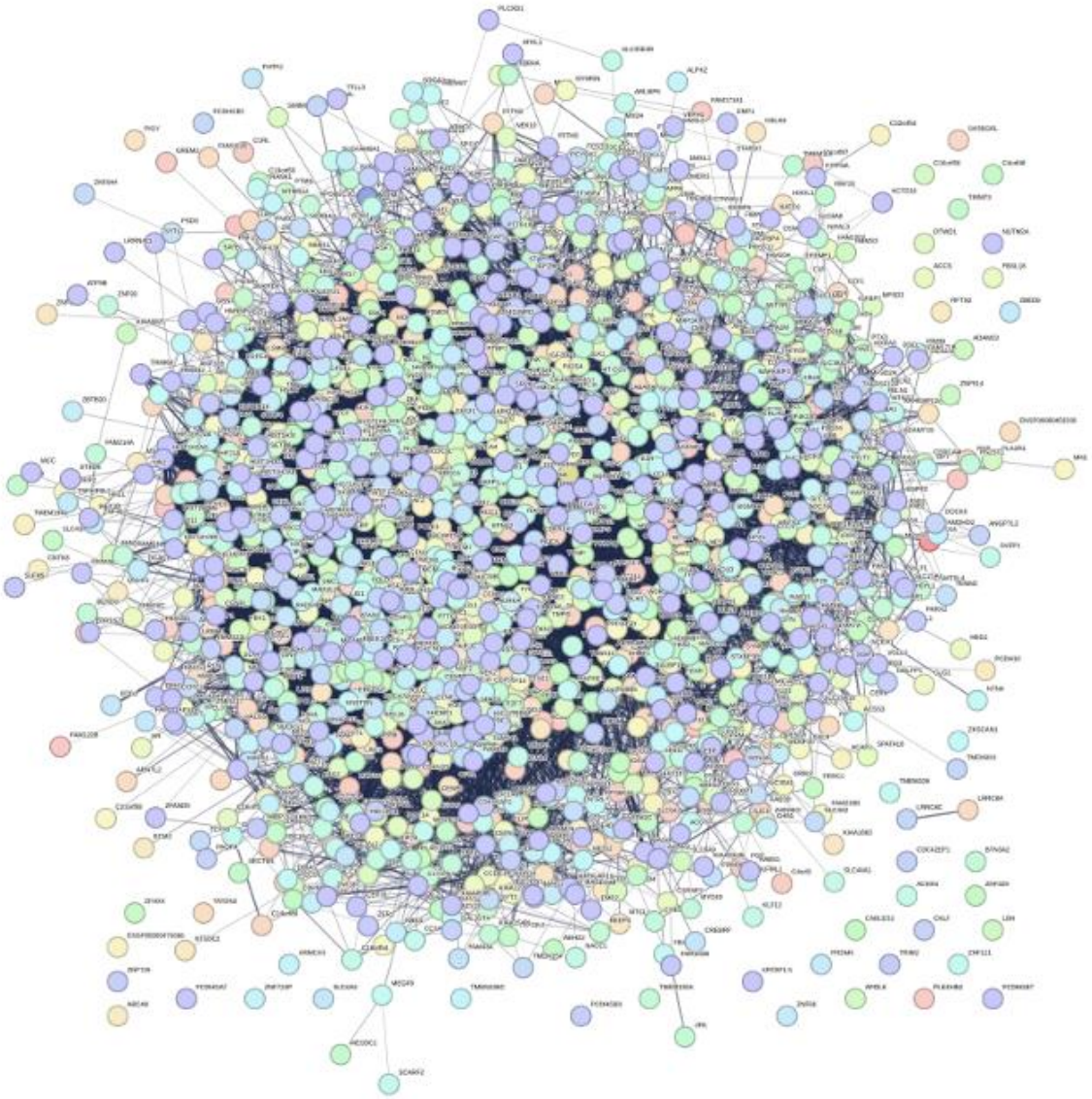

Figure 16. Protein-protein interaction network for DEGs from the comparison between X-ray irradiated cells collected 24 hrs post-irradiation and sham-irradiated ones under 1G.

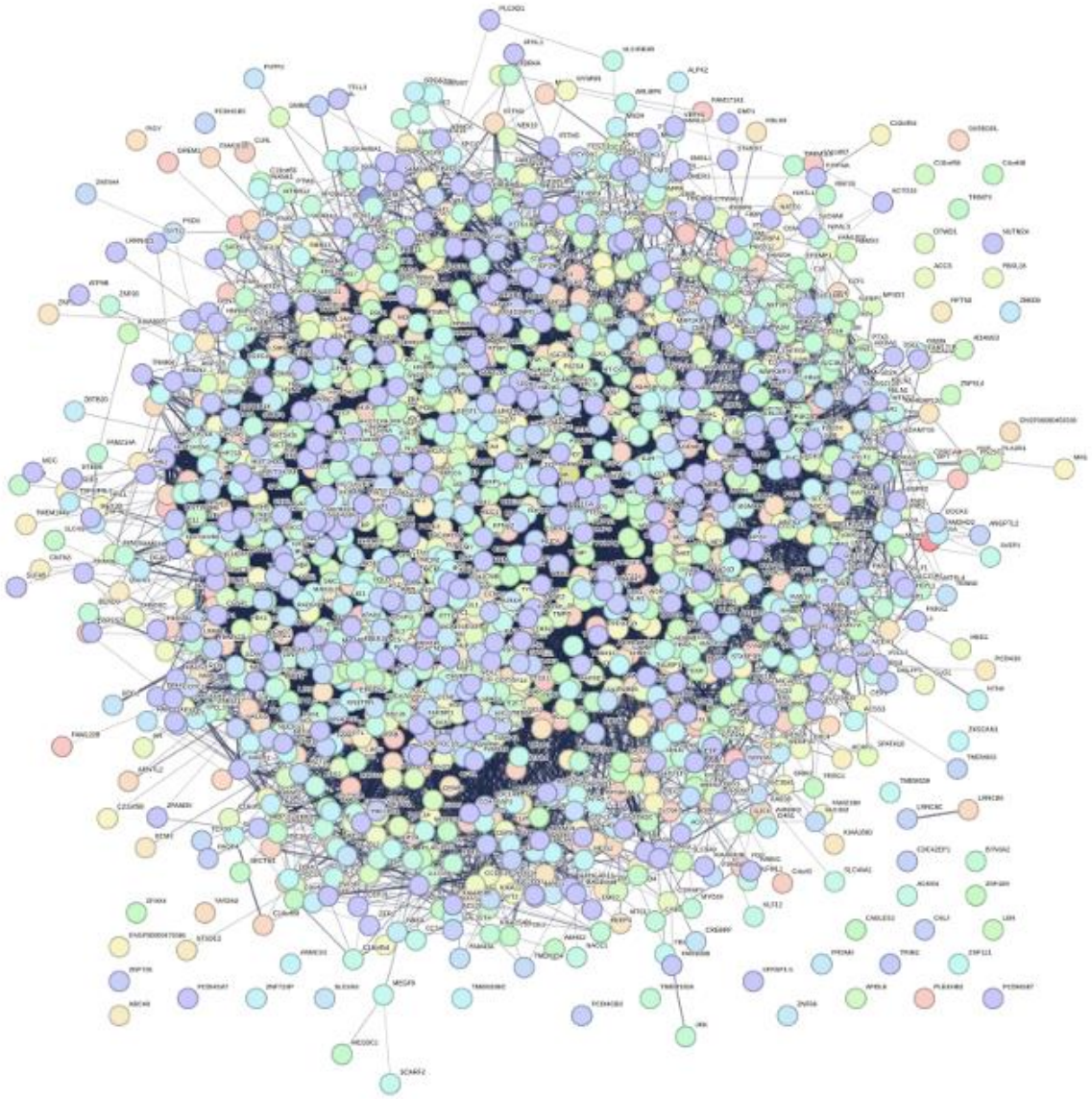

Figure 17. Protein-protein interaction network for DEGs from the comparison between C-ion irradiated cells collected 24 hrs post-irradiation and sham-irradiated ones under 1G.

Table 101. 9 common hub DEGs from the comparisons between X-ray irradiated cells collected 24 hrs post-irradiation and sham-irradiated ones under 1G, as well as between C-ion irradiated cells collected 24 hrs post-irradiation and sham-irradiated ones under 1G.

Ensembl Gene ID	Gene Name	Description
ENSG00000166851	*PLK1*	polo like kinase 1
ENSG00000012048	*BRCA1*	BRCA1 DNA repair associated
ENSG00000134057	*CCNB1*	cyclin B1
ENSG00000178999	*AURKB*	aurora kinase B
ENSG00000170312	*CDK1*	cyclin dependent kinase 1
ENSG00000149554	*CHEK1*	checkpoint kinase 1
ENSG00000051180	*RAD51*	RAD51 recombinase
ENSG00000145386	*CCNA2*	cyclin A2
ENSG00000131747	*TOP2A*	DNA topoisomerase II alpha

3.19. Other DEG analyses

Comparisons involving early (X3μG-X0μG), late (X24μG-X0μG) and late vs early (X24μG-X3μG) responses to X-ray under simulated μG had similar effects to early (X3G-X0G), late (X24G-X0G) and late vs early (X24G-X3G) responses to X-ray under 1G. Comparisons concerning early (C3μG-C0μG), late (C24μG-C0μG) and late vs early (C24μG-C3μG) responses to C-ion radiation under simulated μG had similar effects to early (C3G-C0G), late (C24G-C0G) and late vs early (C24G-C3G) responses to C-ion radiation under 1G.

4. DISCUSSION

In both types of radiation (X-rays or C-ions), the comparisons between 24 hrs post radiation vs 0h identified more DEGs than the comparisons between 3 hrs post radiation vs 0h, although most early response genes were included in the late response gene lists. Late response genes are possibly induced or suppressed by the effects of early response genes.

Based on biological term enrichments, processes related to cellular response to DNA damage stimulus were identified 3-hrs post irradiation, while DNA repair was found to be suppressed 24-hrs post irradiation, as DNA damage repair (DDR) is an early response mechanism (Nickoloff, Boss, Allen, & LaRue, 2017). Signal transduction by p53 class mediator was also identified mainly in early response, as it was previously shown (Okazaki, 2022). Expression of *CDKN1A* is induced by p53 and is a mediator of p53 tumor suppression (el-Deiry et al., 1993). p53 tumor suppressor protein (TP53) plays an important role in DDR mechanisms through signaling responses, as its activation induces the p21 protein, encoded by the *CDKN1A* gene, resulting in G1 arrest (Saini et al., 2012). *CDKN1A* was found to be over-expressed 3 and 24 hrs after irradiation with 1 Gy of X-ray and 1 Gy of C-ion, as it was previously found (H. Ikeda et al., 2019). Cell cycle arrest allows DDR mechanisms to act and prevents non-repaired cells from passing into the phase of synthesis. Cells failing to be repaired undergo apoptosis, a biological process that refers to programmed cell death (Elmore, 2007). Indeed, biological processes related to the intrinsic apoptotic signaling pathway were also identified in the early response to radiation. The transcription factor FOXO4 (Forkhead Box O4) was identified as a transcription factor inducing genes in response to irradiation. FoxO signaling pathway for differentially expressed genes was also identified after exposure to high doses of X-rays, collected 8–24 hrs post-irradiation (Michalettou et al., 2021). FOXOs are transcription factors that play a crucial role in cell fate decision and are involved in the promotion of apoptosis (Z. Fu & Tindall, 2008). E2F was identified as an over-represented gene-targeting transcription factor in down regulated genes. E2F is crucial for the regulation of cell cycle and action of tumor suppressor proteins.

Genes *CDKN1A*, *MDM2*, *PURPL*, *PTCHD4*, *TP53INP1*, *PAPPA* and *BTG2* were found to be up-regulated post-radiation in 1G and simulated μG condition, having the lowest p-values, as well as the highest Log2FoldChanges. *MDM2* was found to be over-expressed after irradiation with 1 Gy of X-ray and 1 Gy of C-ion, as it was previously found (H. Ikeda et al., 2019). *TP53INP1* was found to be up-regulated in human irradiated fibroblasts and is associated with the regulation of apoptosis (Kis et al., 2006; Tachiiri et al., 2006). In a previous study (Venkata Narayanan et al., 2017), it was found that PAPPA levels were higher in response to ionizing radiation. The elevation of BTG2 in response to radiation was also found in non-small cell lung cancer (NSCLC), consequently increasing apoptosis (C. Zhu, Zhang, Xue, Feng, & Fan, 2022).

MKI67 and *CCNB1* had a lower expression in response to radiation, especially 24-hrs post-irradiation in 1G or simulated μG conditions. The decrease of the expression of *MKI67* and *CCNB1* genes as a response to radiation was previously reported (H. Ikeda et al., 2019). Histone clustered genes (*H2AC13*, *H3C2*, *H3C10*, *H3C8* and *H4C3*) were found to be down-regulated genes post-radiation in 1G and simulated μG condition, as radiation suppressed the expression of various histone clustered genes (Ge et al., 2020). Nucleosome occupancy reduction was observed in yeast, as a response to DNA damage. Histone eviction at sites of DNA breaks, facilitates the recruitment of repair factors (Hauer et al., 2017). Minichromosome maintenance genes (*MCM10*, *MCM3* and *MCM4*) were also under-expressed. Minichromosome maintenance (MCM) is associated with cell cycle progression and DNA replication (Maiorano, Lutzmann, & Mechali, 2006).

In this study, the combined effect of C-ion or X-ray and simulated μG resulted in the up regulation of *TNFRSF10B*, *PTCHD4*, and *PURPL* genes. Their expression increased with irradiation alone, but their expression increase was lower when irradiation was combined with simulated μG than when it was combined with 1G. The expression of *CDKN1A* was found to behave in a similar way, but its lower increase was less statistically significant. It has been reported that the combined effect of C-ion radiation and simulated μG results in a lower increase of the expression of *CDKN1A*, compared to the effect of C-ion radiation treatment alone (H. Ikeda et al., 2019). The expression of *TNFRSF10B* significantly increased in irradiated germline stem cells (GSCs) (Ishii et al., 2014). *TNFSF10-TNFRSF10B* pathway was found to be involved in radiation-induced apoptosis. The combined effect of radiation and simulated μG, may reduce the role of the *TNFSF10-TNFRSF10B* pathway that is

crucial in the regulation of response to radiation, suppressing the process of apoptosis, meaning unrepaired cells to not undergo apoptosis, potentially causing the duplication of damaged cells. *PTCHD4* has been found to be up-regulated as a response to ionizing radiation and the binding of p53 to the regulatory region of *PTCHD4* is similar to that of p53 to *CDKN1A* promoter (Chung, Larsen, Chen, & Bunz, 2014). PURPL is a long non-coding RNA (lncRNA) (X. Fu et al., 2019). lncRNAs are RNA molecules of over 200 nucleotides in length that do not encode for proteins, but are instead related to the post-transcriptional regulation, interacting with proteins (Ferrè, Colantoni, & Helmer-Citterich, 2016), mRNAs (Grelet et al., 2017) or miRNAs (M. Ma et al., 2018). PURPL has been reported to be up-regulated after DNA damage (X. L. Li et al., 2017). PURPL expression is anti-correlated with that of TP53. It was suggested that its anti-apoptotic action is due to its regulation of *TP53* gene (X. Fu et al., 2019).

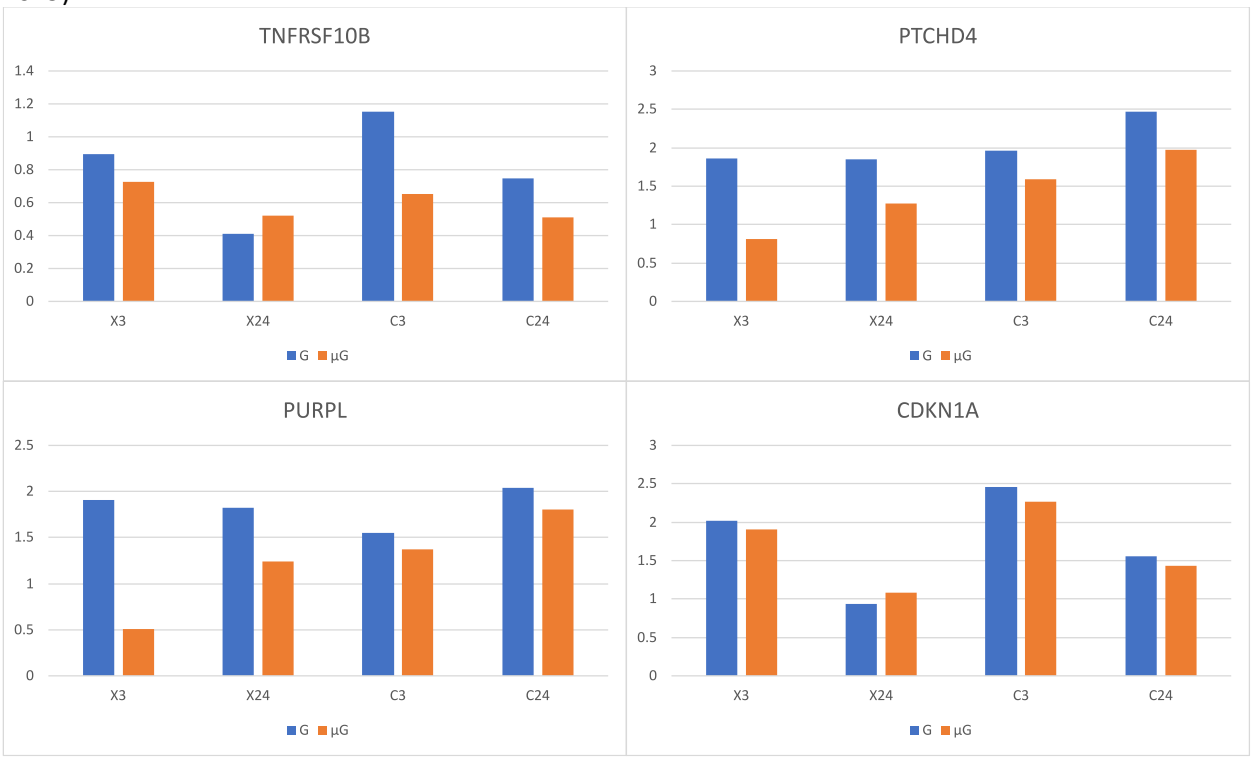

Figure 18. log2 fold changes of up-regulated genes 3 hrs (X3) or 24 hrs (X24) after X-ray exposure vs sham irradiation and 3 hrs (C3) or 24 hrs (C24) after C ion exposure vs sham irradiation under 1G (G)(in blue) or simulated microgravity (µG)(in orange).

It was found that in the 12 genes (*CNF*, *H1-5*, *H2AC13*, *H3C2*, *H3C8*, *H4C3*, *TMPO*, *KIF231*, *RFWD3*, *UHRF1*, *RRM2*, *TICRR*) whose expression was decreased with irradiation alone, simulated µG in combination with irradiation resulted in a lower gene expression decrease. The lowered transcriptional response to irradiation under simulated µG of genes that are related to cell apoptosis and DNA damage repair may explain the observed increase of chromosome aberrations in cells that were exposed simultaneously to radiation and simulated µG (Hada et al., 2018).

Figure 19. log2 fold changes of down-regulated genes 3 hrs (X3) or 24 hrs (X24) after X-ray exposure vs sham irradiation and 3 hrs (C3) or 24 hrs (C24) after C ion exposure vs sham irradiation under 1G (G)(in blue) or simulated microgravity (µG)(in orange).

Comparing sham-irradiated cells under simulated µG and 1G, enrichment analyses in statistically significant down-regulated genes, highlighted terms related to response to oxygen levels, muscle contraction and regulation of blood circulation. Based on their log2 fold changes, *TTN* and *MSTN* were identified as the most prominent down-regulated genes. *TTN* encodes for the lengthiest human protein, Titin which controls sarcomere elasticity and contraction and is linked to the development of muscle atrophy (Ottenheijm et al., 2009). As µG induces skeletal muscle atrophy (Droppert, 1993; Vandenburgh, Chromiak, Shansky, Del Tatto, & Lemaire, 1999), *TTN* under-expression under µG could be responsible for muscle mass loss in space flights. On the other hand, myostatin which is encoded by *MSTN*, is potentially one of the mediators of muscle loss induced by µG (Lee et al., 2020; Smith et al., 2020). Thus, the down-regulation of the expression of *MSTN* may serve as a mechanism to reverse µG -induced mass loss and strength. The under-expression under µG of genes that are related to response to oxygen levels and regulation of blood circulation may be due to lower muscle activity. It has been found that an effect of µG is the reduced human ventilatory response to hypoxia (Prisk, Elliott, & West, 2000).

Biological processes related to defense response (immune effector process and type I interferon signaling pathway) were highlighted in genes that were only differentially expressed under C-ion (high LET) radiation but not in genes that were differentially expressed under X-ray (low LET) radiation. Type I interferons are components of the early immune response (F. Zhang et al., 2020). Strong association between response to radiation and immune system and inflammation have been suggested in the past (Georgakilas et al., 2015). Although DNA repair was identified as an over-represented term in both aforementioned gene subsets, DDR terms such as double-strand break

repair, double-strand break repair via non-homologous end joining (NHEJ) and non-recombinational repair were found exclusively in the genes that were differentially expressed under high LET radiation. NHEJ repair have been found to play a more important role than homologous recombination repair in defining radiosensitivity after exposure to high-LET radiation like carbon, iron, neon and argon ions (Takahashi et al., 2014). The increased complexity of damage often is associated with increase lethality compared to low-LET radiations (Hada et al., 2018). Based on data on X-ray and C-ion irradiated human G2-phase cells, it was suggested that classical NHEJ will make an initial attempt to repair the DSBs (Averbeck et al., 2016; Grabarz, Barascu, Guirouilh-Barbat, & Lopez, 2012). Examining up-regulated genes due to X-ray (low LET) radiation, biological processes related to angiogenesis were discovered. Late down-regulated genes were found to be related to DNA damage repair, as it was previously shown (B. M. Sutherland, Bennett, Sutherland, & Laval, 2002). Last but not least, relating to biological effects of IR, the generation of oxidative stress is expected (Nikitaki, Hellweg, Georgakilas, & Ravanat, 2015). The lysyl oxidase (LOX) family of proteins contains five members: *LOX*, *LOXL1*, *LOXL2*, *LOXL3*, and *LOXL4* (Molnar et al., 2003), all of which were found overexpressed as a response to radiation according to our results. LOX proteins play critical role in the formation and repair of the Extracellular Matrix (ECM) by oxidizing lysine residues in elastin and collagen, thereby initiating the formation of covalent cross linkages which stabilize these fibrous proteins (Pinnell & Martin, 1968; Siegel, Pinnell, & Martin, 1970). Hydrogen peroxide is a side product of this catalytic reaction. LOX proteins are expressed in fibroblasts (Hong, Uzel, Duan, Sheff, & Trackman, 1999). Aberrant expression is involved in tumor invasion and metastasis (W. Wang, Wang, Yao, & Huang, 2022). Thus, lysyl oxidases provide targets for pharmacological and therapeutic intervention. In addition, we have detected an overexpression of all three mitochondrially encoded cytochrome c oxidase subunits (*MT-CO1*, *MT-CO2*, *MT-CO3*), as also previously found (Gong, Chen, & Almasan, 1998). Another upregulated in our experiments cytochrome c oxidase subunit is cytochrome c oxidase subunit 7C (*COX7C*). Cytochrome c Oxidase is related to the regulation of oxidative phosphorylation (Ludwig et al., 2001). Other oxidases that we discovered to be overexpressed due to IR include the following: Acyl-CoA oxidase 2 (*ACOX2*) is involved in the degradation of long branched fatty acids and bile acid intermediates in peroxisomes (Ferdinandusse et al., 2018; Poll-The et al., 1988). Aldehyde oxidase 1 (*AOX1*) produces hydrogen peroxide (Kundu, Hille, Velayutham, & Zweier, 2007) and may be involved in the regulation of reactive oxygen species (ROS) homeostasis (Garrido & Leimkuhler, 2021; Terao, Garattini, Romao, & Leimkuhler, 2020). Quiescin sulfhydryl oxidase 1 (*QSOX1*) catalyzes the oxidation of sulfhydryl groups in peptide and protein thiols to disulfides with the reduction of oxygen to hydrogen peroxide (Chakravarthi, Jessop, Willer, Stirling, & Bulleid, 2007; Grossman, Alon, Ilani, & Fass, 2013; Heckler, Alon, Fass, & Thorpe, 2008; Ilani et al., 2013; Javitt et al., 2019).

Glutathione peroxidase 1 (*GPX1*), a major antioxidant enzyme (de Haan & Cooper, 2011), was also found to be overexpressed as a response to IR in our analysis. *GPX1* belongs to the glutathione peroxidase family, catalyzing the reduction of hydrogen peroxide by glutathione, to protect cells against oxidative damage (M. Sutherland, Shankaranarayanan, Schewe, & Nigam, 2001), therefore its induction underlines the response to a possible oxidative stress induced by IRs also in our case. That in turn, proposes employing a strategy that increases the activity of antioxidants that remove H2O2, such as GPX1, by administering GPX1-mimics, like ebselen (Schewe, 1995).We identify that *PLK1*, *BRCA1*, *CCNB1*, *AURKB*, *CDK1*, *CHEK1*, *RAD51*, *CCNA2*, *TOP2A* are hub genes in protein interaction networks for DEGs from the comparison between X-ray or C-ion irradiated cells collected 24 hrs post-irradiation and sham-irradiated ones under 1G condition. Also, *BRCA1* and *RAD51* are associated with damage repair of DNA breaks. We note that *PLK1*, *CCNB1*, *AURKB*, *CDK1*, *CHEK1*, *CCNA2* and *TOP2A* play a critical role in the process of mitosis.

Our current findings suggest that human cells exposed to microgravity may significantly change their response to a genuine stressor like radiation. Therefore, open the field for use of these results for the development of new tools and methodologies to overcome tumor resistance beyond the current use in space missions.

5. CONCLUSIONS

We conclude that the response to radiation involves the p53 signal cascade, whose function is the preservation of genomic integrity. Upon ionizing irradiation, the DEGs are related to DNA damage response and repair, cell cycle arrest and apoptosis, which are related to the regulation of G1/S and G2/M phase transition of the mitotic cell cycle. High LET radiation induces the expression of genes related to immune response and vesicle-mediated transport, while low LET induces genes related to angiogenesis. Upon microgravity alone, DEGs are related to lower muscle activity. In some cases, the combined effect of irradiation and microgravity in gene expression is lower than the effect of radiation alone. This results in unrepaired cells failing to undergo apoptosis, potentially causing the duplication of damaged cells. Lastly, the lowered transcriptional response to irradiation under simulated μG of genes that are related to cell apoptosis and DNA damage repair may explain the observed increase of chromosome aberrations in cells that were exposed simultaneously to radiation and simulated μG.

This bioinformatics approach will certainly help to gain better understanding on the overview of the biological response mechanisms to the combined stressors like radiation and microgravity during space missions and potentially for the establishment of the countermeasures but also in treatment of tumor cells. The dose of X-ray and C-ion exposure in this experiment was relatively high compared to the radiation dose astronauts are typically exposed to in Space. This study indicates that further research is needed to comprehend the combined effects of different gravitational conditions and radiation environments. Samples exposed to low-dose chronic exposure under simulated μG and partial gravity are currently being studied that simulate prospective future space mission scenarios.

REFERENCES

Ahnstrom, G., Ehrenberg, A., & Graslund, A. (1978). The effect of ionizing radiation on DNA: conclusions and perspectives. *Mol Biol Biochem Biophys, 27*, 348-352. Retrieved from https://www.ncbi.nlm.nih.gov/pubmed/651869

Andrews, S. (2010). FastQC: A Quality Control Tool for High Throughput Sequence Data. Cambridge, UK: Babraham Bioinformatics, Babraham Institute. Retrieved from https://www.bioinformatics.babraham.ac.uk/projects/fastqc/

Averbeck, N. B., Topsch, J., Scholz, M., Kraft-Weyrather, W., Durante, M., & Taucher-Scholz, G. (2016). Efficient Rejoining of DNA Double-Strand Breaks despite Increased Cell-Killing Effectiveness following Spread-Out Bragg Peak Carbon-Ion Irradiation. *Front Oncol, 6*, 28. doi:10.3389/fonc.2016.00028

Benjamini, Y., & Hochberg, Y. (1995). Controlling the False Discovery Rate: A Practical and Powerful Approach to Multiple Testing. *J R Stat Soc Ser B (Methodol), 57*, 289–300. doi:10.1111/j.2517-6161.1995.tb02031.x

Bernhard, E. J., Maity, A., Muschel, R. J., & McKenna, W. G. (1995). Effects of ionizing radiation on cell cycle progression. A review. *Radiat Environ Biophys, 34*(2), 79-83. doi:10.1007/BF01275210

Broude, E. V., Demidenko, Z. N., Vivo, C., Swift, M. E., Davis, B. M., Blagosklonny, M. V., & Roninson, I. B. (2007). p21 (CDKN1A) is a negative regulator of p53 stability. *Cell Cycle, 6*(12), 1468-1471. doi:10.4161/cc.6.12.4313

Castro, J. R., Blakely, E. A., Tsujii, H., & Schulz-Ertner, D. (2010). Carbon Ion Radiotherapy. In *Leibel and Phillips Textbook of Radiation Oncology* (pp. 1511-1522).

Chakravarthi, S., Jessop, C. E., Willer, M., Stirling, C. J., & Bulleid, N. J. (2007). Intracellular catalysis of disulfide bond formation by the human sulfhydryl oxidase, QSOX1. *Biochem J, 404*(3), 403-411. doi:10.1042/BJ20061510

Chapman, B., Kirchner, R., Pantano, L., Naumenko, S., De Smet, M., Beltrame, L., . . . Yoon, J. (2021). Bcbio/Bcbio-Nextgen: V1.2.9. Geneva, Switzerland: Zenodo. Retrieved from https://bcbio-nextgen.readthedocs.io/

Chu, Y., & Corey, D. R. (2012). RNA sequencing: platform selection, experimental design, and data interpretation. *Nucleic Acid Ther, 22*(4), 271-274. doi:10.1089/nat.2012.0367

Chung, J. H., Larsen, A. R., Chen, E., & Bunz, F. (2014). A PTCH1 homolog transcriptionally activated by p53 suppresses Hedgehog signaling. *J Biol Chem, 289*(47), 33020-33031. doi:10.1074/jbc.M114.597203

Crick, F. (1970). Central dogma of molecular biology. *Nature, 227*(5258), 561-563. doi:10.1038/227561a0

Crick, F. H. (1958). On protein synthesis. *Symp Soc Exp Biol, 12*, 138-163. Retrieved from https://www.ncbi.nlm.nih.gov/pubmed/13580867

Cucinotta, F. A., & Durante, M. (2006). Cancer risk from exposure to galactic cosmic rays: implications for space exploration by human beings. *Lancet Oncol, 7*(5), 431-435. doi:10.1016/S1470-2045(06)70695-7

de Haan, J. B., & Cooper, M. E. (2011). Targeted antioxidant therapies in hyperglycemia-mediated endothelial dysfunction. *Front Biosci (Schol Ed), 3*(2), 709-729. doi:10.2741/s182

Dendy, P. P., & Heaton, B. (2011). *Physics for Diagnostic Radiology*.

Dobin, A., Davis, C. A., Schlesinger, F., Drenkow, J., Zaleski, C., Jha, S., . . . Gingeras, T. R. (2013). STAR: ultrafast universal RNA-seq aligner. *Bioinformatics, 29*(1), 15-21. doi:10.1093/bioinformatics/bts635

Droppert, P. M. (1993). A review of muscle atrophy in microgravity and during prolonged bed rest. *J Br Interplanet Soc, 46*(3), 83-86.

el-Deiry, W. S., Tokino, T., Velculescu, V. E., Levy, D. B., Parsons, R., Trent, J. M., . . . Vogelstein, B. (1993). WAF1, a potential mediator of p53 tumor suppression. *Cell, 75*(4), 817-825. doi:10.1016/0092-8674(93)90500-p

Elmore, S. (2007). Apoptosis: a review of programmed cell death. *Toxicol Pathol, 35*(4), 495-516. doi:10.1080/01926230701320337

Ewels, P., Magnusson, M., Lundin, S., & Käller, M. (2016). MultiQC: summarize analysis results for multiple tools and samples in a single report. *Bioinformatics, 32*(19), 3047-3048. doi:10.1093/bioinformatics/btw354

Ferdinandusse, S., Denis, S., van Roermund, C. W. T., Preece, M. A., Koster, J., Ebberink, M. S., . . . Wanders, R. J. A. (2018). A novel case of ACOX2 deficiency leads to recognition of a third human peroxisomal acyl-CoA oxidase. *Biochim Biophys Acta Mol Basis Dis, 1864*(3), 952-958. doi:10.1016/j.bbadis.2017.12.032

Ferrè, F., Colantoni, A., & Helmer-Citterich, M. (2016). Revealing protein-lncRNA interaction. *Brief Bioinform, 17*(1), 106-116. doi:10.1093/bib/bbv031

Fu, X., Wang, Y., Wu, G., Zhang, W., Xu, S., & Wang, W. (2019). Long noncoding RNA PURPL promotes cell proliferation in liver cancer by regulating p53. *Mol Med Rep, 19*(6), 4998-5006. doi:10.3892/mmr.2019.10159

Fu, Z., & Tindall, D. J. (2008). FOXOs, cancer and regulation of apoptosis. *Oncogene, 27*(16), 2312-2319. doi:10.1038/onc.2008.24

Funk, J. O. (1999). Cancer cell cycle control. *Anticancer Res, 19*(6A), 4772-4780. Retrieved from https://www.ncbi.nlm.nih.gov/pubmed/10697591

García-Alcalde, F., Okonechnikov, K., Carbonell, J., Cruz, L. M., Götz, S., Tarazona, S., . . . Conesa, A. (2012). Qualimap: evaluating next-generation sequencing alignment data. *Bioinformatics, 28*(20), 2678-2679. doi:10.1093/bioinformatics/bts503

Garrido, C., & Leimkuhler, S. (2021). The Inactivation of Human Aldehyde Oxidase 1 by Hydrogen Peroxide and Superoxide. *Drug Metab Dispos, 49*(9), 729-735. doi:10.1124/dmd.121.000549

Ge, C., Su, F., Fu, H., Wang, Y., Tian, B., Liu, B., . . . Zheng, X. (2020). RNA Profiling Reveals a Common Mechanism of Histone Gene Downregulation and Complementary Effects for Radioprotectants in Response to Ionizing Radiation. *Dose Response, 18*(4), 1559325820968433. doi:10.1177/1559325820968433

Gene Ontology Consortium. (2023). The Gene Ontology Knowledgebase in 2023. *Genetics, 224*, iyad031. doi:10.1093/genetics/iyad031

Georgakilas, A. G., Pavlopoulou, A., Louka, M., Nikitaki, Z., Vorgias, C. E., Bagos, P. G., & Michalopoulos, I. (2015). Emerging molecular networks common in ionizing radiation, immune and inflammatory responses by employing bioinformatics approaches. *Cancer Lett, 368*(2), 164-172. doi:10.1016/j.canlet.2015.03.021

Gong, B., Chen, Q., & Almasan, A. (1998). Ionizing radiation stimulates mitochondrial gene expression and activity. *Radiat Res, 150*(5), 505-512. doi:10.2307/3579866

Grabarz, A., Barascu, A., Guirouilh-Barbat, J., & Lopez, B. S. (2012). Initiation of DNA double strand break repair: signaling and single-stranded resection dictate the choice between homologous recombination, non-homologous end-joining and alternative end-joining. *Am J Cancer Res, 2*(3), 249-268.

Grelet, S., Link, L. A., Howley, B., Obellianne, C., Palanisamy, V., Gangaraju, V. K., . . . Howe, P. H. (2017). A regulated PNUTS mRNA to lncRNA splice switch mediates EMT and tumour progression. *Nat Cell Biol, 19*(9), 1105-1115. doi:10.1038/ncb3595

Grossman, I., Alon, A., Ilani, T., & Fass, D. (2013). An inhibitory antibody blocks the first step in the dithiol/disulfide relay mechanism of the enzyme QSOX1. *J Mol Biol, 425*(22), 4366-4378. doi:10.1016/j.jmb.2013.07.011

Hada, M., Ikeda, H., Rhone, J. R., Beitman, A. J., Plante, I., Souda, H., . . . Takahashi, A. (2018). Increased Chromosome Aberrations in Cells Exposed Simultaneously to Simulated Microgravity and Radiation. *Int J Mol Sci, 20*(1). doi:10.3390/ijms20010043

Hauer, M. H., Seeber, A., Singh, V., Thierry, R., Sack, R., Amitai, A., . . . Gasser, S. M. (2017). Histone degradation in response to DNA damage enhances chromatin dynamics and recombination rates. *Nat Struct Mol Biol, 24*(2), 99-107. doi:10.1038/nsmb.3347

Hauslage, J., Cevik, V., & Hemmersbach, R. (2017). Pyrocystis noctiluca represents an excellent bioassay for shear forces induced in ground-based microgravity simulators (clinostat and random positioning machine). *NPJ Microgravity, 3*, 12. doi:10.1038/s41526-017-0016-x

Heckler, E. J., Alon, A., Fass, D., & Thorpe, C. (2008). Human quiescin-sulfhydryl oxidase, QSOX1: probing internal redox steps by mutagenesis. *Biochemistry, 47*(17), 4955-4963. doi:10.1021/bi702522q

Hong, H. H., Uzel, M. I., Duan, C., Sheff, M. C., & Trackman, P. C. (1999). Regulation of lysyl oxidase, collagen, and connective tissue growth factor by TGF-beta1 and detection in human gingiva. *Lab Invest, 79*(12), 1655-1667. Retrieved from https://www.ncbi.nlm.nih.gov/pubmed/10616214

Ikeda, H., Muratani, M., Hidema, J., Hada, M., Fujiwara, K., Souda, H., . . . Takahashi, A. (2019). Expression Profile of Cell Cycle-Related Genes in Human Fibroblasts Exposed Simultaneously to Radiation and Simulated Microgravity. *Int J Mol Sci, 20*(19), 4791. doi:10.3390/ijms20194791

Ikeda, H., Souda, H., Puspitasari, A., Held, K. D., Hidema, J., Nikawa, T., . . . Takahashi, A. (2016). A New System for Three-dimensional Clinostat Synchronized X-irradiation with a High-speed Shutter for Space Radiation Research. *Biological Sciences in Space, 30*, 8-16. doi:10.2187/bss.30.8

Ikeda, H., Souda, H., Puspitasari, A., Held, K. D., Hidema, J., Nikawa, T., . . . Takahashi, A. (2017). Development and performance evaluation of a three-dimensional clinostat synchronized heavy-ion irradiation system. *Life Sci Space Res (Amst), 12*, 51-60. doi:10.1016/j.lssr.2017.01.003

Ilani, T., Alon, A., Grossman, I., Horowitz, B., Kartvelishvily, E., Cohen, S. R., & Fass, D. (2013). A secreted disulfide catalyst controls extracellular matrix composition and function. *Science, 341*(6141), 74-76. doi:10.1126/science.1238279

Indo, H. P., Tomiyoshi, T., Suenaga, S., Tomita, K., Suzuki, H., Masuda, D., . . . Majima, H. J. (2015). MnSOD downregulation induced by extremely low 0.1 mGy single and fractionated X-rays and microgravity treatment in human neuroblastoma cell line, NB-1. *J Clin Biochem Nutr, 57*(2), 98-104. doi:10.3164/jcbn.15-20

Ishii, K., Ishiai, M., Morimoto, H., Kanatsu-Shinohara, M., Niwa, O., Takata, M., & Shinohara, T. (2014). The Trp53-Trp53inp1-Tnfrsf10b pathway regulates the radiation response of mouse spermatogonial stem cells. *Stem Cell Rep, 3*(4), 676-689. doi:10.1016/j.stemcr.2014.08.006

Javitt, G., Grossman-Haham, I., Alon, A., Resnick, E., Mutsafi, Y., Ilani, T., & Fass, D. (2019). cis-Proline mutants of quiescin sulfhydryl oxidase 1 with altered redox properties undermine extracellular matrix integrity and cell adhesion in fibroblast cultures. *Protein Sci, 28*(1), 228-238. doi:10.1002/pro.3537

Kanehisa, M., Furumichi, M., Sato, Y., Kawashima, M., & Ishiguro-Watanabe, M. (2023). KEGG for taxonomy-based analysis of pathways and genomes. *Nucleic Acids Res, 51*(D1), D587-D592. doi:10.1093/nar/gkac963

Khatri, P., Sirota, M., & Butte, A. J. (2012). Ten years of pathway analysis: current approaches and outstanding challenges. *PLoS Comput Biol, 8*(2), e1002375. doi:10.1371/journal.pcbi.1002375

Kis, E., Szatmari, T., Keszei, M., Farkas, R., Esik, O., Lumniczky, K., . . . Safrany, G. (2006). Microarray analysis of radiation response genes in primary human fibroblasts. *Int J Radiat Oncol Biol Phys, 66*(5), 1506-1514. doi:10.1016/j.ijrobp.2006.08.004

Kojima, Y., & Machida, Y. J. (2020). DNA-protein crosslinks from environmental exposure: Mechanisms of formation and repair. *Environ Mol Mutagen, 61*(7), 716-729. doi:10.1002/em.22381

Kundu, T. K., Hille, R., Velayutham, M., & Zweier, J. L. (2007). Characterization of superoxide production from aldehyde oxidase: an important source of oxidants in biological tissues. *Arch Biochem Biophys, 460*(1), 113-121. doi:10.1016/j.abb.2006.12.032

L'Annunziata, M. (2003). *Handbook of radioactivity analysis Second edition*. Netherlands: Elsevier Science Publishers.

Lee, S. J., Lehar, A., Meir, J. U., Koch, C., Morgan, A., Warren, L. E., . . . Germain-Lee, E. L. (2020). Targeting myostatin/activin A protects against skeletal muscle and bone loss during spaceflight. *Proc Natl Acad Sci U S A, 117*(38), 23942-23951. doi:10.1073/pnas.2014716117

Li, H., Handsaker, B., Wysoker, A., Fennell, T., Ruan, J., Homer, N., . . . Durbin, R. (2009). The Sequence Alignment/Map format and SAMtools. *Bioinformatics, 25*(16), 2078-2079. doi:10.1093/bioinformatics/btp352

Li, X. L., Subramanian, M., Jones, M. F., Chaudhary, R., Singh, D. K., Zong, X., . . . Lal, A. (2017). Long Noncoding RNA PURPL Suppresses Basal p53 Levels and Promotes Tumorigenicity in Colorectal Cancer. *Cell Rep, 20*(10), 2408-2423. doi:10.1016/j.celrep.2017.08.041

Liao, Y., Smyth, G. K., & Shi, W. (2013). featureCounts: an efficient general purpose program for assigning sequence reads to genomic features. *Bioinformatics, 30*(7), 923-930. doi:10.1093/bioinformatics/btt656

Liao, Y., Wang, J., Jaehnig, E. J., Shi, Z., & Zhang, B. (2019). WebGestalt 2019: gene set analysis toolkit with revamped UIs and APIs. *Nucleic Acids Res, 47*(W1), W199-W205. doi:10.1093/nar/gkz401

Liberzon, A., Birger, C., Thorvaldsdottir, H., Ghandi, M., Mesirov, J. P., & Tamayo, P. (2015). The Molecular Signatures Database (MSigDB) hallmark gene set collection. *Cell Syst, 1*(6), 417-425. doi:10.1016/j.cels.2015.12.004

Love, M. I., Huber, W., & Anders, S. (2014). Moderated estimation of fold change and dispersion for RNA-seq data with DESeq2. *Genome Biol, 15*(12), 550. doi:10.1186/s13059-014-0550-8

Low, F. E. (1958). Bremsstrahlung of Very Low-Energy Quanta in Elementary Particle Collisions. *Physical Review, 110*(4), 974-977. doi:10.1103/PhysRev.110.974

Ludwig, B., Bender, E., Arnold, S., Hüttemann, M., Lee, I., & Kadenbach, B. (2001). Cytochrome c Oxidase and the Regulation of Oxidative Phosphorylation. *ChemBioChem, 2*(6), 392-403. doi:10.1002/1439-7633(20010601)2:6<392::aid-cbic392>3.0.co;2-n

Ma, C. M. C., & Lomax, T. (2012). *Proton and Carbon Ion Therapy*.

Ma, M., Cai, B., Jiang, L., Abdalla, B. A., Li, Z., Nie, Q., & Zhang, X. (2018). lncRNA-Six1 Is a Target of miR-1611 that Functions as a ceRNA to Regulate Six1 Protein Expression and Fiber Type Switching in Chicken Myogenesis. *Cells, 7*(12), 243. doi:10.3390/cells7120243

Maalouf, M., Durante, M., & Foray, N. (2011). Biological effects of space radiation on human cells: history, advances and outcomes. *J Radiat Res, 52*(2), 126-146. doi:10.1269/jrr.10128

Maiorano, D., Lutzmann, M., & Mechali, M. (2006). MCM proteins and DNA replication. *Curr Opin Cell Biol, 18*(2), 130-136. doi:10.1016/j.ceb.2006.02.006

Malatesta, P., Kyriakidis, K., Hada, M., Ikeda, H., Takahashi, A., Saganti, P. B., . . . Michalopoulos, I. (2024). Differential Gene Expression in Human Fibroblasts Simultaneously Exposed to Ionizing Radiation and Simulated Microgravity. *Biomolecules, 14*(1). doi:10.3390/biom14010088

Mavragani, I. V., Nikitaki, Z., Souli, M. P., Aziz, A., Nowsheen, S., Aziz, K., . . . Georgakilas, A. G. (2017). Complex DNA Damage: A Route to Radiation-Induced Genomic Instability and Carcinogenesis. *Cancers (Basel), 9*(7). doi:10.3390/cancers9070091

Maxwell, C. A., Fleisch, M. C., Costes, S. V., Erickson, A. C., Boissiere, A., Gupta, R., . . . Barcellos-Hoff, M. H. (2008). Targeted and nontargeted effects of ionizing radiation that impact genomic instability. *Cancer Res, 68*(20), 8304-8311. doi:10.1158/0008-5472.CAN-08-1212

Mazrani, W., McHugh, K., & Marsden, P. J. (2007). The radiation burden of radiological investigations. *Arch Dis Child, 92*(12), 1127-1131. doi:10.1136/adc.2006.101782

Michalettou, T. D., Michalopoulos, I., Costes, S. V., Hellweg, C. E., Hada, M., & Georgakilas, A. G. (2021). A Meta-Analysis of the Effects of High-LET Ionizing Radiations in Human Gene Expression. *Life (Basel), 11*(2). doi:10.3390/life11020115

Molnar, J., Fong, K. S., He, Q. P., Hayashi, K., Kim, Y., Fong, S. F., . . . Csiszar, K. (2003). Structural and functional diversity of lysyl oxidase and the LOX-like proteins. *Biochim Biophys Acta, 1647*(1-2), 220-224. doi:10.1016/s1570-9639(03)00053-0

Moreno-Villanueva, M., & Wu, H. (2019). Radiation and microgravity – Associated stress factors and carcinogensis. *Reach, 13*, 100027. doi:10.1016/j.reach.2019.100027

Mullis, K. B. (1990). The unusual origin of the polymerase chain reaction. *Sci Am, 262*(4), 56-61, 64-55. doi:10.1038/scientificamerican0490-56

Nelson, G. A. (2016). Space Radiation and Human Exposures, A Primer. *Radiat Res, 185*(4), 349-358. doi:10.1667/rr14311.1

Nickoloff, J. A., Boss, M. K., Allen, C. P., & LaRue, S. M. (2017). Translational research in radiation-induced DNA damage signaling and repair. *Transl Cancer Res, 6*(Suppl 5), S875-s891. doi:10.21037/tcr.2017.06.02

Nikitaki, Z., Hellweg, C. E., Georgakilas, A. G., & Ravanat, J. L. (2015). Stress-induced DNA damage biomarkers: applications and limitations. *Front Chem, 3*, 35. doi:10.3389/fchem.2015.00035

Nikitaki, Z., Michalopoulos, I., & Georgakilas, A. G. (2015). Molecular inhibitors of DNA repair: searching for the ultimate tumor killing weapon. *Future Med Chem, 7*(12), 1543-1558. doi:10.4155/fmc.15.95

Nikitaki, Z., Velalopoulou, A., Zanni, V., Tremi, I., Havaki, S., Kokkoris, M., . . . Georgakilas, A. G. (2022). Key biological mechanisms involved in high-LET radiation therapies with a focus on DNA damage and repair. *Expert Rev Mol Med, 24*, e15. doi:10.1017/erm.2022.6

Nishikawa, M. (2008). Reactive oxygen species in tumor metastasis. *Cancer Lett, 266*(1), 53-59. doi:10.1016/j.canlet.2008.02.031

Okazaki, R. (2022). Role of p53 in Regulating Radiation Responses. *Life (Basel), 12*(7). doi:10.3390/life12071099

Ottenheijm, C. A., Knottnerus, A. M., Buck, D., Luo, X., Greer, K., Hoying, A., . . . Granzier, H. (2009). Tuning passive mechanics through differential splicing of titin during skeletal muscle development. *Biophys J, 97*(8), 2277-2286. doi:10.1016/j.bpj.2009.07.041

Patro, R., Duggal, G., Love, M. I., Irizarry, R. A., & Kingsford, C. (2017). Salmon provides fast and bias-aware quantification of transcript expression. *Nat Methods, 14*(4), 417-419. doi:10.1038/nmeth.4197

Pflaum, J., Schlosser, S., & Müller, M. (2014). p53 Family and Cellular Stress Responses in Cancer. *Front Oncol, 4*, 285. doi:10.3389/fonc.2014.00285

Pinnell, S. R., & Martin, G. R. (1968). The cross-linking of collagen and elastin: enzymatic conversion of lysine in peptide linkage to alpha-aminoadipic-delta-semialdehyde (allysine) by an extract from bone. *Proc Natl Acad Sci U S A, 61*(2), 708-716. doi:10.1073/pnas.61.2.708

Poll-The, B. T., Roels, F., Ogier, H., Scotto, J., Vamecq, J., Schutgens, R. B., . . . et al. (1988). A new peroxisomal disorder with enlarged peroxisomes and a specific deficiency of acyl-CoA oxidase (pseudo-neonatal adrenoleukodystrophy). *Am J Hum Genet, 42*(3), 422-434. Retrieved from https://www.ncbi.nlm.nih.gov/pubmed/2894756

Porter, L. E. (1985). Bethe-bloch stopping power parameters for light projectiles at energies near the stopping power maximum. *Nuclear Instruments and Methods in Physics Research Section B: Beam Interactions with Materials and Atoms, 12*(1), 50-55. doi:10.1016/0168-583x(85)90699-8

Preston, D. L., Pierce, D. A., Shimizu, Y., Cullings, H. M., Fujita, S., Funamoto, S., & Kodama, K. (2004). Effect of recent changes in atomic bomb survivor dosimetry on cancer mortality risk estimates. *Radiat Res, 162*(4), 377-389. doi:10.1667/rr3232

Prisk, G. K., Elliott, A. R., & West, J. B. (2000). Sustained microgravity reduces the human ventilatory response to hypoxia but not to hypercapnia. *J Appl Physiol (1985), 88*(4), 1421-1430. doi:10.1152/jappl.2000.88.4.1421

Radstake, W. E., Gautam, K., Miranda, S., Vermeesen, R., Tabury, K., Rehnberg, E., . . . Baatout, S. (2023). The Effects of Combined Exposure to Simulated Microgravity, Ionizing Radiation, and Cortisol on the In Vitro Wound Healing Process. *Cells, 12*(2), 246. doi:10.3390/cells12020246

Rodriguez-Rocha, H., Garcia-Garcia, A., Panayiotidis, M. I., & Franco, R. (2011). DNA damage and autophagy. *Mutat Res, 711*(1-2), 158-166. doi:10.1016/j.mrfmmm.2011.03.007

Russ, E., Davis, C. M., Slaven, J. E., Bradfield, D. T., Selwyn, R. G., & Day, R. M. (2022). Comparison of the Medical Uses and Cellular Effects of High and Low Linear Energy Transfer Radiation. *Toxics, 10*(10). doi:10.3390/toxics10100628

Saiki, R. K., Scharf, S., Faloona, F., Mullis, K. B., Horn, G. T., Erlich, H. A., & Arnheim, N. (1985). Enzymatic amplification of beta-globin genomic sequences and restriction site analysis for diagnosis of sickle cell anemia. *Science, 230*(4732), 1350-1354. doi:10.1126/science.2999980

Saini, D., Shelke, S., Mani Vannan, A., Toprani, S., Jain, V., Das, B., & Seshadri, M. (2012). Transcription profile of DNA damage response genes at G_0 lymphocytes exposed to gamma radiation. *Mol Cell Biochem, 364*(1-2), 271-281. doi:10.1007/s11010-012-1227-9

Schewe, T. (1995). Molecular actions of ebselen--an antiinflammatory antioxidant. *Gen Pharmacol, 26*(6), 1153-1169. doi:10.1016/0306-3623(95)00003-j

Schwenn, R., Raymond, J. C., Alexander, D., Ciaravella, A., Gopalswamy, N., Howard, R., . . . Zhang, J. (2006). Coronal observations of CMEs: Report of working group A. *Space Sci Rev, 123*, 127–176. doi:10.1007/s11214-006-9016-y

Seal, R. L., Braschi, B., Gray, K., Jones, T. E. M., Tweedie, S., Haim-Vilmovsky, L., & Bruford, E. A. (2023). Genenames.org: the HGNC resources in 2023. *Nucleic Acids Res, 51*(D1), D1003-D1009. doi:10.1093/nar/gkac888

Shi, L., Tian, H., Wang, P., Li, L., Zhang, Z., Zhang, J., & Zhao, Y. (2021). Spaceflight and simulated microgravity suppresses macrophage development via altered RAS/ERK/NFκB and metabolic pathways. *Cell Mol Immunol, 18*(6), 1489-1502. doi:10.1038/s41423-019-0346-6

Shiraishi, I., Shikazono, N., Suzuki, M., Fujii, K., & Yokoya, A. (2017). Efficiency of radiation-induced base lesion excision and the order of enzymatic treatment. *Int J Radiat Biol, 93*(3), 295-302. doi:10.1080/09553002.2017.1239849

Siegel, R. C., Pinnell, S. R., & Martin, G. R. (1970). Cross-linking of collagen and elastin. Properties of lysyl oxidase. *Biochemistry, 9*(23), 4486-4492. doi:10.1021/bi00825a004

Simpson, J. A. (1983). Elemental and Isotopic Composition of the Galactic Cosmic Rays. *Ann Rev Nuclear Part Sci, 33*(1), 323-382. doi:10.1146/annurev.ns.33.120183.001543

Sinden, R. R. (1994). *DNA Structure and Function*. Cambridge: Academic Press.

Smith, R. C., Cramer, M. S., Mitchell, P. J., Lucchesi, J., Ortega, A. M., Livingston, E. W., . . . Stodieck, L. S. (2020). Inhibition of myostatin prevents microgravity-induced loss of skeletal muscle mass and strength. *PLoS One, 15*(4), e0230818. doi:10.1371/journal.pone.0230818

Soneson, C., Love, M. I., & Robinson, M. D. (2016). Differential analyses for RNA-seq: transcript-level estimates improve gene-level inferences. *F1000Res, 4*, 1521. doi:10.12688/f1000research.7563.2

Steinbaugh, M. J., Pantano, L., Kirchner, R. D., Barrera, V., Chapman, B. A., Piper, M. E., . . . Ho Sui, S. (2018). bcbioRNASeq: R package for bcbio RNA-seq analysis. *F1000Res, 6*, 1976. doi:10.12688/f1000research.12093.2

Stephens, M. (2016). False discovery rates: a new deal. *Biostatistics, 18*(2), 275-294. doi:10.1093/biostatistics/kxw041

Sutherland, B. M., Bennett, P. V., Sutherland, J. C., & Laval, J. (2002). Clustered DNA Damages Induced by X Rays in Human Cells. *Radiat Res, 157*(6), 611-616. doi:10.1667/0033-7587(2002)157[0611:CDDIBX]2.0.CO;2

Sutherland, M., Shankaranarayanan, P., Schewe, T., & Nigam, S. (2001). Evidence for the presence of phospholipid hydroperoxide glutathione peroxidase in human platelets: implications for its involvement in the regulatory network of the 12-lipoxygenase pathway of arachidonic acid metabolism. *Biochem J, 353*(Pt 1), 91-100. doi:10.1042/bj3530091

Szklarczyk, D., Kirsch, R., Koutrouli, M., Nastou, K., Mehryary, F., Hachilif, R., . . . von Mering, C. (2022). The STRING database in 2023: protein–protein association networks and functional enrichment analyses for any sequenced genome of interest. *Nucleic Acids Res, 51*(D1), D638-D646. doi:10.1093/nar/gkac1000

Tachiiri, S., Katagiri, T., Tsunoda, T., Oya, N., Hiraoka, M., & Nakamura, Y. (2006). Analysis of gene-expression profiles after gamma irradiation of normal human fibroblasts. *Int J Radiat Oncol Biol Phys, 64*(1), 272-279. doi:10.1016/j.ijrobp.2005.08.030

Takahashi, A., Kubo, M., Ma, H., Nakagawa, A., Yoshida, Y., Isono, M., . . . Nakano, T. (2014). Nonhomologous end-joining repair plays a more important role than homologous recombination repair in defining radiosensitivity after exposure to high-LET radiation. *Radiat Res, 182*(3), 338-344. doi:10.1667/rr13782.1

Terao, M., Garattini, E., Romao, M. J., & Leimkuhler, S. (2020). Evolution, expression, and substrate specificities of aldehyde oxidase enzymes in eukaryotes. *J Biol Chem, 295*(16), 5377-5389. doi:10.1074/jbc.REV119.007741

Teyssier, F., Bay, J. O., Dionet, C., & Verrelle, P. (1999). [Cell cycle regulation after exposure to ionizing radiation]. *Bull Cancer, 86*(4), 345-357. Retrieved from https://www.ncbi.nlm.nih.gov/pubmed/10341340

Topal, U., & Zamur, C. (2021). Microgravity, Stem Cells, and Cancer: A New Hope for Cancer Treatment. *Stem Cells Int, 2021*, 5566872. doi:10.1155/2021/5566872

Van Allen, J. A., McIlwain, C. E., & Ludwig, G. H. (1959). Radiation observations with satellite 1958 ε. *Journal of Geophysical Research, 64*(3), 271-286. doi:10.1029/JZ064i003p00271

Vandenburgh, H., Chromiak, J., Shansky, J., Del Tatto, M., & Lemaire, J. (1999). Space travel directly induces skeletal muscle atrophy. *Faseb j, 13*(9), 1031-1038. doi:10.1096/fasebj.13.9.1031

Venkata Narayanan, I., Paulsen, M. T., Bedi, K., Berg, N., Ljungman, E. A., Francia, S., . . . Ljungman, M. (2017). Transcriptional and post-transcriptional regulation of the ionizing radiation response by ATM and p53. *Sci Rep, 7*, 43598. doi:10.1038/srep43598

von Steiger, R., Schwadron, N. A., Fisk, L. A., Geiss, J., Gloeckler, G., Hefti, S., . . . Zurbuchen, T. H. (2000). Composition of quasi-stationary solar wind flows from Ulysses/Solar Wind Ion Composition Spectrometer. *Journal of Geophysical Research: Space Physics, 105*(A12), 27217-27238. doi:10.1029/1999ja000358

Wang, T., Sun, Q., Xu, W., Li, F., Li, H., Lu, J., . . . Bian, P. (2015). Modulation of modeled microgravity on radiation-induced bystander effects in Arabidopsis thaliana. *Mutat Res, 773*, 27-36. doi:10.1016/j.mrfmmm.2015.01.010

Wang, W., Wang, X., Yao, F., & Huang, C. (2022). Lysyl Oxidase Family Proteins: Prospective Therapeutic Targets in Cancer. *Int J Mol Sci, 23*(20), 12270. doi:10.3390/ijms232012270

Wang, Z., Gerstein, M., & Snyder, M. (2009). RNA-Seq: a revolutionary tool for transcriptomics. *Nat Rev Genet, 10*(1), 57-63. doi:10.1038/nrg2484

Watts, D. J., & Strogatz, S. H. (1998). Collective dynamics of 'small-world' networks. *Nature, 393*(6684), 440-442. doi:10.1038/30918

Yamanouchi, S., Adachi, T., Yoshida, Y., Rhone, J., Mao, J.-H., Fujiwara, K., . . . Hada, M. (2021). The combined effect of simulated microgravity and radiation on chromosome aberrations in human peripheral blood lymphocytes. *Biol Sci Space, 35*, 15-23. doi:10.2187/bss.35.15

Zhang, F., Manna, S., Pop, L. M., Chen, Z. J., Fu, Y. X., & Hannan, R. (2020). Type I Interferon Response in Radiation-Induced Anti-Tumor Immunity. *Semin Radiat Oncol, 30*(2), 129-138. doi:10.1016/j.semradonc.2019.12.009

Zhang, Y., Cui, Y., Li, M., Cui, K., Li, R., Xie, W., . . . Xiao, Z. (2022). DNA-assembled visible nanodandelions with explosive hydrogen-bond breakage achieving uniform intra-tumor distribution (UITD)-guided photothermal therapy. *Biomaterials, 282*, 121381. doi:10.1016/j.biomaterials.2022.121381

Zhu, A., Ibrahim, J. G., & Love, M. I. (2018). Heavy-tailed prior distributions for sequence count data: removing the noise and preserving large differences. *Bioinformatics, 35*(12), 2084-2092. doi:10.1093/bioinformatics/bty895

Zhu, A., Ibrahim, J. G., & Love, M. I. (2022). Effect size estimation with apeglm. Retrieved from https://bioconductor.org/packages/devel/bioc/vignettes/apeglm/inst/doc/apeglm.html

Zhu, C., Zhang, S., Xue, A., Feng, G., & Fan, S. (2022). Elevated BTG2 improves the radiosensitivity of non-small cell lung cancer (NSCLC) through apoptosis. *Thorac Cancer, 13*(10), 1441-1448. doi:10.1111/1759-7714.14410

Ziegler, J. F., Ziegler, M. D., & Biersack, J. P. (2010). SRIM – The stopping and range of ions in matter (2010). *Nuclear Instruments and Methods in Physics Research Section B: Beam Interactions with Materials and Atoms, 268*(11-12), 1818-1823. doi:10.1016/j.nimb.2010.02.091